

BENT-CORE MESOGENS – SUBSTITUENT EFFECT AND PHASE BEHAVIOR

DISSERTATION

zur Erlangung des akademischen Grades
doctor rerum naturalium (Dr. rer. nat)

vorgelegt der

Mathematisch-Naturwissenschaftlich-
Technischen Fakultät

(mathematisch-naturwissenschaftlicher Bereich) der Martin-Luther-Universität
Halle-Wittenberg

von Frau Dipl.- Chem. Hajnalka Nádasi
geboren am 14.08.1975 in Budapest

Gutachter 1. Prof. Wolfgang Weissflog
 2. Prof. Gerhard Pelzl
 3. Dr. Katalin Fodor-Csorba

Halle (Saale), den 06. 05. 2004

urn:nbn:de:gbv:3-000007274

[<http://nbn-resolving.de/urn/resolver.pl?urn=nbn%3Ade%3Agbv%3A3-000007274>]

To the memory of my grandfather

Chapter 1 Introduction	1
1.1 Bent-shaped mesogens: a topic area of liquid crystals	1
1.1.1 Structure of bent-core mesogens	1
1.1.2 Structure of liquid crystalline phases of bent-shaped molecules	3
1.1.3 Experimental techniques	4
1.2 This thesis	5
Chapter 2 The field of bent-shaped mesogens	7
2.1 Mesophases of bent-shaped mesogens	7
2.1.1 Predicted banana mesophases	7
2.1.2 Realization of banana mesophases	9
2.2 Experimental techniques	12
2.2.1 Polarizing microscopy	12
2.2.2 Calorimetric studies	12
2.2.3 X-ray diffraction	13
2.2.4 Electro-optical studies	14
2.2.5 Nuclear magnetic resonance studies	16
2.2.6 Dielectric spectroscopy	18
2.3 Chemical structure-property relationships in bent-shaped molecules	21
2.3.1 The central unit	22
2.3.2 The connecting groups	23
2.3.3 Lateral substitution	26
2.3.4 The terminal chains	28
2.4 Objectives	30
Chapter 3 Substituted resorcinol derivatives	32
3.1 Synthetic work	32
3.2 Two-ring substances	36
3.2.1 4-(4-n-Alkyloxy-3-fluoro-phenyliminomethyl)benzoic acids	36
3.2.2 4-(4-n-Alkyloxy-2-fluoro-phenyliminomethyl)benzoic acids	37
3.3 Bent-shaped compounds derived from resorcinol and substituted resorcinols	40
3.3.1 Resorcinol derivatives without substitution on the central ring	40
3.3.1.1 1,3-Phenylene bis[4-(4-n-alkyloxy-3-fluoro-phenyliminomethyl)benzoates]	40

3.3.1.2 1,3-Phenylene bis[4-(4-n-alkyloxy-2-fluoro-phenyliminomethyl)benzoates]	46
3.3.2 2-Nitroresorcinol derivatives	49
3.3.3 2-Methylresorcinol derivatives	51
3.3.3.1 2-Methyl-1,3-phenylene bis[4-(4-n-alkyloxy-3-fluoro-phenyliminomethyl)benzoates]	51
3.3.3.2 2-Methyl-1,3-phenylene bis[4-(4-n-alkyloxy-2-fluoro-phenyliminomethyl)benzoates]	57
3.3.4 4-Cyanoresorcinol derivatives	59
3.3.4.1 4-Cyano-1,3-phenylene bis[4-(4-n-alkyloxy-3-fluoro-phenyliminomethyl)benzoates]	59
3.3.4.2 4-Cyano-1,3-phenylene bis[4-(4-n-alkyloxy-2-fluoro-phenyliminomethyl)benzoates]	63
3.3.5 4-Chlororesorcinol derivatives	65
3.3.5.1 4-Chloro-1,3-phenylene bis[4-(4-n-alkyloxy-3-fluoro-phenyliminomethyl)benzoates]	65
3.3.5.2 4-Chloro-1,3-phenylene bis[4-(4-n-alkyloxy-2-fluoro-phenyliminomethyl)benzoates]	67
3.3.6 4,6-Dichlororesorcinol derivatives	70
3.3.6.1 4,6-Dichloro-1,3-phenylene bis[4-(4-n-alkyloxy-3-fluoro-phenyliminomethyl)benzoates]	70
3.3.6.2 4,6-Dichloro-1,3-phenylene bis[4-(4-n-alkyloxy-2-fluoro-phenyliminomethyl)benzoates]	75
3.3.7 5-Fluororesorcinol derivatives	77
3.3.7.1 5-Fluoro-1,3-phenylene bis[4-(4-n-alkyloxy-3-fluoro-phenyliminomethyl)benzoates]	77
3.3.7.2 5-Fluoro-1,3-phenylene bis[4-(4-n-alkyloxy-2-fluoro-phenyliminomethyl)benzoates]	83
3.3.7.3 5-Fluoro-1,3-phenylene bis[4-(4-n-alkyloxyphenyliminomethyl)benzoates]	84
Chapter 4 m-Phenylene-diamine derivatives	87
4.1 The synthetic work	87
4.2 Characterization	89
Chapter 5 Isophthalydene bis[4-(4-subst.-phenoxy)carbonyl]anilines]	91
5.1 The synthetic work	91
5.2 Characterization	92
Chapter 6 Conclusion	97
6.1 The role of the linking groups	97
6.2 The role of lateral fluoro-substituents	99

Chapter 7 Summary/Zusammenfassung	104
Chapter 8 Experimental part	116
8.1 Substituted fluorinated 1,3-phenylene bis[4-(4-n-alkyloxy-2/3-fluoro-phenyliminomethyl)benzoates]	117
8.1.1 4-n-Alkyloxy-2/3-fluoro-nitrobenzene	117
8.1.1.1 Mitsunobu etherification	117
8.1.1.2 Williamson etherification	117
8.1.2 4-n-Alkyloxy-2/3-fluoro-anilines	119
8.1.3 4-(4-n-Alkyloxy-2/3-fluoro-phenyliminomethyl)benzoic acids	121
8.1.4 5-Fluororesorcinol and 5-chlororesorcinol	122
8.1.5 Substituted 1,3-phenylene bis[4-(4-n-alkyloxy-2/3-fluoro-phenyliminomethyl)benzoates]	123
8.2 N,N'-bis[4-(4-n-Octyloxybenzoyloxy)benzylidene]phenylene-1,3-diamines	130
8.2.1 2-Fluoro-4-hydroxy-benzaldehyde	130
8.2.2 4-n-Octyloxybenzoic acid 3-fluoro-4-formylphenyl ester	130
8.2.3 4-Fluoro-m-phenylenediamine	131
8.2.4 N,N'-bis[4-(4-n-Octyloxybenzoyloxy)benzylidene]phenylene-1,3-diamines	131
8.3 Isophthalaldene bis[4-(4-substituted-phenyloxycarbonyl)anilines]	132
Bibliography	134
Symbols and abbreviations	139
Curriculum Vitae	141
Acknowledgement	142

Chapter 1 Introduction

Since application of thermotropic liquid crystals has always been of wide interest, discovery of bent-shaped (banana, boomerang, bow) liquid crystals [1] opened a very promising field concerning new mesophases.

Banana-shaped mesogens exhibit rich variety of liquid crystalline state: new so-called banana as well as conventional mesophases have been observed. The properties of banana mesophases are affected by the transversal anisotropy of the bent-shape of the molecules. In banana mesophases bent-core molecules organize into liquid-like layers but the mesophase character is different from conventional smectic phases inasmuch as conventional smectic and banana phases are not miscible. Some banana mesophases are switchable: they display ferro- and/or antiferroelectric switching behavior. The molecules are achiral, however. The unique properties of bent-core mesogens have stimulated intensive work: comprehensive studies have been carried out to make a better understanding on structure-property relationship in bent-shaped liquid crystals. You can find an extensive review in ref. [2].

1.1 Bent-shaped mesogens: a topic area of liquid crystals

1.1.1 Structure of bent-core mesogens

According to the IUPAC recommendation [3] banana-shaped mesogens are constituted of two mesogenic groups linked through a rigid group in such a way as not to be co-linear (Fig. 1.1). The mesogenic groups are mostly calamitic molecules consisting of two aromatic rings with varied linking groups (Y, Y') between them, and a terminal chain in para position on one of the aromatic rings with respect to this linking group, e.g. 4-(4-n-octyloxyphenyliminomethyl)- phenylcarbonyloxy fragment. These calamitics are connected to a rigid mainly six-member-aromatic ring, so that the angle between the two calamitic wings (bending angle) is around 120 degrees. In case of a benzene ring it means that the mesogens are connected in position 1 and 3, respectively. Thus, the origin of the non-linear shape is the meta-substituted benzene ring.

There are some examples for varying the central ring while keeping the bending angle around 120 degrees. Possible alternatives were found by replacing the benzene ring with 2,7-disubstituted naphthalene [4] or 2,5-disubstituted 1,3,4-oxadiazol or 2,5-disubstituted-thiophene [5]. The latter two compounds exhibit but conventional smectic and nematic mesophases, though.

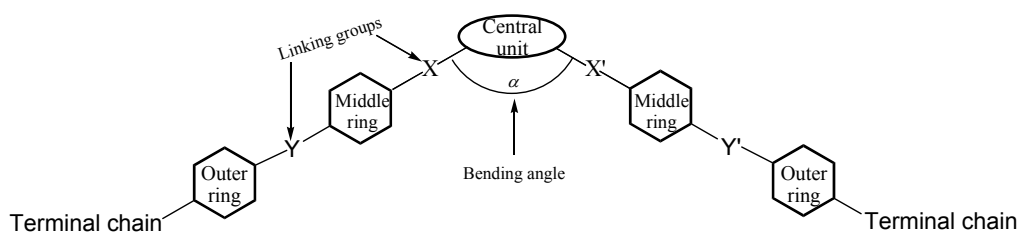


Fig. 1.1 General scheme of bent-shaped molecules

The mesogenic groups can be connected by a spacer, too. Thisayukta et al. made a comparative study of such so-called twins connected through “one-unit spacer” like methylene, carbonyl, ether and thioether [6]. X-ray measurements proved that all compounds exhibit smectic mesophases: the compounds with methylene and carbonyl spacers have a conventional, with ether spacer a frustrated smectic layer structure. The texture observations do not provide additional information about the mesophase structure. X-ray data obtained from the thioether derivative also suggest a smectic layer structure. Although the microscopic texture gives a hint suggests a more complex structure than in the above-mentioned three cases. All compounds exhibit smectic mesophases: the results do not give any indication if the substances display conventional or banana smectic mesophases. An explicit odd-even effect occurs connecting the mesogenic wings through a longer spacer [7, 8, 9]. An additional important structural factor is the proportion of the length of the spacer and the terminal chains. If the length of the terminal chains is smaller or comparable to the central spacer an intercalated SmC phase appears [8, 9]. If the terminal chains are significantly longer than the spacer they segregate from each other resulting in a biaxial structure [10, 11].

Pelz et al. synthesized two kinds of asymmetric twins with methyleneoxycarbonyl spacer [12]. The molecules differ in the linking groups: the benzene rings are connected only by carbonyloxy groups in one compound while by carbonyloxy and

azomethine groups in the other one. They found that the substances exhibit B_1 phase, whereas two different kinds of – tilted and non-tilted - B_1 phase.

Recently, Schröder et al. presented bent-core liquid crystals with very unusual benzoylpiperazine and benzoylpiperidine central moiety [13]. These mesogens exhibit both, banana and/or conventional mesophases.

Linking groups employed for calamitic mesogens can be used in bent-core molecules, too. Varying the connection between the rings may bring about drastic changes in the mesophase behavior.

1.1.2 Structure of liquid crystalline phases of bent-shaped molecules

What makes these molecules different from calamitic ones so that banana smectic mesophases can show macroscopic electric polarization? Two directors can define orientation of a bent-shaped molecule. One \mathbf{n} along the long molecular axis and another in the direction of the bow \mathbf{p} . Because of packing constraints, bent-core molecules tend to segregate into planes, with their polar axis defined by \mathbf{p} aligned along a common direction. Since the layer normal \mathbf{k} defines a direction independently of \mathbf{n} and \mathbf{p} a large variety of mesophases with different symmetries may result. Because an electric polarization exists the polar axis can be controlled by application of an electric field, in other words, the mesophase is switchable. You will find a detailed description in chapter 2.

As it has been mentioned above rich variety of banana mesophases are conceivable. There are several possibilities of arrangement of the molecules in smectic layers. A detailed description is given in chapter 2.

There are two nomenclatures for banana mesophases. One based on the nomenclature of conventional liquid crystals. A subscription behind the phase symbol signs the interface arrangement of the molecules from layer to layer, viz. S for synclitic, A for anticlitic one. Additionally the letter P indicates if the mesophase is polar. There may be a subscription behind it describing the switching behavior. A stands for antiferroelectric and F for ferroelectric mesophases. Thus, $SmC_S P_F$ describes a mesophase where the long axes of the bent-shaped molecules are tilted with respect to the layer normal, from layer to layer parallel with each other, showing ferroelectric switching behavior in electric field. Detailed description of this mesophase see in chapter 2.

The other nomenclature was suggested in the workshop Banana-Shaped Liquid Crystals: “Chirality by Achiral Molecules” held in Berlin in December 1997. According to this regulation B denotes that the mesophase is formed by banana molecules. Furthermore numbering from one to seven behind indicates the similarity or the sameness with one of those banana phases discovered at first. This nomenclature was declared preliminary, and does not cover the whole spectra of banana mesophases known nowadays. However, for instance B₇ and B₅ phases cannot be described with the conventional nomenclature because of our incomplete knowledge about it. The necessity of developing a new nomenclature has been formulated on the workshop “Banana Liquid Crystals: Chirality and Polarity” held in Boulder in August 2002. As a result Clark, Pleiner, Pelzl et al. have been developing a new nomenclature based on the symmetry of the phases.

Neither banana mesophase is miscible with any smectic phase of calamitic compounds. Detailed descriptions of the mesophases see in chapter 2.

1.1.3 Experimental techniques

Characterization of the mesophases requires combination of several techniques such as polarizing microscopy, calorimetry, X-ray diffraction, electro-optics, dielectric spectroscopy and NMR. None of these techniques can give complete picture about the mesophase, even if each has particular contribution to the full characterization. A short overview is given below. The consequence of the methods is in accordance with the usual consequence of investigations.

Polarizing microscopy	Phase assignment based on microscopic texture and the topology of defects
Differential scanning calorimetry	Transition temperatures T Transition enthalpy ΔH in some cases order of transition
X-ray diffraction	Structural analysis: symmetry of the molecular arrangement layer thickness d of smectics Phase assignment

Electro-optics	Switching behavior switching time τ_s switching polarization P_s Elastic constants K Viscosity γ
Dielectric spectroscopy	Dielectric properties dielectric permittivity ε conductivity σ Molecular dynamics elastic constants K viscosity γ relaxation processes: relaxation times τ and activation energies E_A Intermolecular interactions
Nuclear magnetic resonance	Degree of orientational order S, D Molecular conformation angles torsions interatomic distances Relaxation processes τ Elastic constants K

1.2. This thesis

In 1932 Vorländer reported about the first bent-shaped molecules [14]. In 1994 Akutagawa et al. gave an account of some bent-core mesogens without characterization of the high-temperature smectic phases [15]. The article of Niori et al. [1] turned the attention to the bent-shaped compounds. Several bent-shaped compounds have been prepared and investigated since then, but still there is a lot to do to complete the picture about this field. This work is an attempt to make a better understanding on structure-property relationships.

In chapter 2 there is a description of physical studies (polarizing microscopy, DSC, XRD, electro-optics, dielectric spectroscopy and NMR) applied for characterization the substances. Additionally, it gives an account of banana phases as well as structure-property relationships in bent-shaped mesogens known up to the beginning of this work. Here you will read about the objectives of this work.

In chapter 3 resorcinol derivatives and the intermediates of the synthesis are introduced and characterized. In chapter 4 a description about m-phenylenediamine derivative bent-compounds will be given. In chapter 5 an account is given about isophthalaldehyde derivative bent-core compounds. In chapter 6 conclusions will be drawn. Chapter 7 provides the summary, chapter 8 contains the experimental part of this work.

Chapter 2 The field of bent-shaped mesogens

2.1 Mesophases of bent-shaped mesogens

2.1.1 Predicted banana mesophases

It is important to notice that achiral bent-shaped compounds show mesogenic behavior. One of the striking features of the mesophases formed by achiral bent-shaped molecules is that they show spontaneous breaking of achiral symmetry. In case of smectic liquid crystals formed by bent-shaped molecules possible arrangements have been proposed by Brand et al. [16]. So-called “minimal banana smectics” have one polarization vector and corresponding arrangements and symmetries are sketched in Fig. 2.1 and Table 2.1. Among these polar structures two phases with C_2 and C_1 symmetries are chiral.

Class	Symmetry	Electro-optics	Helix
C_P	C_{2v}	Ferri- or ferroelectric $P = (P_x, 0, 0)$	no
$C_{P'}$	C_{2v}	Ferri- or ferroelectric $P = (0, 0, P_z)$	no
C_{B2}	C_2	Ferri- or ferroelectric $P = (P_x, 0, 0)$	yes
C_{B1}	C_{1h}	Ferri- or ferroelectric $P = (P_x, 0, P_z)$	no
C_G	C_1	Ferri- or ferroelectric $P = (P_x, P_y, P_z)$	yes

Table 2.1 Character of banana smectics

Thisayukta et al. synthesized bent-core compounds with chiral terminal chains and studied the effect of chiral dopants on the formation of smectic phases of achiral mesogens [18, 19]. They have supposed that the chirality of the phase has been determined by the intermolecular steric interactions and not by the handedness of the mole-

cules. Although it has not been proved yet if the effect of the molecular chirality and interactions can be interpreted independently.

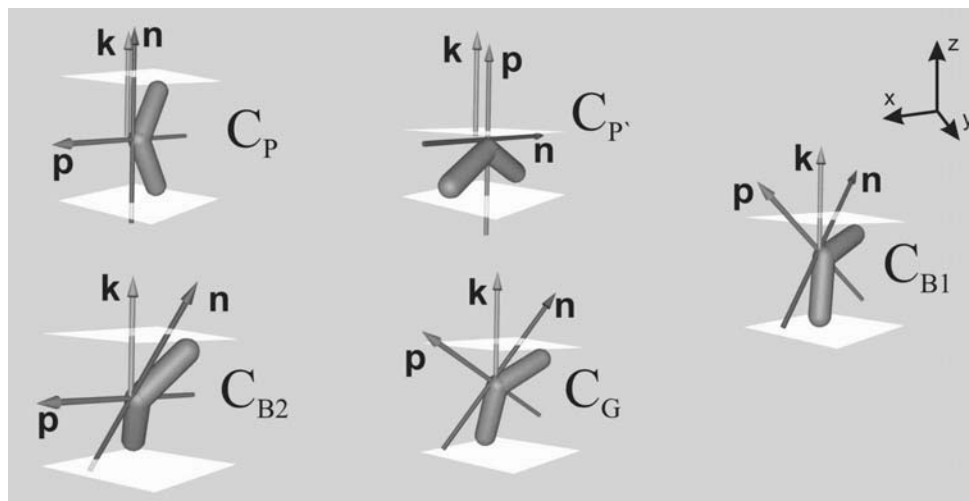


Fig. 2.1 Possible arrangement of the molecules in smectic layers [17]

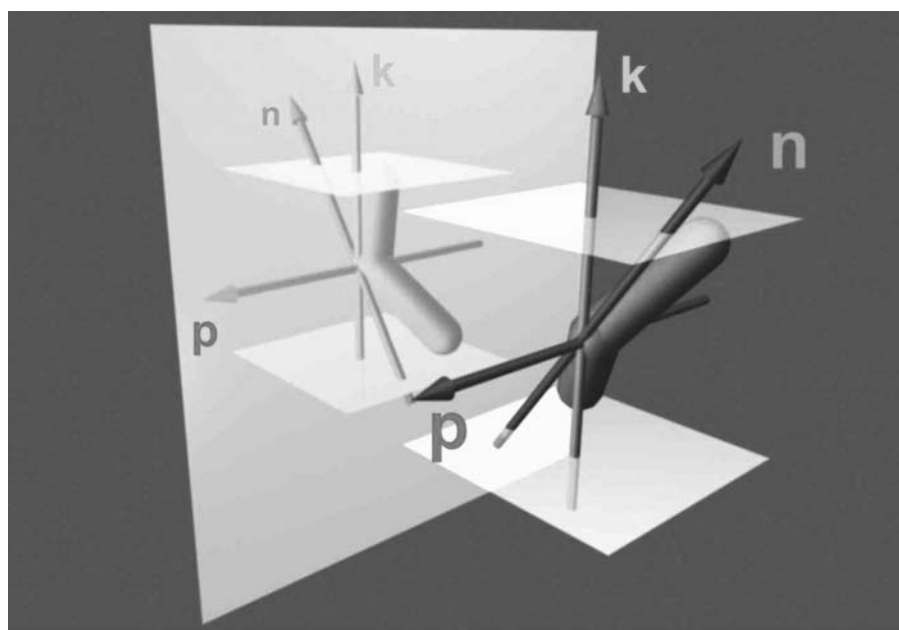


Fig. 2.2 Structural chirality of the SmC phase [17]

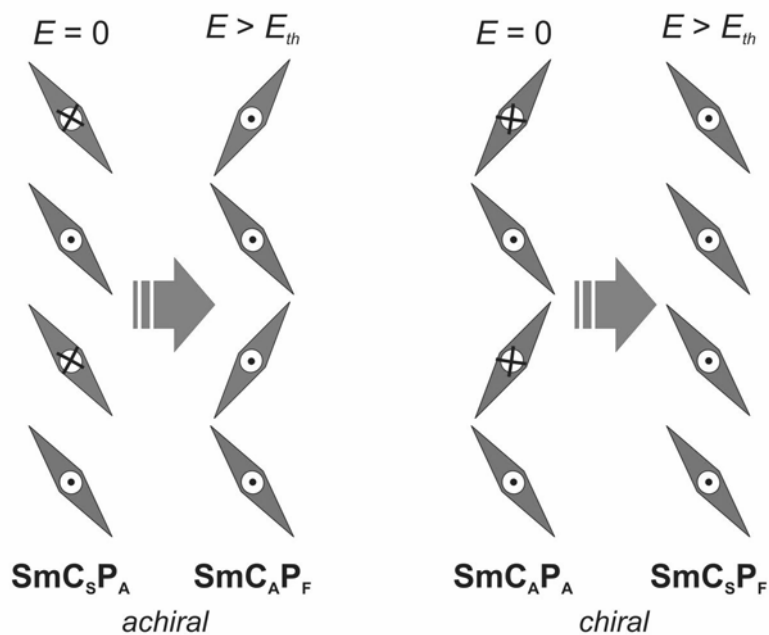


Fig. 2.3 Various arrangement of smectic layers in SmCP phase and the effect of the switching on the structure of the layers. E electric field, E_{th} threshold field

2.1.2 Realization of banana mesophases

Theoretical models predict tremendously rich variety of smectic and nematic mesophases of various symmetries, yet only few unusual smectic phases have been observed experimentally. Among them there are two phases with a simple layer structure of C_2 and C_{2v} symmetry and no order within the layers as well as there are some higher ordered phases. Recently some evidence has been found for the phase with the C_1 symmetry [20].

A phase with C_{2v} symmetry is called C_P or SmAP. The bent molecules are arranged orthogonally in liquid-like smectic layers. The molecules are packed in the direction of the bow within each layer, which results in spontaneous macroscopic polarization. Therefore the SmAP phase is different from the SmA phase where there is no preferred direction perpendicular to the layer normal. A similar phase (SmAP) was found in side-chain polymers [21] quite a while ago, however, in low-molecular bent-shaped compounds it was observed and described for the first time only recently [22].

Up to date the most common phase is the one with C_2 symmetry. There is no all-accepted nomenclature so far and this phase is designated by different authors as C_{B2} or

B_2 or SmCP. The structure of the phase consists of smectic liquid-like layers with tilted molecules and the polar order in the direction perpendicular to the layer normal. It is a unique mesophase since despite liquid disorder within the layers it shows a breaking of achiral symmetry, natural for solids but has never been found in liquids. The molecules are achiral and the chirality appears in consequence of the mesophase structure. Indeed the structure is defined by three vectors \mathbf{p} , \mathbf{n} and \mathbf{k} . These vectors are coplanar unless the value of $[\mathbf{n} \times \mathbf{k}] \cdot \mathbf{p} = q \neq 0$ which, actually, defines the chirality since the vector product is a pseudo-vector. The states with $q < 0$ and $q > 0$ are of opposite handedness: have no mirror symmetry (Fig. 2.2). Whereas the state with $q = 0$ is achiral. In our system the latter case corresponds to the SmAP phase. An excellent review of the topic of chirality and its measure can be found in ref. [23, 24].

An extensive research made on thin SmCP films [25] showed that besides the polar packing of the molecules within the smectic layers, the arrangement of the layers with respect to each other plays an important role. In particular, there are two possible interface arrangements: synclinal and anticlinal as well as two possible orientations of the polarization vectors in the adjacent layers: ferroelectric (FE) and antiferroelectric (AFE). In most cases the ground state is antiferroelectric and applying an electric field along the layers one can switch to the ferroelectric state. As it has already been mentioned above each layer is chiral. However, among these four different structures two are macroscopically chiral (SmC_AP_A and SmC_SP_F) and the other two are achiral (or racemic as designated in ref. [25]) (SmC_SP_A and SmC_AP_F). Application of an electric field leads to an electro-optical switching from the ground AFE state into the FE state (Fig. 2.3). The chirality of the layers usually remains conserved.

Among other mesophases the B_5 phase is similar to the SmCP phase: it consists of smectic layers with tilted molecules and shows electro-optical switching. In contrast to the SmCP phase, the B_5 phase possesses an in-plane density modulation which can be described by a rectangular two-dimensional network [2, 26]. So far, it is not fully characterized and probably is a candidate to an analogue to hexatic phases of calamitics.

An intercalated version of the SmCP phase is called B_6 . It occurs rarely and in contrast to the SmCP phase, it does not show electro-optical switching [2, 27, 28].

A long search for simple smectic phases with triclinic (C_1) symmetry seems to have good chances to be of success in the field of bent-shaped liquid crystals. Recently

some candidates for the general SmC_G phase have been found in our laboratory [20]. In chapter 3 you will find an account about these substances. Jáklí et al. suggested at first that one of these candidates exhibit SmC_G phase [29].

The family of the B_7 phases which are under intense discussions nowadays [30]. Unusual bright and artistic textures attracted many liquid-crystal researchers and endeavored them to unravel the structure of this enigmatic phase. However, difficulties to form free-standing films and absence of oriented samples is a main obstacle since the X-ray shows a complex two- or three- dimensional superstructure of the mesophase. Currently, columnar models with triclinic symmetry [31] as well as modulated lamellar structures with C_2 symmetries are under consideration [32]. However, there could not be observed incommensurable reflections – typical for B_7 phase – in the X-ray pattern of the compound researched by Clark et al. A description about materials exhibiting B_7 phase is issued in chapter 3.

Additionally except for smectic phases described above, the bent-shaped mesogens form some exotic columnar phases designated as B_1 (it is rather a group of phases of different symmetries) [2, 33]. Lately Pelz et al. suggested that there exists two kinds of B_1 phase with rectangular lattice: an orthogonal and a tilted one [12]. Two more crystalline phases “belong” to the banana class: the crystalline B_3 phase [2], and the distorted soft-crystalline B_4 phase [34].

2.2 Experimental techniques

2.2.1 Polarizing microscopy

The texture characterization of liquid crystal mesophases has been essential in primary phase assignment. The birefringence and the defects of a liquid crystal are responsible for the patterns seen in a polarizing microscope wherein light first passes through a polarizer, then through the liquid crystal specimen, and finally through a second polarizer. The latter is situated at 90 degrees to the first one. Because of the crossed polarizers no light gets to the observer's eyes unless the liquid crystal changes the polarization state of the light.

2.2.2 Calorimetric studies

Measurement of the temperature dependence of the heat capacity C_p and/or the enthalpy ΔH determines the thermal behavior of the liquid crystal phases and helps to characterize the phase transitions which occur.

By far the most common thermal technique used to study liquid crystals has been differential scanning calorimetry (DSC). This method has the advantages of high sensitivity for detecting enthalpy changes, very small sample size, rapid and convenient operation. However, DSC is not well suited to making detailed quantitative measurements near liquid crystal phase transitions.

The disadvantage of DSC measurements is the difficulty to distinguish first- and second-order transitions. In operation, a constant heating (or cooling) rate dH_{ref}/dt is imposed on the reference sample, which results in a constant and rapid linear temperature ramp. Scan rates dT/dt of 5-10 K/min are commonly used. Although slower rates can be used, DSC machines work best for fairly rapid scans ($dT/dt \geq 1$ K/min) and require minimum scan rates of 0.1 K/min. A servosystem forces the sample temperature to follow that of the reference by varying the power input dH_{sample}/dt . The differential power $dH/dt = dH_{sample}/dt - dH_{ref}/dt$ is measured, and the integral $\int (dH/dt)dt$ for a DSC peak approximates the enthalpy associated with the corresponding transition.

A quantitative distinction between first and second order transitions could be found by making a series of measurements at different scan rates with further extrapolating of the transition enthalpy to rate zero. Strongly first order transition does not exhibit dependence of the latent heat on the cooling/heating rate. Whereas the enthalpy H shows almost linear dependence in case of the second or weakly first order transitions.

2.2.3 X-ray diffraction

X-ray diffraction provides one of the most definite ways to determine the structure of liquid crystalline phases. This technique has played a key role in the identification of liquid crystalline phases and in the quantitative study of several liquid crystal phase transitions.

The basic mantra of X-ray diffraction is the Bragg law. This law states that X-rays reflected from adjacent atomic planes separated by a distance d of a crystal interfere constructively when the path difference between them is an integer multiple of the wavelength λ , i.e.

$$2d \sin \theta = n\lambda \quad (2.1)$$

Here n , an integer, is the order of the reflection. The reflected rays make an angle of 2θ with the direction of the incident beam. X-ray “reflection” is present only when the planes are oriented (e.g. under the influence of an external field) at the correct angle to satisfy the Bragg condition. There is no reflection at other angles. For this reason it is called X-ray diffraction.

One of the goals on an X-ray experiment is to determine the Bragg angle(s), which can be related to the inter-planar distance or lattice constant. Conceptually, it seems to be simple but in liquid crystal experiments one needs to carefully consider the details.

An X-ray diffraction experiment provides information not only about the inter-planar distance, but also about the relative orientation and spatial orientational distribution of different sets of planes.

Basically the diffraction patterns of banana mesophases do not differ much of the calamitic liquid crystals. Thus, one cannot make difference between the SmC and

SmCP phases of banana compounds. However, clear distinction lies between the diffraction patterns of banana phases [2].

2.2.4 Electro-optical studies

The strong anisotropy of the molecular shape of bent-core mesogens can promote a polar packing within the smectic layers. The expressed sterical moment of such molecules accounts for ferroelectric properties observed in some banana mesophases (SmCP, B₅). One of the most intensively studied features of the ferroelectric liquid crystals is their ability to switch the direction of optical axes under the influence of external electric field. The bistable ferroelectric switching in ferroelectric chiral smectic C phase has found to be suitable to a lot of application. The macroscopic polarization in the ferroelectric phase does not linearly depend on the external field: it shows a hysteresis-like behavior. A typical one-loop ferroelectric hysteresis curve is shown in the Fig. 2.4. In the limit of large fields ($E > E_{th}$) the macroscopic polarization is saturated. When the field goes to zero the macroscopic polarization remains non-zero. In this case two stable states are allowed; with spontaneous polarization “up” ($+P_s$) and “down” ($-P_s$). Application of the field above a certain threshold E_{th} results in the transition (switching) between these states. The rate of the switching is characterized by the switching time τ . In antiferroelectric mesophases the macroscopic polarization in the absence of the external field is zero. However, applying the field E ($E > E_{th}$) a transition into the ferroelectric state can be induced. In this case the field-dependent macroscopic polarization shows a typical antiferroelectric two-loop hysteresis curve (Fig. 2.5).

The measurements of the spontaneous polarization can be made by applying electric field to a capacitor filled with the liquid crystalline sample. In the triangular wave voltage technique the applied electric field has a triangular shape. When the voltage over the capacitor exceeds a threshold voltage U_{th} ($U_{th} = E_{th} \times d$, where d is the distance between the capacitor plates) the reorientation of the macroscopic polarization in the sample induces a current impulse through the capacitor. The value of this switching polarization is:

$$P_{sw} = \frac{1}{S} \int_{\text{over the pulse}} I(t) dt \quad (2.2)$$

where S is the area of the capacitor. In the ferroelectric material there is only one transition with the threshold E_{th} between the FE^+ and FE^- states. Thus, one peak in half a period of the applied voltage represents the current response.

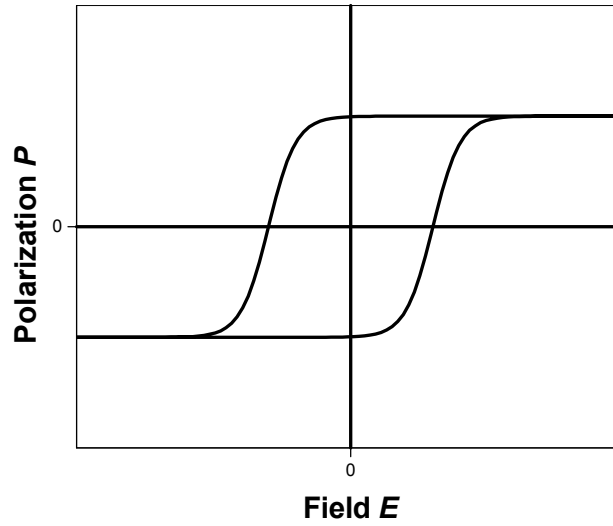


Fig. 2.4 One-loop ferroelectric hysteresis curve

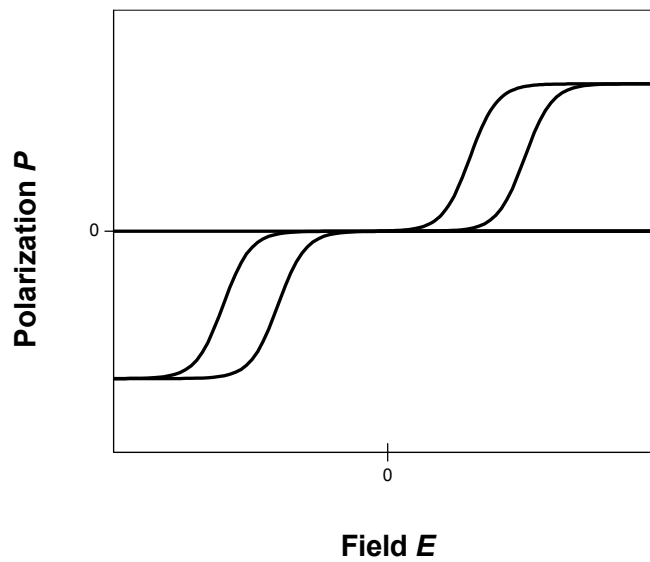


Fig. 2.5 Two-loop antiferroelectric hysteresis curve

In the antiferroelectrics there are two transitions: AFE→FE with E_{th1} and the inversed FE→AFE transition with E_{th2} what provides two current impulses per half a period. The switching times can be extracted from the current response curves for the step-like shape of the external field.

2.2.5 Nuclear magnetic resonance studies

NMR offers numerous ways to study dynamic aspects over a large range of characteristic motional rates. The main advantage of NMR is its unprecedented selectivity. Since the discovery of NMR technique it has been intensively used in liquid crystal research [35, 36]. The most important aspect of NMR for study of liquid crystals is that the splitting of the proton and deuterium NMR lines is directly related to the orientational order parameter S and to the orientation of the nematic director \mathbf{n} . NMR has a variety of applications in liquid crystals: study of structure and conformation of mesogens [37], study of orientational order [35, 38], determination of elastic constants [39], etc.

Application on bent-shaped liquid crystals [17]

If we consider, for example, an aromatic ring in a bent-shaped molecule, the dynamic and the orientation of the group with respect to the molecular frame should be taken into account. In Fig. 2.6 the direction of the principle axis frame of chemical-shift tensor is schemed. In presence of a π -flip only two components of the tensor are non-zero: parallel and perpendicular to the para-axis:

$$\begin{aligned}\overline{W}_{11} &= W_{11} \cos^2 \pi/3 + W_{22} \sin^2 \pi/3 \\ \overline{W}_{22} &= W_{22} \cos^2 \pi/3 + W_{11} \sin^2 \pi/3\end{aligned}\quad (2.3)$$

Allowing the aromatic rings be tilted in the molecular frame, we can express the components of the tensor in terms of the angle ε and the torsion angle φ (Fig. 2.4)

$$W_{\zeta\zeta} = \overline{W}_{11} - (\overline{W}_{11} - \overline{W}_{22}) \sin^2 \varepsilon - (\overline{W}_{11} + 2\overline{W}_{22}) \sin^2 \varepsilon \sin^2 \varphi \quad (2.4)$$

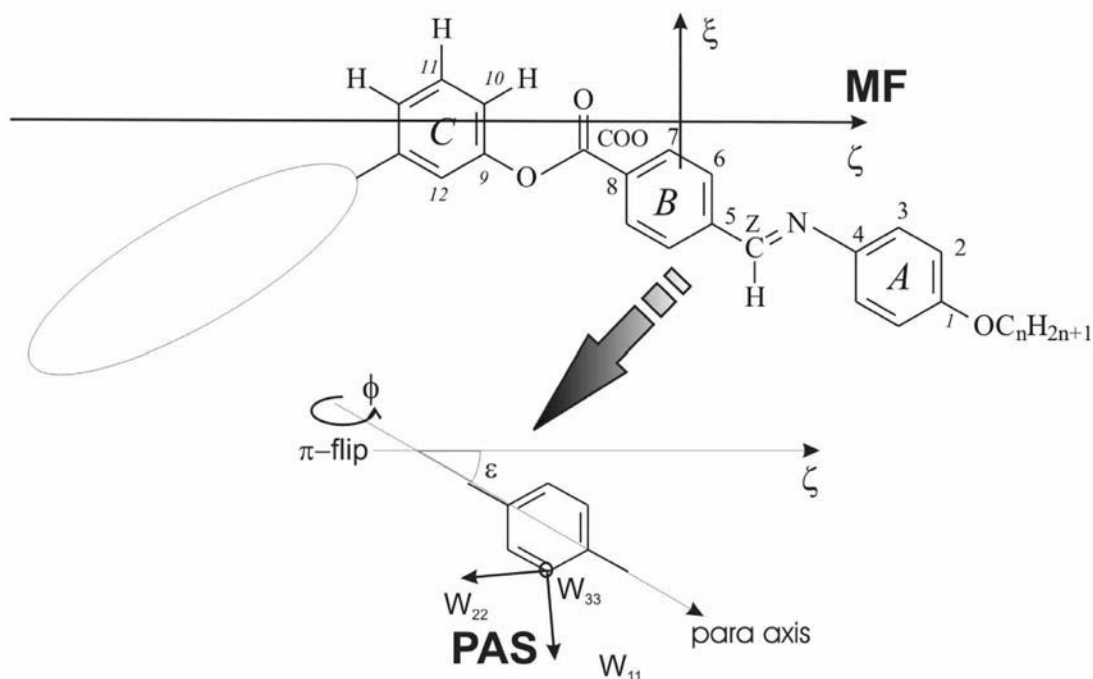


Fig. 2.6 Co-ordinate frames and the assignment of the atomic positions in a bent-shaped molecule. MF - molecular fixed frame: a coordinate frame fixed on the long and the short molecular axes, PAS – principle axis system: coordinate frame in which the corresponding interaction tensor (dipolar, quadrupolar or chemical shift tensor) is diagonal [40]

The experiments performed on the compounds included the following steps:

- *Determination of the orientational order parameter S .* It is made by observing dipolar splitting of H in positions 10 and 11 in $^1\text{H-NMR}$ (when these positions are not substituted). The three-spin system formed by a proton H11 and two protons H10 gives in the molecular frame an outer splitting $\Delta\nu_0 = k \Delta\nu_0^{(2)}$, where $\Delta\nu_0^{(2)}$ is the splitting in a two-spin system with a field parallel to the vector connecting the protons H10 and H11. The coefficient k depends on the precise geometry of the ring. Neglecting the transversal order parameter D the dipole splitting can be expressed by Eq. 2.7

$$\Delta\nu = \Delta\nu_0 S \left(\frac{3}{2} \cos^2 \beta - \frac{1}{2} \right) \quad (2.5)$$

where $\Delta\nu_0^{(2)} = -\frac{3K}{r^3}$ with $K = \frac{\gamma_i \gamma_j}{2\pi} \hbar$, $\Delta\nu_0^{(2)} = 47.25$ ppm for $r = 2.48$ Å, and

β regards to an angle between the symmetry axis and the molecular long axis. Shift anisotropy of carbons in positions 9 and 10 (11, 12) was measured, too. If the position 11 was substituted by fluorine, then the order parameter S could be found directly from ^{19}F -NMR measurements. The values of chemical shift anisotropy tensor were taken from literature [41]. Since there are no data on exactly the same molecules with similar groups and substituents had to be chosen. Using their data on shift anisotropy as initial parameters, a refinement was made with respect to the geometry of the rings to obtain a better agreement between different methods.

- The bending angles $\alpha = (180 - 2\varepsilon)$ and torsion angles φ for the rings A and B have been determined from ^{13}C -NMR from the corresponding positions in the rings A and B with a help of Eq. 2.4. If the ring A is fluorinated, the angle ε could be found from the dipolar splitting by the neighboring proton.

2.2.6 Dielectric spectroscopy

The dielectric permittivity determines the response of the material to the external field. In case of static electric field the dielectric permittivity is dielectric constant ε . For anisotropic materials dielectric constant is a tensor (depends on the direction in space). For example for uniaxial liquid crystals in the principal axis frame dielectric permittivity can be expressed by two values: ε_{\parallel} (component parallel to the optical axis) and ε_{\perp} (component perpendicular to the optical axis). The dielectric anisotropy $\Delta_a \varepsilon = \varepsilon_{\parallel} - \varepsilon_{\perp}$ can be positive like in case of 2,3-bis(trifluoromethyl)-4-methoxyphenyl trans-4-(trans-4-n-propylcyclohexyl)-cyclohexanecarboxylate, or negative like in 2,3-bis(trifluoromethyl)-4-methoxyphenyl trans-4-n-propylcyclohexylmethyl ether [42]. If the sample is non-oriented the dielectric response is governed by the average dielectric permittivity: $\varepsilon_{iso} = \frac{1}{3}\varepsilon_{\parallel} + \frac{2}{3}\varepsilon_{\perp}$ for uniaxial phase. If the applied field varies with time, then the frequency dependence of the permittivity is an additional property of the mate-

rial. A complication with any time-dependent response is that it may not be in-phase with the applied field. Thus to describe the frequency-dependent dielectric response of a material, the amplitude and phase of the induced polarization must be measured. A convenient way of representing phase and amplitude is through complex notation, so that ε' (real) measures the in-phase response, and ε'' (imaginary) is the phase delay of the dielectric response (dielectric loss).

$$\varepsilon^*(f) = \varepsilon'(f) - i\varepsilon''(f) \quad (2.6)$$

In presence of the relaxation process with characteristic relaxation time τ the dispersion curve looks like in Fig. 2.7.

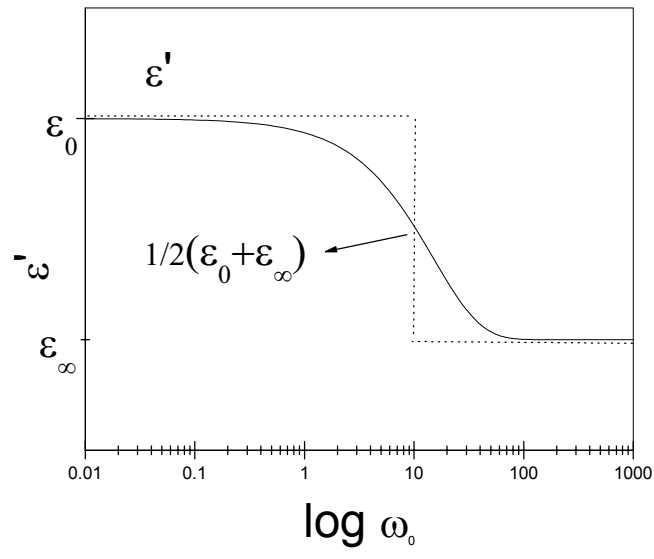


Fig. 2.7 Typical dispersion curve of the dielectric permittivity

The real part ε' shows step-like behavior changing from its low-frequency limit ε_0 ($f < f_{\text{relaxation}}$) to ε_∞ ($f > f_{\text{relaxation}}$). Thus, the relaxation process is characterized by the dielectric strength $\Delta\varepsilon$:

$$\Delta\varepsilon = \varepsilon_0 - \varepsilon_\infty \quad (2.7)$$

In case of several relaxation processes the characteristics can be extracted from the dielectric spectra using Debye and Cole-Cole approaches. Dielectric measurements on liquid crystals probe the dipole organization of molecules, and changes in the permittivity components as a liquid crystal undergoes phase transitions will primarily reflect changes in orientational order and symmetry changes. Dielectric spectroscopy gives us indispensable information about molecular dynamics in the mesophase, dipolar correlations, viscosity and diffusion.

2.3 Chemical structure-property relationships in bent-shaped molecules

In order to determine what types of molecular structures form mesophases numerous compounds have been synthesized and their mesomorphic properties determined to establish structure-property relationships. Yet the accurate prediction of properties for a new compound is still not possible. The best that can be done is to use known trends in the design of a molecule with the desired properties, and hope that this will be one of the many that do follow these known trends, but not be surprised if it does not.

Structure-property relations in bent-shaped mesogens are even less predictable than those of calamitics. The only criterion certainly need to be applied is that two mesogenic groups should be connected non-linearly. This condition is not guaranteed to obtain mesogens, but need to be prevailed for banana mesophases. In many cases, such a bent structure is non-mesogenic or exhibits common mesophases like in calamitics. Hence, the golden rule in banana-field is the compounds showing banana mesophases always consist of bent-shaped molecules, whereas the bent-shape of molecules does not assure (banana) mesophase at all. On top of all, it has not been clarified either why or in what case macroscopically chiral mesophases (SmCP/B_2 , $\text{SmAP/C}_{\text{PA}}$, B_5 , and SmC_G) appear.

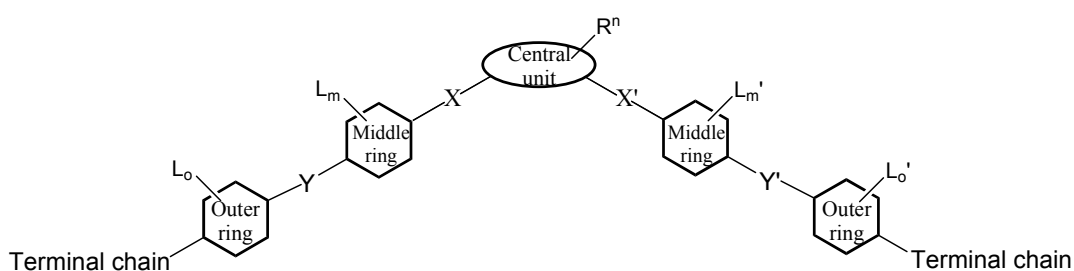


Fig. 2.8 General scheme of a bent-shaped molecule. X , X' , Y , Y' are the connecting or linking groups. L_m , L_m' , L_o , L_o' represent the lateral substituents, i.e. substituents on the rings of the wing. R^n designates lateral substituent(s) on the central ring, where n indicates the position of the substituents.

In this section the up to date trends in structure-property relationships in bent mesogens will be discussed in the following sequence: central ring, connecting groups,

lateral substituents, and terminal chains (Fig. 2.8). However, it should be noted that these structural factors together determine the physical properties of the mesogens. Contribution of a particular unit of the molecules cannot be discussed independently. Moreover the influence of the different structural factors, especially of the lateral substituents, is strongly dependent on the size of the molecules.

2.3.1 The central unit

The central unit in banana mesogens plays the key role in the bent. If the connection between the wings of the molecule through the central ring is established not in the right angle, there is no chance to obtain banana mesogens even if the construction of the molecule in all other building stones corresponds to the structure of bananas [43, 44]. The loss of the bent results in rod-like molecules with an extensive ring system, most probably with inconvenient, high transition temperatures and with no chance for macroscopically chiral phase formed by achiral molecules. At the same time one should note that bent-core mesogens might also exhibit “classical” mesophases like N, SmA and SmC phases. Examples will be shown in chapter 3.

In the literature, one may mostly find two aromatic systems used as central ring in bent-shaped compounds: 1,3-disubstituted benzene ring [1, 2, 45, 46] and 2,7-disubstituted naphthalene ring [4, 6, 18, 47] (Fig. 2.9).

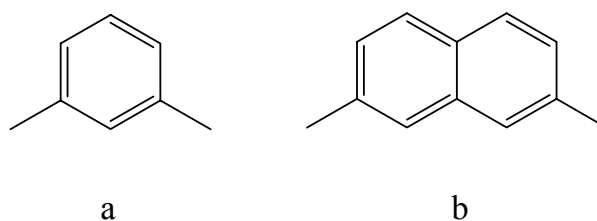


Fig. 2.9 1,3-Disubstituted benzene (a) and 2,7-disubstituted naphthalene (b) rings

Additionally there are some examples for heterocyclic central ring, e.g. 2,5-disubstituted 1,3,4-oxadiazol or 2,5-disubstituted-tiophene [5], 2,6-disubstituted-pyridine [48, 49, 50] (Fig. 2.10). In fact, only the pyridine derivative exhibited banana mesophase. The five-ring heterocycle derivatives exhibit smectic and nematic mesophases.

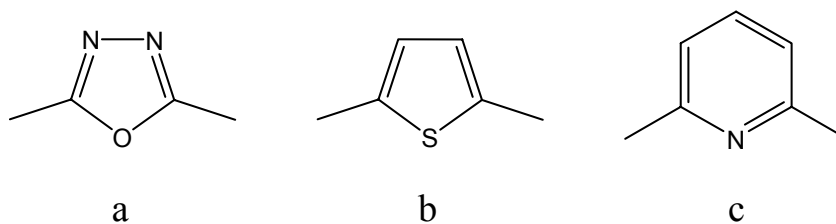


Fig. 2.10 2,5-Disubstituted-1,3,4-oxadiazol (a), 2,5-disubstituted-thiophene (b) and 2,6-disubstituted-pyridine (c) cores

As it has already been mentioned, it is impossible to consider only a particular element of the bent-shaped molecules as responsible moiety for the mesophase behavior. That brings us to the next topic of this chapter: the role of the connecting groups.

2.3.2 The connecting groups

Connecting or linking groups are as essential elements in bent-shaped molecule as the bent-core. They connect the rigid core system of bananas together. Connecting groups used for calamitic mesogens are suitable for bent-core compounds, too. Some typical examples for connecting groups in bent-shaped molecules are depicted in Fig. 2.11.

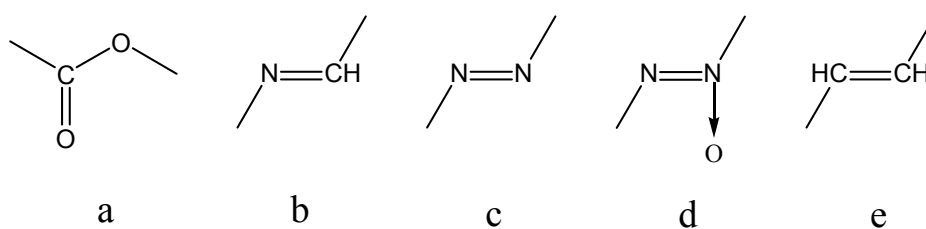


Fig. 2.11 Examples for connecting groups in bent-shaped molecules: a) carboxylic b) azomethine c) azo d) azoxy e) ethylene linking groups

Additionally there are some instances of linking the aromatic rings with thiocarbonyl connection [51] or extensive acroyloxy group [52].

Connecting groups exert a powerful effect on the mesophase behavior: they establish the flexibility and influence the polarity of the molecules.

The electron withdrawing or donating effect of the connecting groups determines the electron density and so the partial polarity of the aromatic rings. Obviously, the direction of a non-symmetric linking group between two aromatic rings does matter. Some symmetric five-ring bent-shaped compounds with varied (in direction and/or chemical class) linking groups were compared [53]. Mesomorphic properties were observed in the case where the donor or acceptor nature of the four linking groups leads to an alternate sequence of positive and negative charges on the five benzene rings according to molecular modeling and electrostatic potential map computation (Fig. 2.12).

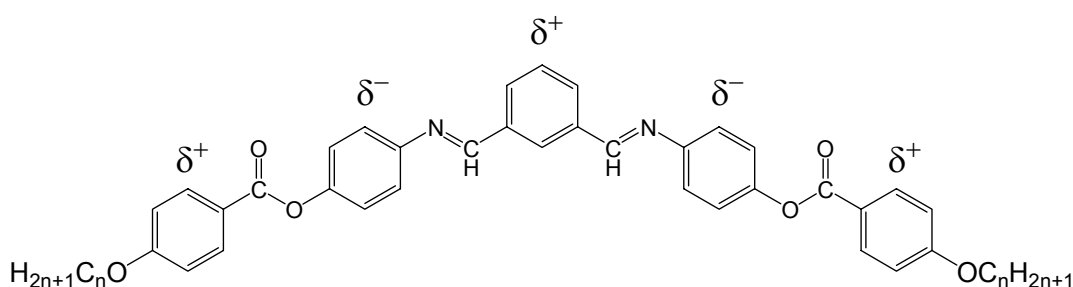


Fig. 2.12 Alternating partial charges on a five-ring bent-core molecule

In the meantime, some linking groups (e.g. azomethine, ethylene) together with the aromatic rings establish an extensive conjugated system, whereas ester group is not a completely conjugated unit. The role of conjugation in banana molecules, however, has not been cleared up yet. Furthermore free rotation around the single bond of the ester linking group is possible (with consideration of spatial hindrance and electrostatic repulsion, attraction), while the double bond in imino, ethylene, etc group hinders rotation. In other words, segments of bent-shaped molecules with ester linking group may have more kinds of rotational arrangement than with imino connecting group. Regarding bent-shaped molecules where $X=X'=-O-CO-$ rotation around this bond may strongly influence the bending angle itself [40]. Additionally polarized FT-IR measurements of 1,3-phenylene-bis[4-(4-decylphenyliminomethyl)benzoate] in SmCP (B_2) phase indicate that the ester groups are twisted with respect to the central phenyl ring, and on average only one of the possible twisted conformations exists in B_2 phase what could result in molecular chirality [54]. So far, many points of conformation in bent molecules remains open to question.

The most successful bent-core mesogenic materials exhibiting several (switchable) mesophases contain the sensitive azomethine group: it is thermally instable and sensitive to proton and metal surfaces. Some Schiff bases decompose above around 150°C, while others are stable even above 200°C. Hence, the thermal instability is dependent on the structure of the molecule. Moreover, only compounds containing azomethine linking groups e.g. 2-methyl-1,3-phenylene bis[4-(4-n-alkyloxyiminomethyl)benzoate] exhibit polymorphism like SmCP-B₅ [55]. As we shall see later, even richer polymorphism was found in a laterally substituted derivative of this compound (chapter 3) [56].

Shen et al. reported about bent-shaped mesogens containing central unit derived from 1,3-phenylene ring so that there is no connecting group between the central ring and one of the middle rings [57, 58, 59, 60] (Fig. 2.13). Biphenyl derivatives exhibit either a wide range SmCP_A (B₂) phase or a rectangular columnar phase designated as Col_r or B₁.

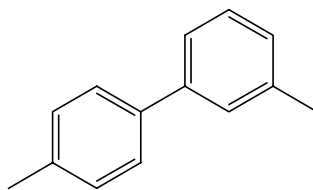


Fig. 2.13 3,4'-Disubstituted-biphenyl core

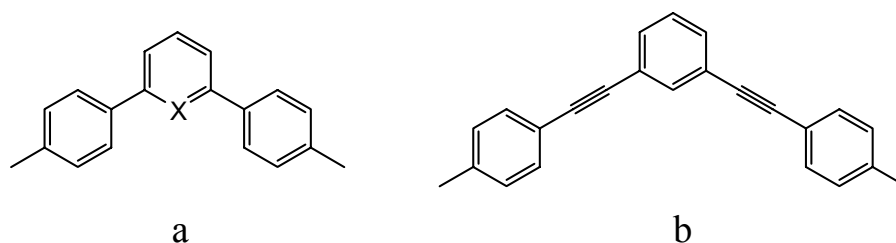


Fig. 2.14 a) *m*-Terphenyl (X=H) and 2,6-diphenylpyridine (X=N) central units, b) tolane central core

They gave an account about compounds without any connecting group between the central and middle rings: 2,6-diphenylpyridine and *m*-terphenyl derivatives [48, 58] (Fig.

2.14a) were synthesized. In the same work they also reported about tolane derivatives (Fig. 2.14b). Actually, only 2,6-diphenylpyridine derivatives exhibited liquid crystalline (B_1 , B_x , B_{x1}) phase.

2.3.3 Lateral substitution

In case of lateral substitution three major factors are involved: the size (spatial contribution) and the polarity namely inter- and intramolecular forces of attraction, repulsion of the substituents, and the position of the substitution. These factors influence molecular conformation. Molecular conformation effects on molecular packing and vice versa. Consequently, lateral substitution has an impact on the liquid crystalline state, i.e. on the liquid crystalline phase stability. It is not easy to predict the influence of lateral substitution on bent-shaped molecules: the above-discussed structural factors and the lateral substituents not independently influence the liquid crystalline behavior. Systematic study of banana substance classes one by one, may advance understanding on this subject.

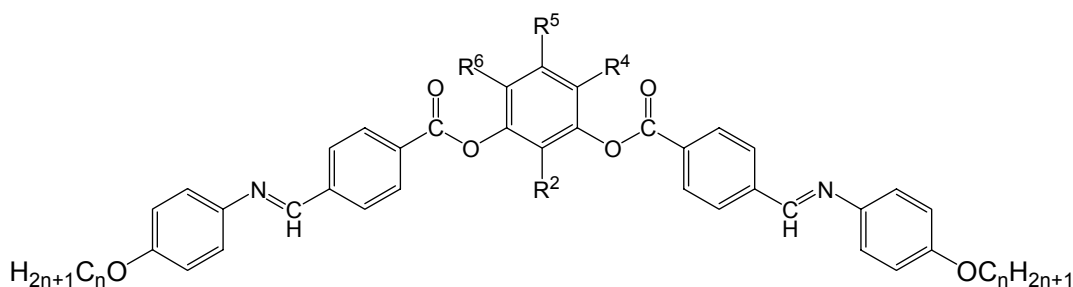


Fig. 2.15 General formula of substituted 1,3-phenylene bis[4-(4-n-alkoxyphenyliminomethyl)benzoate]

On the way to investigate the influence of lateral substitution of bent-core substances, several new banana mesophases were discovered [2]. In this work among others, the results obtained by investigating substituted resorcinol derivatives (Fig. 2.15) are summarized. Some of them exhibited new, up to that time not known mesophases: B_5 and B_7 . Moreover, B_5 turned out to be switchable. On top of that, the 2-methyl-resorcinol derivative bent mesogen exhibited both, SmCP (B_2) and B_5 , switchable mesophases. These are the main conclusions to which detailed investigation of mesogenic five-ring resorcinol bananas led:

- substitution of the central core strongly effects on the liquid crystalline properties: voluminous substituents like ethyl- ($-\text{C}_2\text{H}_5$), acetyl- ($-\text{COCH}_3$), hexyl- ($-\text{C}_6\text{H}_{13}$) groups adversely (no mesophase), small substituents like methyl- ($-\text{CH}_3$), nitro- (NO_2), chloro- (Cl), cyano- (CN) groups depending on the position of the substituent positively influence them,
- substitution in position R^5 results in non-mesogenic compounds, independently of the class of substituents. The only exception ($\text{R}^5=\text{F}$) found will be described in this work (Chapter 3) [61]. Another exception was found in perfluorinated terminal chain containing bananas, but for a different substance class [62],
- in the case when $\text{R}^2=\text{NO}_2$ a new mesophase, called B_7 , with very unusual texture was discovered [30, 63],
- in the case when $\text{R}^2=\text{CH}_3$ a new mesophase (B_5) and a first a banana polymorphism ($\text{SmCP}(\text{B}_2)\text{-B}_5$) were observed [26],
- 4,6-dichlororesorcinol derivative bananas exhibit SmA and SmC mesophases, owing to the stretched (rather rod-like) conformation of the molecules [40, 64],
- a later study of 4-cyanoresorcinol derivatives ($\text{R}^4=\text{CN}$) [65] reported about SmCP-SmC-SmA polymorphism, in the case of $\text{R}^4=\text{Cl}$ switchable $\text{SmCP}(\text{B}_2)$ phase was found [64, 66, 67, 68] as well as in the homologue serie of the resorcinol derivative. The 4-chlororesorcinol bananas have lower melting and clearing points, while the resorcinol bananas exhibit some additional crystalline, B_3 and B_4 phases. The temperature ranges of the mesophases are in the same order of magnitude.

Substitution of the central ring of bent-shaped molecules turned out to be a fruitful field in liquid crystal research, and so several research groups have been working on this area [28, 49, 70, 50, 69, 71, 72, 73]. Recently, another 5-methylresorcinol derivative, 5-methyl-1,3-phenylene bis(alkoxycinnamoyloxy)benzoate was declared to exhibit banana mesophase (B_6 and crystalline B_3) [28]. Although, this is the only substance class where the 5-substituted resorcinol derivatives show more favorable phase behavior than the 2-substituted resorcinol compounds.

2.3.4 The terminal chains

The molecular organization of bent-shaped molecules depends on the balance of electrostatic interactions developed by the polar segment of the molecule and the van der Waals interactions established by the terminal chains. The most often occurring terminal chains are alkyl- and alkoxy chains [e.g. 2]. As it has already appeared in several above-mentioned examples, the mesophase character of bananas is exposed to the influence of the length of the alkyl/alkoxy chain. Namely, short-chain homologues of otherwise chemically equivalent bent-shaped molecules exhibit B₁, long-chain homologues SmCP (B₂) mesophase [74, 75]. There are few examples for banana molecules with alkyloxycarbonyl [76] and alkenyloxy terminal chains [69, 77]. By comparison, replacing alkyloxy chains with unsaturated alkenyl chains decreases the clearing points by 10-20°C.

Heppke et al. synthesized bent-core compounds with terminal alkylthio chains [45]. The substances exhibit crystalline B₃ and a high-temperature switchable phase. They found that the transition temperatures fall down replacing alkyloxy with alkylthio terminal chains.

Walba et al. prepared a racemic asymmetric bent-core compound with achiral alkyloxy and chiral alkyloxycarbonyl chain [78]. By means of polarization microscopy and electro-optical measurements on freely suspended films with differing layers they observed a ferroelectric mesophase.

Dantlgraber et al. synthesized asymmetric bent-core mesogens with a dodecyloxy chain and a bulky oligosiloxane unit connected through a flexible alkyloxy chain to the outer ring [60]. The compounds exhibit switchable SmCP mesophase. X-ray investigations proved that each moiety (aromatic cores, aliphatic chains, oligosiloxane units) is organized into sublayers. Furthermore, they found that the mesophase stability is nearly independent of the size of the siloxane unit.

Bent-shaped materials were synthesized even with perfluoroalkyloxy terminal chains [62, 79]. They possess the individual property exhibiting (banana) mesophase despite the voluminous methyloxycarbonyl substituent on the top of the central ring (R⁵= -COOCH₃). The rigid perfluoroalkyloxy chains often intercalate. Additionally, it might drive on separation of the perfluoroalkyloxy chains from the aliphatic and aro-

matic parts of the molecules. It results in increased mesophase stability. Unfortunately, the transition temperatures are strongly elevated, and so the mesophase behavior cannot always be completely characterized. Decreasing the number of aromatic rings to three in bent-shaped molecules or introduction of substituents may reduce the transition temperature of bent-core materials with perfluoroalkoxy chains, however they exhibit only conventional smectic phases [80, 81].

2.4 Objectives

Rich variety of banana phases was discovered by introducing lateral substituent(s) on the central ring [2]. It was found that these substituents bring about changes in the bending angle α thereby influencing the mesophase behavior and characteristics of the mesogens.

Lateral substitution has an essential influence on the sterical and electrical characteristic and thereby on the intermolecular distance. Consequently, it can generate mesophase characteristics different from the related non-substituted mesogens.

Up to the beginning of this work no bent-core molecules with lateral substituents on the outer as well as central rings had been presented. There had not been any information about the effect of such lateral substitutions on the phase behavior of the substances. Therefore substitution on the outer rings of central-ring substituted bent-shaped molecules has attracted our interest. At first we turn our attention to the small but strongly electronegative fluorine substituent. Since it has the highest electronegativity among the chemical elements it always brings strong dipole moment in corresponding positions of the molecule. Would it affect in altering spontaneous polarization values of bananas either? Furthermore, do lateral substituents on the outer rings bring about changes in the bending angle α as substituents on the central ring do?

NMR measurements can develop our understanding about these questions and even more in connection with structure-property relationships of these bent-core mesogens. They can provide additional information (molecular conformation – bending angle, torsion angles, longitudinal and transversal order parameter) if the molecules contain heteronucleides or isotopes different from ^1H and ^{13}C .

Thus, fluorinated and/or deuterated five-ring bent-core mesogens have been synthesized for two reasons:

- to study the influence of lateral fluoro-substituents on mesophase behavior
- to make it possible to apply not only ^1H and ^{13}C , but also ^2H and ^{19}F NMR techniques for the investigation of bent-core mesogens in liquid crystalline state.

There had been found some evidence that the direction of the connecting groups in bent-core compounds influences the phase behavior [2]. Therefore, isomers of the first banana 1,3-phenylene bis[4-(4-n-alkyloxyphenyliminomethyl)benzoates] have been

synthesized. How lateral substitution of these substances influences the mesophase character?

Besides, the effect of several kinds of terminal chains on the mesophase properties of isophthalydene bis[4-(4-subst.-phenyloxycarbonyl)anilines] has been studied.

Chapter 3 Substituted resorcinol derivatives

In the first part of this chapter there is a description of the synthetic work led to substituted resorcinol (1,3-dihydroxybenzene) derivative bent-shaped molecules fluorinated on the outer rings in different positions. In the second part, there is a description of the mesophase behavior of these compounds. Additionally, the intermediate two-ring calamitic materials are introduced.

The electro-optical and X-ray measurements were made in the work team of Professor Gerhard Pelzl (Martin-Luther-University Halle-Wittenberg, Germany) on the following instruments:

- the electro-optical measurements were performed with the help of LEICA DMRXP polarizing microscope equipped with METTLER-TOLEDO FP900 heating stage (Switzerland).
- the X-ray measurements were made on Guinier goniometer (Huber Diffractionstechnik GmbH, Cu-K α line) and either with a camera or with a 2D detector (HI-Star, Siemens AG) recorded.

The dielectric measurements were carried out in the work team of Professor Horst Kresse (Martin-Luther-University Halle-Wittenberg, Germany): the samples were put into a two-plate condensator and the signals were recorded by Hewlett Packard (HP 4192) impedance analyzer.

The NMR investigations were performed in the work team of Professor Siegbert Grande (University Leipzig, Germany) on Bruker MSL 500 spectrometer.

3.1 Synthetic work

The resorcinol derivatives were synthesized according to the following strategy (Fig 3.1):

1. Nucleophilic substitution of the commercially available 2- or 3-fluoro-4-nitrophenol was done to obtain 4-n-alkyloxy-3-fluoronitrobenzene (**1**) and 4-n-alkyloxy-2-fluoro-nitrobenzene (**2**) (hereafter abbreviated as 2/3-fluoro...). Mitsunobu reaction (n-alkanol/PPh₃/DEAD in tetrahydrofuran, room temperature) [82] produced higher yield in some cases than the considerably cheaper modified

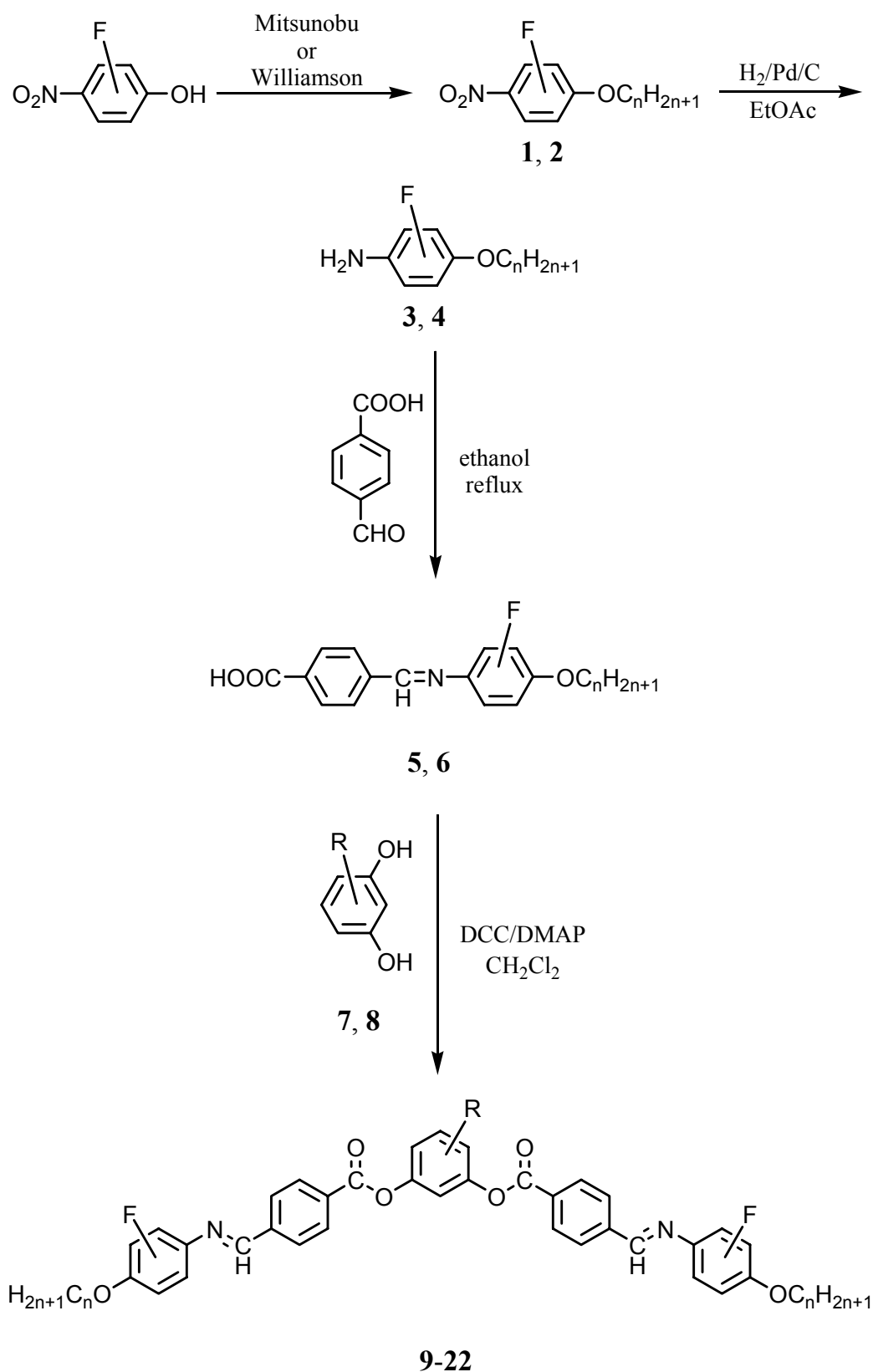


Fig. 3.1 General scheme of the synthesis of resorcinol derivative bent-shaped compounds. R=H (**9, 10**), R²=NO₂ (**11, 12**), CH₃ (**13, 14**), R⁴=CN (**15, 16**), Cl (**17, 18**), R⁴=R⁶=Cl (**19, 20**), R⁵=F (**21, 22**).

Williamson etherification (n-alkylbromide/ K_2CO_3 /KI in acetone or DMF under reflux) [83]. The reaction after Mitsunobu takes shorter time (2 days vs. 1 week), but the purification is more time-consuming in this case (removing $O=PPh_3$ derived from PPh_3 requires column chromatography). The difference in yield is not significant if the Williamson etherification is carried out in DMF under reflux (61% in Mitsunobu reaction vs. 53% in Williamson reaction for 2-fluoro-4-n-octyloxy-nitrobenzene). Note that 2-fluoro-4-nitrophenol becomes 4-n-alkyloxy-3-fluoro-nitrobenzene and 3-fluoro-4-nitrophenol turns into 4-n-alkyloxy-2-fluoro-nitrobenzene.

2. Nitro group reduction was carried out with hydrogen in ethylacetate with Pd catalyst. The resulting compounds are 4-n-alkyloxy-3-fluoro-anilines (**3**) and 4-n-alkyloxy-2-fluoro-anilines (**4**).
3. The anilines were led into condensation reaction with 4-formylbenzoic acid in ethanol under reflux. The resulting Schiff bases – 4-(4-n-alkyloxy-3-fluorophenyliminomethyl)benzoic acids (**5**) and 4-(4-n-alkyloxy-2-fluorophenyliminomethyl)benzoic acids (**6**) – exhibit mesomorphism.
4. 5-Fluoro-resorcinol (**7a**) and 5-chloro-resorcinol (**7b**) are not commercially available. They were prepared by cleavage of the corresponding 3,5-dimethoxyhalobenzenes with BBr_3 in dichloromethane (Fig. 3.2) [84, 85].

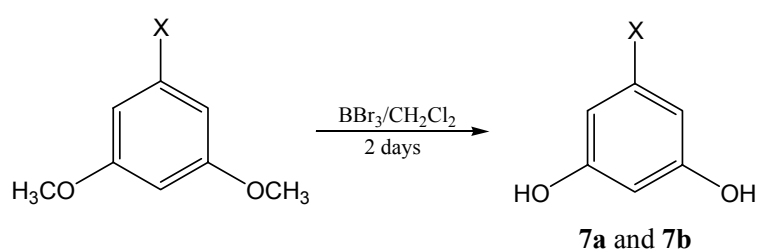


Fig. 3.2 Synthesis of 5-halogenoresorcinol, X=F, Cl

4-cyanoresorcinol was available in the laboratory of the work team. Partially deuterated resorcinol and 2-methylresorcinol were prepared in the laboratory of Katalin Fodor-Csorba (Research Institute for Solid State Physics and Optics of the Hungarian Academy of Sciences, Budapest, Hungary).

There were several attempts to synthesize 4-fluoro and 4,6-difluororesorcinols using Selectfluor as fluorinating agent [85]. Since the first attempt had not been successful, the reaction circumstances were changed. The proportion of the reagents, the solvent, the reaction time and temperature had been varied. GC-MS investigations pointed out that always mixture of mono-, di- and even trifluorinated resorcinols were obtained. Fluorination of 2-methylresorcinol with Selectfluor was not successful either.

Some attempted synthesis were done to get 2-cyanoresorcinol from 2,6-dihydroxy-benzaldehyde and 2,6-dihydroxybenzamide. Reddy et al. could obtain this substance from 2,6-dimethoxybenzotrile under extreme reaction circumstances: they hydrolyzed the diether by borontribromide at high temperature [73].

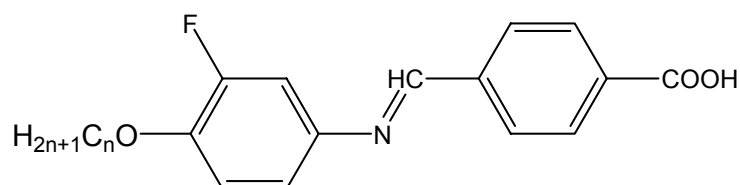
5. Reaction between (substituted) resorcinols (resorcinol **8a**, 2-nitroresorcinol **8b**, 2-methylresorcinol **8c**, 4-cyanoresorcinol **8d**, 4-chlororesorcinol **8e**, 4,6-dichlororesorcinol **8f**) and the 4-(4-n-alkyloxy-3-fluoro-phenyliminomethyl) benzoic acids (**5**) or the 4-(4-n-alkyloxy-2-fluoro-phenyliminomethyl)benzoic acids (**6**) in presence of N,N'-dicyclohexylcarbodiimide (DCC) and 4-dimethylaminopyridine (DMAP) catalyst [87, 88] produced the bent-shaped compounds (**9-23**).

3.2 Two-ring substances

3.2.1 4-(4-n-Alkyloxy-3-fluoro-phenyliminomethyl)benzoic acids (5)

On the way to synthesize new bent-shaped compounds rod-like mesogens (**5**, **6**) were prepared, too.

All mesogens exhibit SmC and a low-temperature SmX phase (Fig. 3.3). Preliminary X-ray studies point to a new higher ordered smectic phase. The transition temperatures marginally change with increasing chain length. The transition temperatures and transition enthalpy values are shown in Table 3.1. In Fig. 3.4 the tendency of decreasing transition temperatures is illustrated.



Sign.	n	Cr	SmX	SmC	I
5.1	8	• 147	• 181	• 261	•
		[19.7]	[5.4]	[16.3]	
5.2	9	• 133	• 176	• 255	•
		[18.2]	[5.5]	[15.4]	
5.3	10	• 112	• 175	• 254	•
		[18.4]	[5.4]	[15.5]	
5.4	11	• 116	• 171	• 251	•
		[20.4]	[5.0]	[14.7]	
5.5	12	• 114	• 169	• 246	•
		[22.6]	[5.5]	[17.3]	

Table 3.1 Transition temperatures (°C) and transition enthalpy values [kJ/mol] of 4-(4-n-alkyloxy-3-fluorophenyliminomethyl)benzoic acids (**5.1-5.5**)

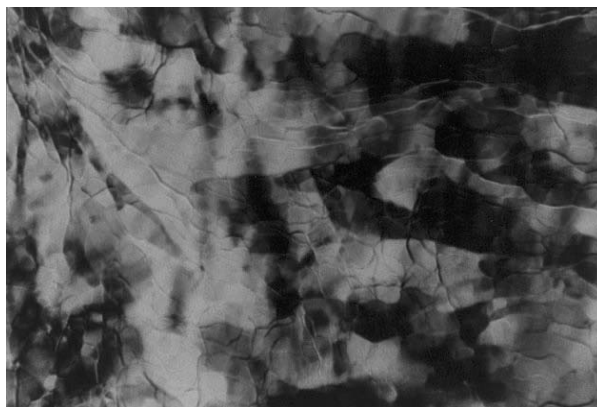


Fig. 3.3 The low-temperature SmX phase of compound 5.2 at 124°C

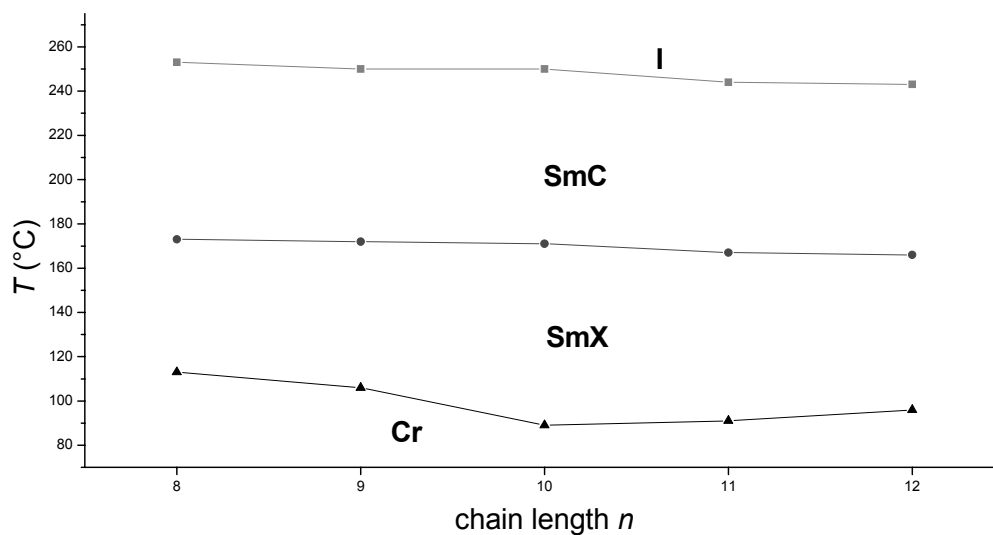
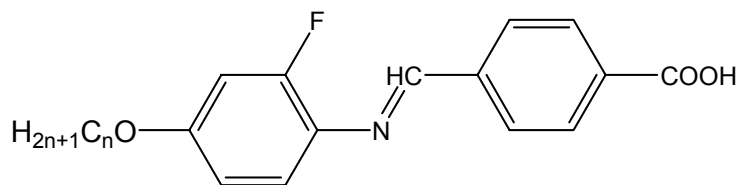


Fig. 3.4 Phase behavior of 4-(4-n-alkyloxy-3-fluoro-phenyliminomethyl)benzoic acids (5.1-5.5)

3.2.2 4-(4-n-Alkyloxy-2-fluoro-phenyliminomethyl)benzoic acids (6.1 and 6.2)

These compounds exhibit nematic and smectic C mesophases. The difference is minimal between the clearing points of the two homologues. The melting points significantly decrease with lengthening the terminal chains (Table 3.2).



Sign.	n	Cr	SmC	N	I
6.1	8	• 192 [16.3]	• 239 [3.6]	• 253 [6.3]	•
6.2	12	• 165 [15.3]	• 237 [16.2]	-	•

Table 3.2 Transition temperatures (°C) and transition enthalpy values [kJ/mol] of the 4-(4-n-alkoxy-2-fluoro-phenyliminomethyl)benzoic acids (**6.1** and **6.2**)

Comparing the phase behavior of the non-fluorinated [40] and the fluorinated mesogens the following conclusions could be drawn (Table 3.3):

- the 4-(4-n-alkoxy-phenyliminomethyl)benzoic acids as well as the **6.1** and **6.2** exhibit smectic C and/or nematic mesophases. Compounds **5.1-5.5** exhibit two smectic mesophases.
- fluorination slightly decreases the clearing points (8-20°C),
- melting points hardly change if fluorine is introduced into position 2 (**6.1** and **6.2**), while significantly decreased if the compound is fluorinated in position 3 (**5.1-5.5**).

Sign.	n	Phase behavior
[40]	8	Cr 190 SmC 255 N 261 I
5.1	8	Cr 147 SmX 181 SmC 261 I
6.1	8	Cr 192 SmC 239 N 253 I
[40]	12	Cr 155 SmC 255 I
5.5	12	Cr 114 SmX 169 SmC 246 I
6.2	12	Cr 165 N 237 I

Table 3.3 Comparison of fluorinated and non-fluorinated 4-(4-n-alkoxy-phenyliminomethyl)benzoic acids

Introduction of fluoro-substituent next to the position of the terminal chain positively influence width of the phase range. Furthermore a new mesophase (SmX) appeared. Fluoro substitution next to the position of the azomethine connection does not remarkably effect on the transition temperatures and the phase behavior.

3.3 Bent-shaped compounds derived from resorcinol and substituted resorcinols

In this chapter resorcinol-derivative compounds substituted or non-substituted on the central ring and fluorinated on the outer rings will be described. The chapter is divided in sections according to the chemical structure of the central ring, the consequence of the discussion follows the position of the substitution on the central ring, e.g. the first section is about the non-substituted resorcinol derivatives, the second about the 2-nitroresorcinol derivative, the last section is about the 5-fluororesorcinol derivative banana compounds. You will find an account of several novelties concerning the phase behavior of these substances:

- the first mesogens (**9**) probably exhibit SmC_G phase (Section 3.3.1),
- the first bent-shaped compounds (**15**) with biaxial SmA (SmAP or C_{PA}) phase (Section 3.3.4),
- some examples of exceptionally rich polymorphism of switchable banana mesophases (Section 3.3.3 polymorphic SmCP (**13**) and Section 3.3.7 polymorphic B₅ phases (**21**)),
- the first issue (**18.1**) about SmCP phase formed on cooling the nematic phase (Section 3.3.5).

3.3.1 Resorcinol derivatives without substitution on the central ring (**9, 10**)

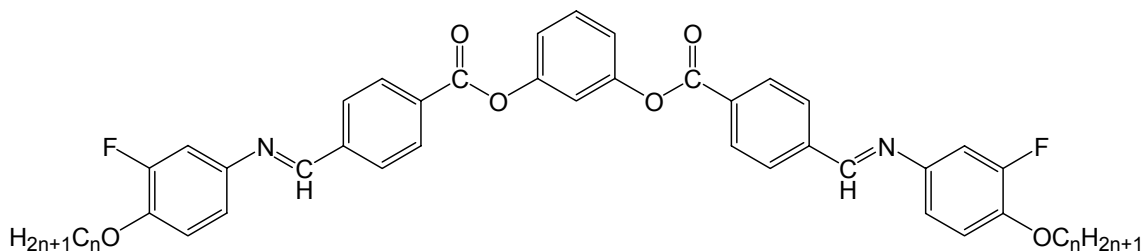
3.3.1.1 1,3-Phenylene bis[4-(4-n-alkyloxy-3-fluoro-phenyliminomethyl)benzoates] (**9**)

In this section liquid crystalline materials exhibiting B₄, SmCP and most probably SmC_G phase will be introduced [20]. All mesophases were experimentally proved.

Phase behavior (DSC)

As it is shown in Table 3.4 three mesophases appear on cooling. The SmC_G - SmCP transition is not detectable with DSC. The B₄ soft-crystalline phase appears on the first cooling, and does not crystallize in reasonably long time. The melting and clearing points hardly, the transition temperatures slightly decrease with the length of

the terminal chains (Fig. 3.5). The shorter the terminal chains the wider SmCP and shorter SmC_G phase ranges exist.



Sign.	n	Cr	B ₄ ^a	SmCP	SmC _G	I
9.1 [§]	8	• 129 [40.6]	(• 98) [26.0]	• 164*	• 166 [20.5]	•
9.2	9	• 123 [39.8]	(• 101) [32.7]	• 153*	• 163 [20.7]	•
9.3 [§]	10	• 123 [44.7]	(• 99) [29.2]	• 147*	• 163 [23.1]	•
9.4	11	• 121 [44.5]	(• 98) [38.6]	• 141*	• 162 [22.3]	•
9.5	12	• 120 [49.8]	(• 98) [50.4]	• 132*	• 160 [22.5]	•

^a the B₄ phase can be supercooled up to room temperature, the inverse transition B₄ → SmCP takes place about 10-12°C above this temperature

* not detectable with DSC, [§] [89], [§] [90]

Table 3.4 Transition temperature (°C) and enthalpy values [kJ/mol] of substances **9.1-9.5** according to the DSC measurements

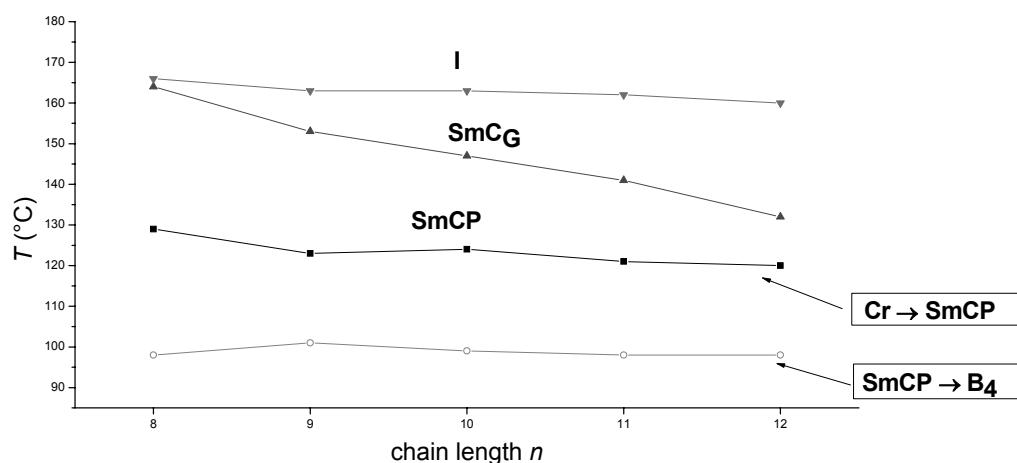


Fig. 3.5 Transition temperatures vs. chain length for compounds 9.1-9.5

X-ray studies

Sign.	Molecular length L (Å)	Spacing $d \pm 0.5$ (Å)	Tilt angle (deg)
9.1	45.3	38.5	31.3
9.2	47.5	40.5	31.4
9.3	49.5	41.8	32.5
9.4	51.6	43.5	32.6
9.5	54.4	45.5	33.2

Table 3.5 Molecular lengths, temperature-independent layer spacings and tilt angles found in compounds 9.1-9.5

XRD measurements performed on powder sample produced the outcome as follows:

- the layer spacing d is temperature independent, it does not change either during the SmC_G-SmCP or during the SmCP-B₄ transition (Table 3.5),
- the layer spacing linearly depends on the length of the terminal chain,
- from the proportion of the layer spacing to the effective molecular length (L) the tilt of the molecules within the layer is estimated about 32°,

- the correlation length ξ determined from the full width at half maximum of the small angle X-ray reflection is temperature independent in the SmC_G phase, while it continuously increases at the transition to the SmCP phase and abruptly decreases at the SmCP-B₄ transition.

XRD measurements on surface-oriented sample

In the SmC_G phase four reflections occur in the small angle region (Fig. 3.6). They originate from differently oriented domains where the smectic layers are parallel and perpendicular to the substrate surface. The longer chained homologues (9.5) prefer orienting perpendicular, while the short chain homologue (9.1) parallel to the substrate surface. For compound 9.2 the probability is equal for growing in both directions.

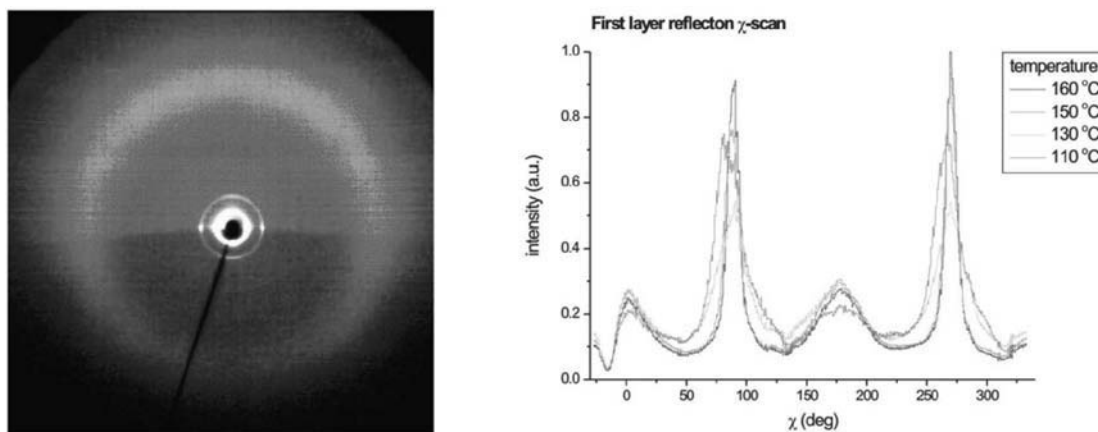


Fig. 3.6 X-ray pattern of the surface oriented sample for compound 9.5

The maxima in the wide-angle region have been found to be out of the equator, what means the molecules are tilted with respect to the layer normal. The estimated tilt angle about 33 degrees is in good agreement with the values obtained from the diffuse scattering measurements. The SmC_G phase is a smectic phase without in-plane order formed by tilted molecules. Orientation completely disappears in the B₄ phase.

Electro-optical investigations and texture observations

Cooling the sample quickly from the isotropic phase non-specific grainy texture appears, while at slow cooling rate colored and gray ribbon-like growing domains as well as screw-like and telephone-wire filaments have been observed (Fig. 3.7).

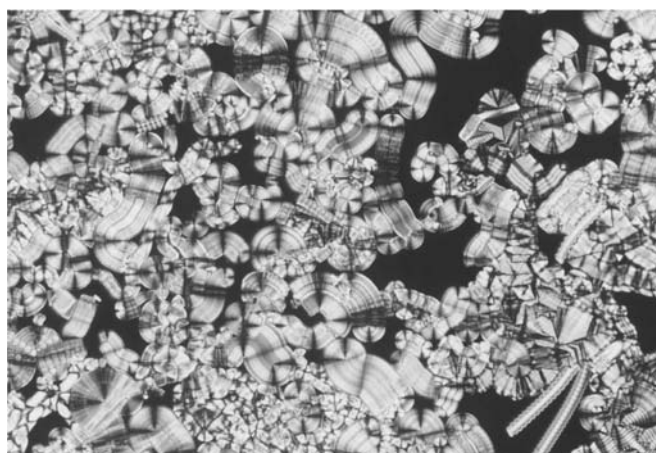


Fig. 3.7 Formation of SmC_G phase on cooling the compound 9.2

When the growing domains are surrounded with isotropic liquids application of electric field affects on the texture. Depending on the polarity of the field the grey ribbons grow or shrink. Exposing the ribbons to an electric field they coil into spirals formed clockwise or anticlockwise depending on the polarity of the field. The behavior of the ribbons in electric field tallies with the observations given by A. Jáklí et al. in favor of SmC_G phase [29]. The screw-like filaments coil, moreover grow as flat nuclei in case of long-time exposure even grow as flat nuclei in electric field (Fig. 3.8). When the texture covers the whole view-field of the microscope electric field does not markedly effect on the texture. On further cooling the fan-shaped texture changes into a grainy one, it indicates a phase transition. In this low-temperature phase the field-induced texture is independent from the polarity of the field.

On cooling the SmC_G phase the chiral domains remain unchanged at the transition into the SmCP and B₄ phases. In the B₄ phase the texture shows nearly extinction between the crossed polarizers and the contrast between the domains of opposite handedness is less pronounced. These domains neither change upon a reversed transition on

heating from the B₄ phase. Only the formation of the SmCP phase from the B₄ phase is delayed, taking place at about 10 degrees higher temperature. Similar hysteresis behavior will be reported in chapter 5 [91].

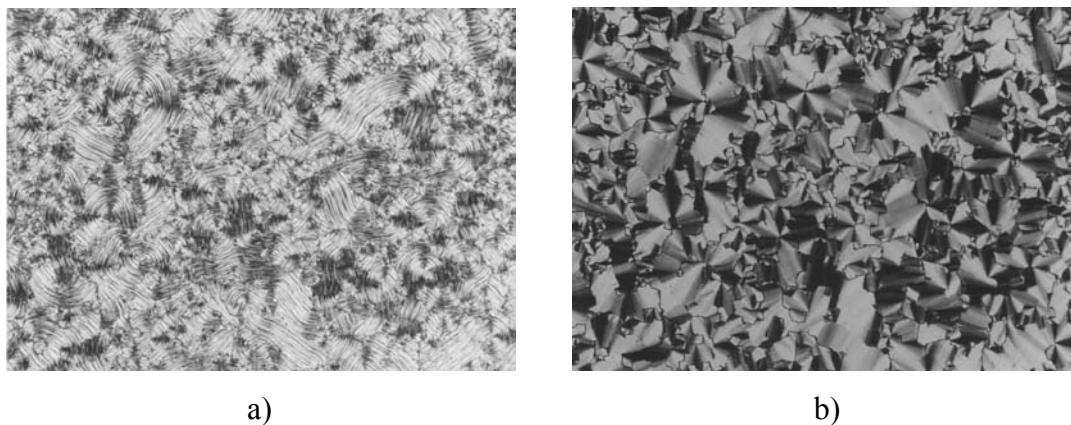


Fig. 3.8 Microscopic texture of SmCP phase of the compound **9.3** at 133°C a) $E=0 \text{ V}\mu\text{m}^{-1}$ b) $E= \pm 20 \text{ V}\mu\text{m}^{-1}$

Depending on the experimental conditions (cooling rate; surface treatment) different behavior have been observed. During the nucleation of the SmC_G phase one-dimensionally growing screw-like domains as well as large chiral domains grow simultaneously (Fig. 3.9). The screw-like domains further transform into a grainy texture, whereas the large chiral domains remain unchanged.

The high temperature SmC_G phase is not switchable: the strong sterical hindrance inhibits turning of the leaning molecules in the smectic plane. The low temperature phase is an antiferroelectric mesophase with synclincic symmetry, i.e. SmC_SP_A mesophase. Unexpectedly, the spontaneous polarization shows pronounced odd-even effect in spite of the long terminal chains.

As it has already been mentioned in section 2.2 the molecules in the SmCP phase can adjust four kinds of structures: AFE anticlinic and synclincic (SmC_AP_A, SmC_SP_A), FE anticlinic and synclincic (SmC_AP_F, SmC_SP_F) [25, 92]. The two states AFE and FE are separated by a small energy barrier. In most instances the energy of the AFE state is somewhat lower than one of the FE state resulting in the AFE ground state either synclincic or anticlinic. Application of an electric field leads to the transition from the AFE into FE state. The chirality of the layers is mainly conserved (observed transitions are SmC_AP_A → SmC_SP_F and SmC_SP_A → SmC_AP_F). Recent Fourier transform infrared

spectroscopic measurements also indicated a motion of the long molecular axis on the cone as in the SmC* phase [93].



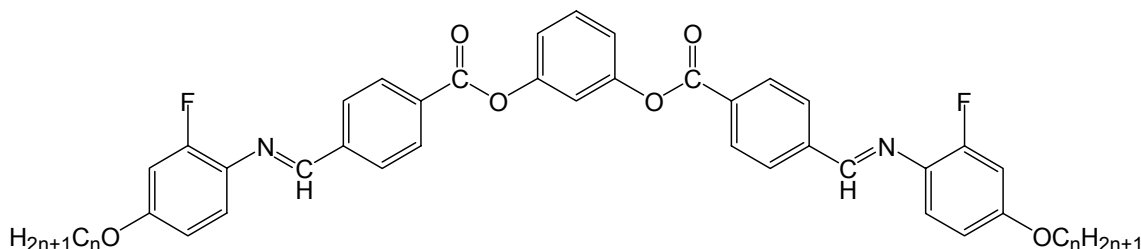
Fig. 3.9 Nucleation of SmC_G phase in compound 9.5

A detailed investigation of the switching in the SmCP phase is reported in the ref. [94]. They observed that the appearance of the synclinic or anticlinic ground state can also be influenced by the shape of the oscillating external field. However, the SmC_SP_A ground state has lower energy. Dielectric spectroscopy measurements separately performed on racemic and homochiral samples showed quite different properties of the domains. In the racemic state the switching is about twice as fast as in chiral state. The dielectric strength $\Delta\epsilon$, however, is about twice as high in the chiral state. Further analysis of the effects of the chiral and racemic domains in the SmCP phase has been reported by L.M. Blinov et al. [95] on the base of the analysis of the fine structure of the current response peaks.

3.3.1.2 1,3-Phenylene bis[4-(4-n-alkyloxy-2-fluoro-phenyliminomethyl)benzoates] (10.1 and 10.2)

These compounds exhibit switchable SmCP mesophase. Since there is a tiny change in the clearing point and a slight decrease in the melting point with chain-

lengthening the mesophase range is wider in the dodecyloxy (**10.2**) homologue (Table 3.6).



Sign.	n	Cr	SmCP	I
10.1	8	•	127 [38.9]	•
10.2	12	•	117 [42.6]	•

Table 3.6 Transition temperature (°C) and enthalpy values [kJ/mol] of compounds **10.1** and **10.2** according to the DSC measurements

The mesophase appears with Schlieren and non-specific grainy texture. At the freezing point this texture freezes and becomes glassy. NMR measurements pointed out that in **10.1** the bending angle between the two wings is about 118-120 deg, what means that the molecule is really bent. The order parameter S is around 0.82 corresponding to S values found in banana mesophases in earlier studies [2].

Comparing the phase behavior of fluorinated (**9.1-9.5**, **10.1** and **10.2**) and non-fluorinated* [1, 33] resorcinol derivatives:

- fluorination decreases the melting points, in case of compounds **9.1-9.5** they are slightly changed, whilst in **10.1** and **10.2** there is a significant difference between them,
- the clearing points change similarly to the melting points,
- all three kinds of bananas exhibit enantiotropic SmCP mesophase. The mesophase range is wider in the fluorinated substances.
- a new mesophase SmC_G appears in **9.1-9.5**,

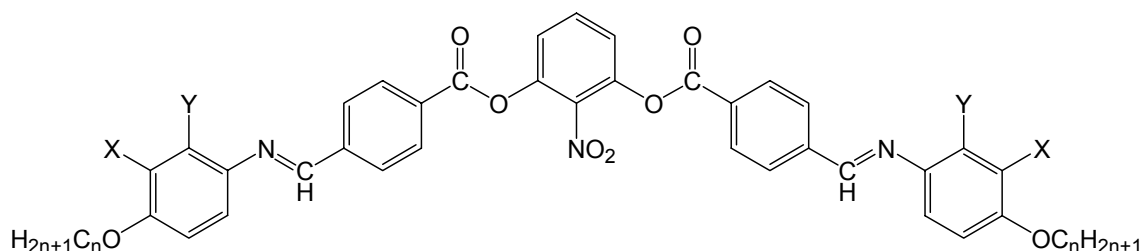
- in **10.1** and **10.2** crystalline banana phases (B_3 , B_4) disappear.

* The non-fluorinated substances, 1,3-phenylene bis[4-(4-n-alkyloxyphenyliminomethyl)benzoates] display the following phase behavior [1, 33]: if $n=8$ B_4 139 B_3 152 B_2 174 I and if $n=12$ B_4 141 B_2 170 I.

3.3.2 2-Nitroresorcinol derivatives (11, 12)

All fluorinated bananas derived from 2-nitroresorcinol derivatives exhibit the exotic B₇ mesophase [61] (Table 3.7) as well as the non-fluorinated compounds [30]. This phase appears with two-dimensional patterns indicating a helical superstructure. However, neither substance could be oriented, therefore detailed characterization of B₇ phase is one of the most challenging tasks of the future.

Dielectric measurements point to a crystalline-like monotropic low-temperature phase in compound **11.1** [96]. The mesophase B₇ does not crystallize anymore after the first heating of **11.1**.



Sign.	X	Y	n	Cr	B _x	B ₇	I
11.1*	F	H	8	• (142 [#])	•	147 [3.8]	• 169 [26.2]
11.2	F	H	12	•	-	148 [3.2]	• 167 [25.5]
12.1	H	F	8	• 81 [38.6]	-	• 157 [29.3]	•
12.2	H	F	12	• 88 [10.0]	-	• 156 [30.0]	•

* for compound **11.1** data are given on cooling

this transition is not detectable on DSC

Table 3.7 Transition temperature (°C) and enthalpy values [kJ/mol] according to the DSC measurements

Comparison of compounds **11** and **12** and non-fluorinated 2-nitroresorcinol derivatives* [30] points to the following conclusions:

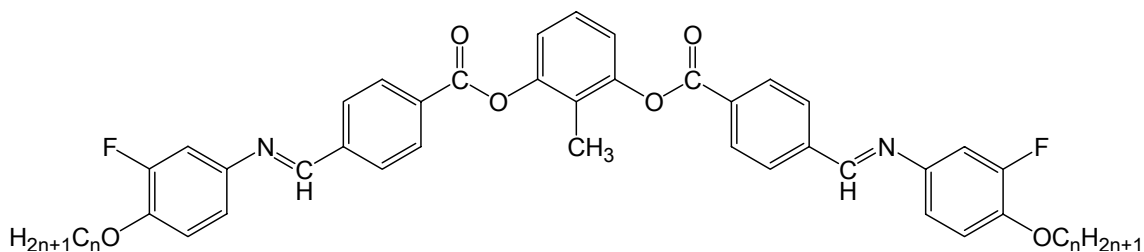
- all compounds exhibit B₇ mesophase,
- the melting point decreases by about 60°C if fluoro-substituent is introduced in position 3, while fluoro-substitution in position 2 hardly changes it,
- the clearing point decreases by about 10°C in **11.1** and **11.2**, and 20°C in **12.1** and **12.2**. Since characterization of B₇ phase is in an early state compounds with sunk transition temperatures might be good candidates for extensive studies.
- dielectric measurements suggest that the octyloxy homologue of the non-fluorinated substance and **11.1** have a low temperature B_x phase.

* The non-fluorinated mesogens, 2-nitro-1,3-phenylene bis[4-(4-n-alkyloxyphenyliminomethyl) benzoates] have the following phase behavior [30]: n=8 X=Y=H Cr 87 B_x 129 B₇ 177 I and if n=12 X=Y=H Cr 85 B₇ 173 I.

3.3.3 2-Methylresorcinol derivatives

3.3.3.1 2-Methyl-1,3-phenylene bis[4-(4-n-alkoxy-3-fluorophenyliminomethyl)benzoates] (13)

In this section substances with polymorphic switchable banana mesophases (SmCP, B₅, B_x) will be introduced. The octyloxy homologue (n=8) was thoroughly researched [56], even its deuterated analogue was synthesized to enable extensive NMR investigations never have been carried out before.

Phase behavior (DSC)

Sign.	n	Cr	B _x	B ₅	B ₂ ''	B ₂ '	B ₂	I
13.1	8	• 103	• 112	• 136	• 142	• 147	• 153	•
		[11.4]	[0.5]	[0.4]	[0.04]	[*]	[18.1]	
13.2	9	• 99	110	• 127	• 133	•	150	•
		[10.4]	[0.5]	[0.3]	[0.06]		[16.1]	
13.3	10	• 97	108	• 121	• 127	•	151	•
		[11.4]	[0.6]		[1.2]~		[19.7]	
13.4	11	• 94	109	• 120	• 124	•	151	•
		[15]	[0.7]		[1.5]		[21.0]	
13.5	12	• 92	106	• 115	• 119	•	149.5	•
		[17.2]	[0.6]		[1.9]~		[21.0]	

* this transition not seen on DSC

~ sum of ΔH at B₂''-B₂' and B₂-B₅ transitions

Table 3.8 Transition temperature (°C) and enthalpy values [kJ/mol] of **13.1-13.5** on cooling provided by DSC measurements

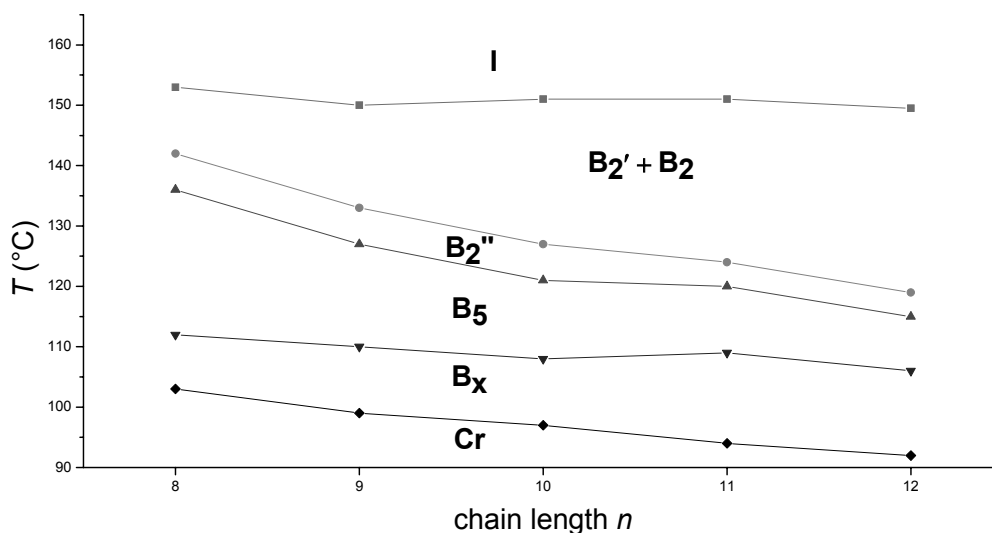


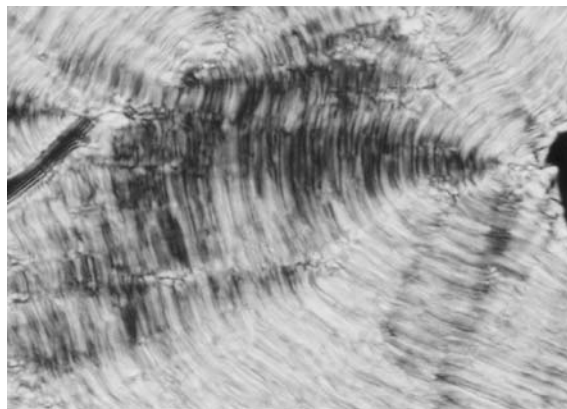
Fig. 3.10 The phase behavior of substances 13.1-13.5

These substances exhibit very rich variety of mesophases. The long chain homologues were not fully investigated, so the phase assignment is a preliminary. Neither polarization microscopy nor DSC measurements can provide information about the B_2 - B_2' transition of compound 14.1. At the same time the B_2' - B_2'' transition is detectable with both techniques. Therefore the existence of B_2' mesophase in compounds 13.2-13.5 could be determined preliminary. The B_x phase is not identical with the B_x phase mentioned in section 3.3.2. As you can see on Fig. 3.10 the clearing point hardly, the melting point slightly decreases with increasing terminal chain length. The longer terminal chain the wider SmCP and B_x and the narrower B_5 phase ranges were found.

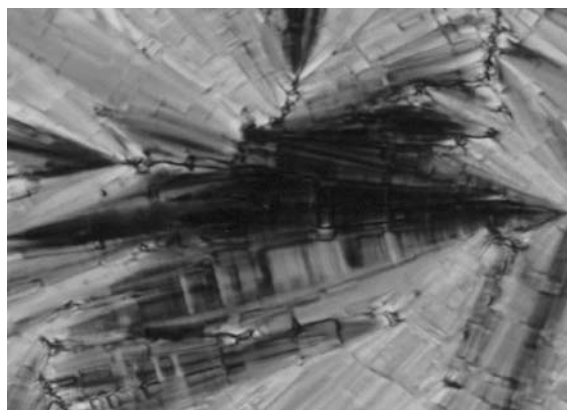
Polarizing microscopy and electro-optical measurements

These observations were made on compound 13.1. The B_2 phase appears on cooling of the isotropic liquid exhibiting a grainy or fan-shaped texture (Fig. 3.11a). There is no texture change at the transitions $B_2 \rightarrow B_2'$, whereas at the transition $B_2' \rightarrow B_2''$ paramorphic smooth fan-shaped textures appears (Fig. 3.11b). There is a minor change in the texture at the transition into the B_5 phase: a small change of the birefringence and the formation of irregular stripes perpendicular to the fans have been ob-

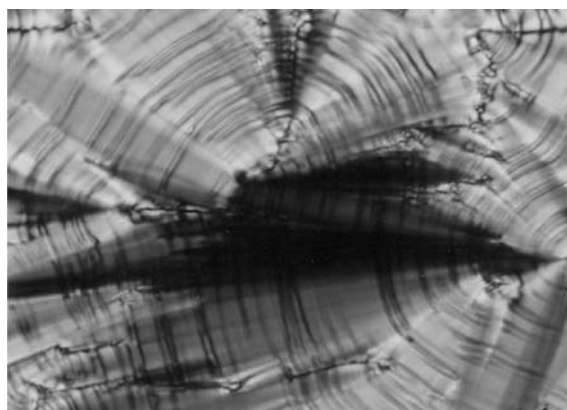
served (Fig. 3.11c). The transition into the low-temperature phase B_X could not be seen by polarizing microscopy.



a)



b)



c)

Fig. 3.11 Optical textures of compound **13.1** at 148°C B_2 phase (a), 140°C B_2' phase (b) and at 130°C B_5 phase (c)

All four phases showed similar electro-optical responses to the applied d.c. electric field. The initial fan-shaped texture transformed into a smooth SmA-like fan-shaped texture at the field higher than a threshold 0.5 - 0.8 V/ μm for the mesophases B_2 , B_2' , B_2'' and B_5 (Fig. 3.12 and 3.13). The textures relaxed into their initial state when the external field was removed (at $E = 0$).

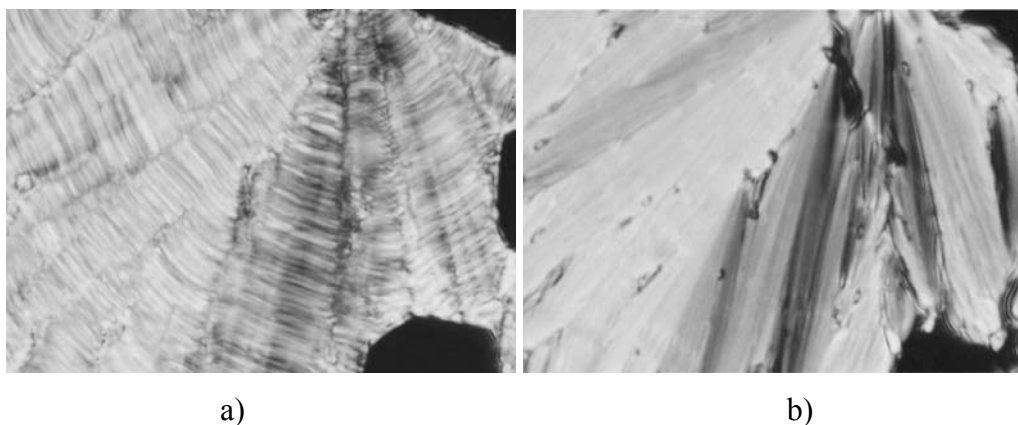


Fig. 3.12 Field induced texture change of the B_2' phase at 143°C a) field-off state b) $E = \pm 2.8 \text{ V}\mu\text{m}^{-1}$

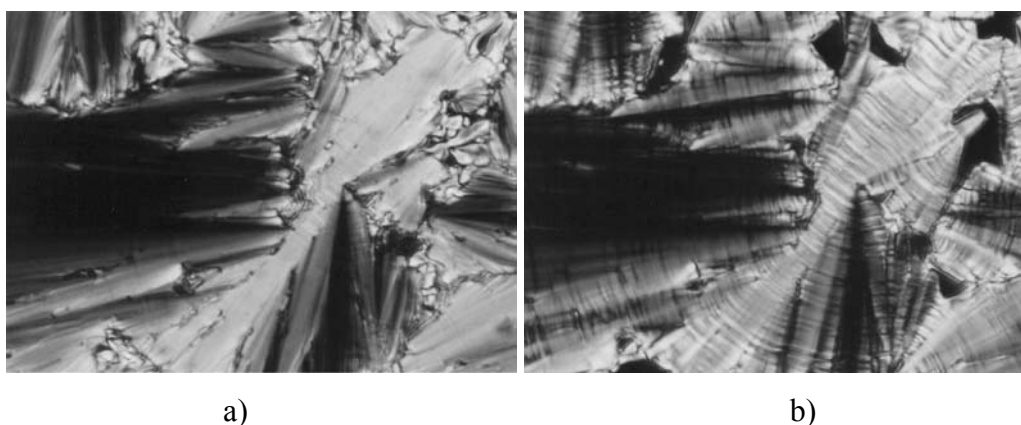


Fig. 3.13 Field induced texture change of the B_5 phase at 132°C a) field-off state b) $E = \pm 4.8 \text{ V}\mu\text{m}^{-1}$

The spontaneous polarization is temperature dependent, its maximum value is 800 nCcm⁻². At the transition into the low-temperature phase B_X the threshold significantly increases. The relaxation from the polarized state into the ground state is quite

slow, probably due to high viscosity of the sample; otherwise the switching behavior is quite similar to that of the B₅ phase.

X-ray measurements

The patterns of oriented samples provide important details about the mesophases. The high temperature phase exhibits a pattern without in-plane order, typical for SmCP: the layer reflections are observed on the meridian of the pattern; the maxima of the broad outer diffuse scattering are situated out of the equator indicating an inclination of the molecules and the absence of the long-range positional order within the layers. From the χ -scan the tilt angle of about 25 deg has been derived. On cooling the sample into the B₂' phase the meridian reflections reproducibly split up into pairs. This splitting corresponds to an angle \sim 6 deg between the layer normal and the fiber axis. This additional tilt is too small to be detected from the wide-angle diffuse outer scattering. However, this change conforms to alterations in the NMR spectra. The split peaks merge again on the meridian at the transition into the B₂'' phase at 142°C. Below 135 °C the scattering diagram shows formation of a two-dimensional rectangular cell within the layers on a short-range scale characteristic of B₅ phase [26]. The pattern of the B_X phase indicates the positional correlation of the molecules in adjacent layers. The phase is assumed as a three-dimensional crystalline one with large amount of disorder. Furthermore an in-plane organization of the molecules described by an orthorhombic cell can be inferred. The pattern also hints at more complex structure could not have been proved yet. The next change of the X-ray pattern takes place below $T \cong 102$ °C to a true crystalline phase.

Dielectric measurements

The phase transition B₂'/B₂'' could be interpreted with the help of dielectric spectroscopy: the decrease of the parameters Δ_2 and τ_2 at the B₂'/B₂'' transition may indicate that in the B₂'' phase the interaction of the dipoles is reduced with respect to that in the B₂' phase. The detected high strength Δ_2 is in the same order of magnitude as in case of B₂ modifications and indicates a strong positive dipole correlation in the B₅ as well as in

the B_2 phase. The decrease of Δ_2 at the B_5/B_X transition may be connected either with a complete disappearance or a stepwise decrease of the relaxation frequency of some decades (phase transition into a highly ordered solid-like B phase).

NMR studies

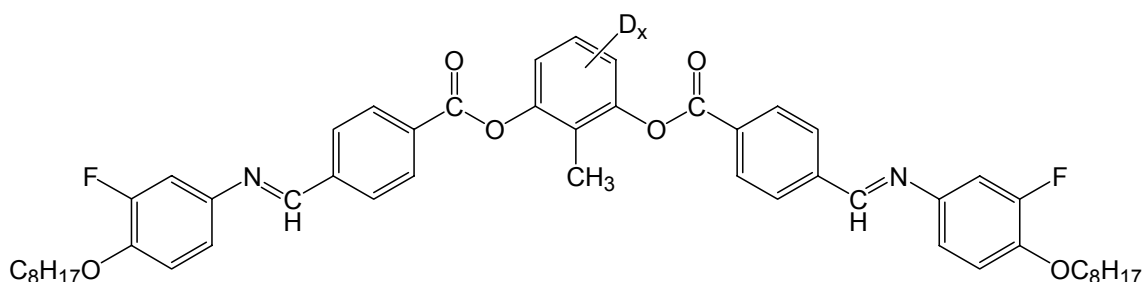


Fig. 3.13 Compound **13.1d**: bent-core molecule deuterated on the central ring

NMR measurements were made on the compound **13.1** and deuterated **13.1** (**13.1d**, see Fig. 3.13). There is no difference between the phase behavior of **13.1** and **13.1d**. Partial substitution by deuterium enables finding both the longitudinal (S) and the transversal (D) order parameters. The order parameter S in the high-temperature B_2 phase was obtained using both $^1\text{H-NMR}$ and $^2\text{H-NMR}$ techniques under the assumption that the molecules are oriented parallel to the magnetic field. Three regions can be distinguished in the temperature interval of the B_2 -like phases ($152\text{ }^\circ\text{C} - 136\text{ }^\circ\text{C}$) (Fig. 3.14). The first interval between the clearing point and $\sim 145\text{ }^\circ\text{C}$ where the splitting is almost independent of the temperature, then the splitting experiences a jump and again a small plateau up to $142\text{ }^\circ\text{C}$. This region we designate as the B_2' phase. The transition into the B_2'' phase is accompanied by a small latent heat detected on the DSC curve. The proton splitting is monotonically increasing with decreasing temperature and at $136\text{ }^\circ\text{C}$ it reaches saturation upon the transition into the B_5 phase. The calculated value of D in high-temperature range is very small: $D < 0.01$. Therefore at lower temperatures D was assumed to be negligibly small, and only S was calculated from the splitting of ^2H .

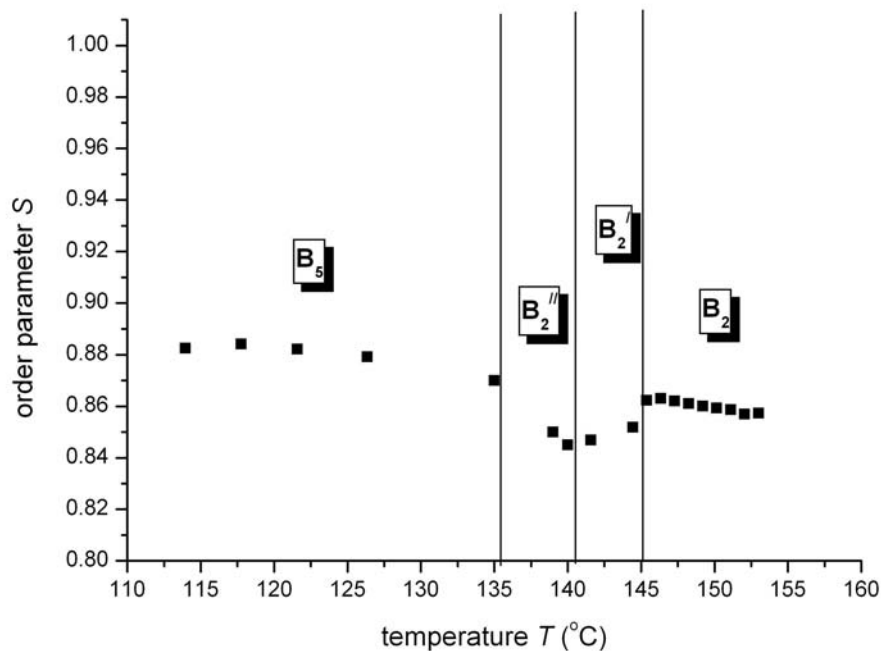
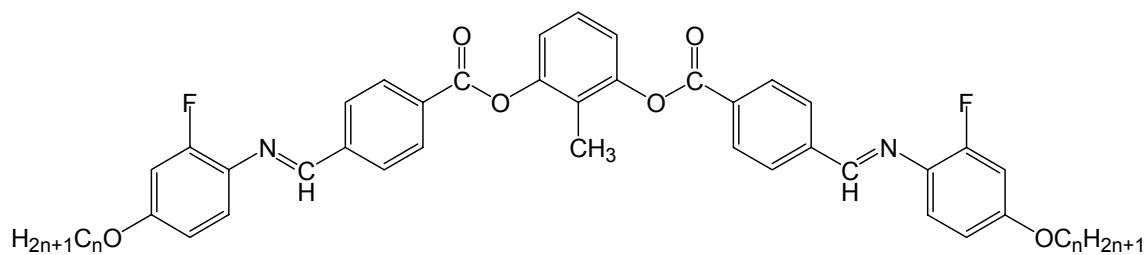


Fig. 3.14 Order parameter of compound **13.1d** obtained from NMR measurements

The long-chain homologues ($n=9-12$) show similar phase behavior under polarizing microscope and according to the DSC studies as **13.1**. XRD measurements are necessary to provide unambiguous information, though.

3.3.3.2 2-Methyl-1,3-phenylene bis[4-(4- n -alkoxy-2-fluoro-phenyliminomethyl) benzoates] (**14.1** and **14.2**)

The compounds **14.1** and **14.2** were preliminary studied by polarizing microscopy and electro-optics. These substances have lost polymorphism owing to fluorination in position 2 on the outer rings. Fluorination in this position influenced the phase behavior so unfavorably that the short-chain homologue exhibits only a monotropic non-switchable B_1 mesophase. Terminal chain lengthening, as usual, led to the appearance of B_2 phase. However, B_2 - B_5 polymorphism does not show up either.



Sign.	n	Cr	B ₁	B ₂	I
14.1	8	• 135 [33.2]	(• 131) [15.8]	-	•
14.2	12	• 125 [21.0]	-	• 135 [20.6]	•

Table 3.9 Transition temperature (°C) and enthalpy [kJ/mol] values of compounds **14.1** and **14.2**

Comparing the non-fluorinated mesogens* [26] and **13.1-13.5** and **14.1**, **14.2** the following points can be raised:

- fluorination considerably changes the phase behavior in the case of 2-methylresorcinol derivatives,
- the short-chain (n=8) homologue of the non-fluorinated compound exhibit B₂ and B₅, the dodecyloxy homologue B₂ mesophases,
- in compounds **13.1-13.5** unique polymorphism of switchable mesophases appears,
- in compounds **14.1** and **14.2** only the dodecyloxy homologue exhibits switchable B₂ mesophase,
- additionally, fluorination in both positions considerably decreases the melting points,
- the clearing points fall due to fluorination.

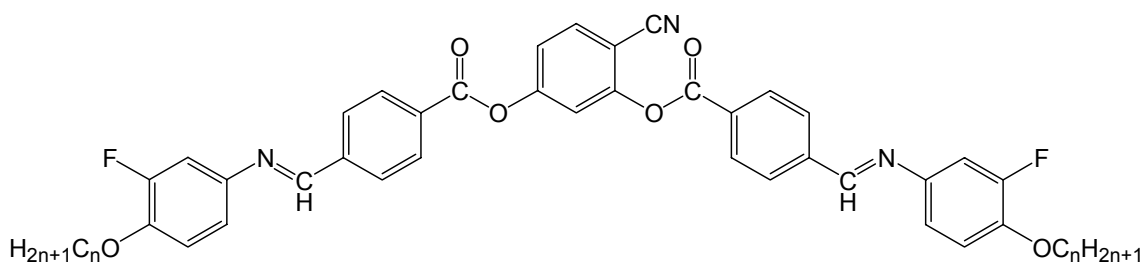
* The 2-methyl-1,3-phenylene bis[4-(4-n-alkoxyphenyliminomethyl)benzoates], the non-fluorinated mesogens, have the following phase behavior [26]: if n=8 Cr 161 B₅ 165 B₂ 172 I and if n=12 Cr 148 B₂ 164 I.

3.3.4 4-Cyanoresorcinol derivatives

In this section you will read about materials exhibiting SmAP (C_{PA}) – an orthogonal, but switchable – mesophase. Brand et al. [16, 97] predicted this kind of phase behavior of bent-shaped mesogens. These are the first substances where the existence of SmAP was found and could be proved [22].

3.3.4.1 4-Cyano-1,3-phenylene bis[4-(4-n-alkoxy-3-fluoro-phenyliminomethyl)benzoates] (15)

These substances exhibit a high-temperature SmA and a low-temperature SmAP switchable mesophase. Both mesophases are enantiotropic and appear independently of the chain length.



Sign.	n	Cr	SmAP	SmA	I
15.1	8	• 73	• 145	• 180	•
		[74.6]	[1.2]	[16.7]	
15.2	9	• 78	• 143	• 180	•
		[30.8]	[0.4]	[8.1]	
15.3	10	• 81	• 140	• 183	•
		[33.7]	[0.7]	[8.2]	
15.4	11	• 72	• 137	• 184	•
		[20.5]	[0.6]	[8.1]	
15.5	12	• 75	• 133	• 182	•
		[18.2]	[0.7]	[8.1]	

Table 3.10 Transition temperature ($^{\circ}\text{C}$) and enthalpy [kJ/mol] values of compounds 15.1-15.5.

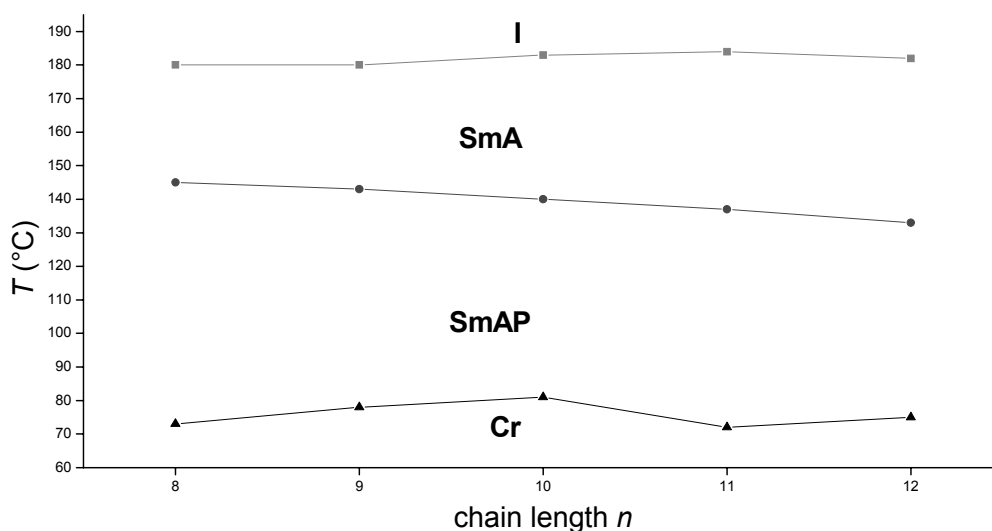


Fig. 3.15 The phase behavior of substances 15.1-15.5

As you can see in Fig. 3.15 the clearing and melting points marginally deviate from a value. The transition temperature of the phase transition SmAP-SmA slightly decreases with increasing chain length what means that the SmA phase range becomes wider with chain-lengthening, the change is not considerably, though. The compound **15.1** was investigated in details, and will be introduced in the following.

Polarizing microscopy and electro-optical measurements

Both mesophases can be observed by polarizing microscopy. SmA phase appears with fan-shaped or homeotropic texture as usual. The SmAP phase shows up with a subtle change in the fan-shaped texture: irregular fine stripes parallel to the smectic layers appear (Fig. 3.16). The homeotropic texture, at the same time, turns into a strongly fluctuating schlieren one. At further cooling the fluctuation in the schlieren texture disappears, in the meantime it becomes more birefringent.

The SmA phase is not switchable. Applying electric field to the fan-shaped texture of SmAP phase the stripes disappear. Meanwhile, the birefringence has been changing. At lower temperatures the switching becomes slower and happens within

seconds. The current response proves the antiferroelectric nature of this phase. The polarization is unusually high in the SmAP phase: its value reaches 1000 nCcm^{-2} .

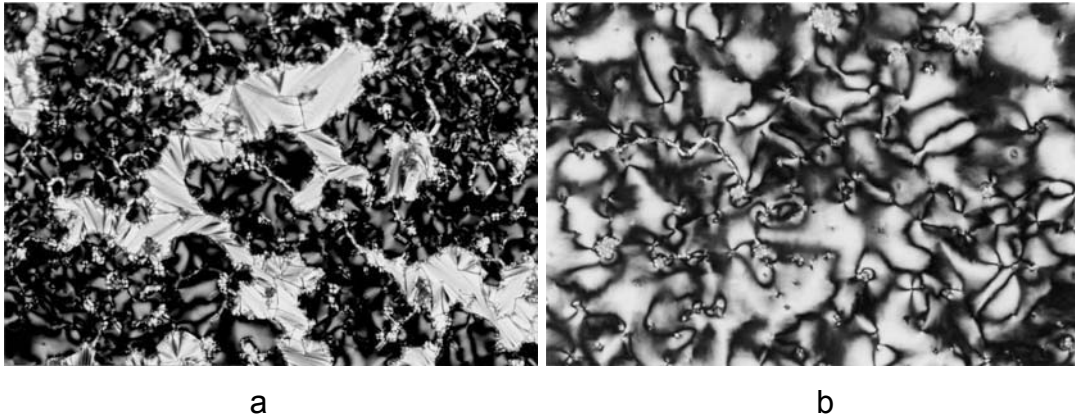


Fig. 3.16 Fan-shaped (a) and schlieren texture (b) of the SmAP phase

X-ray measurements

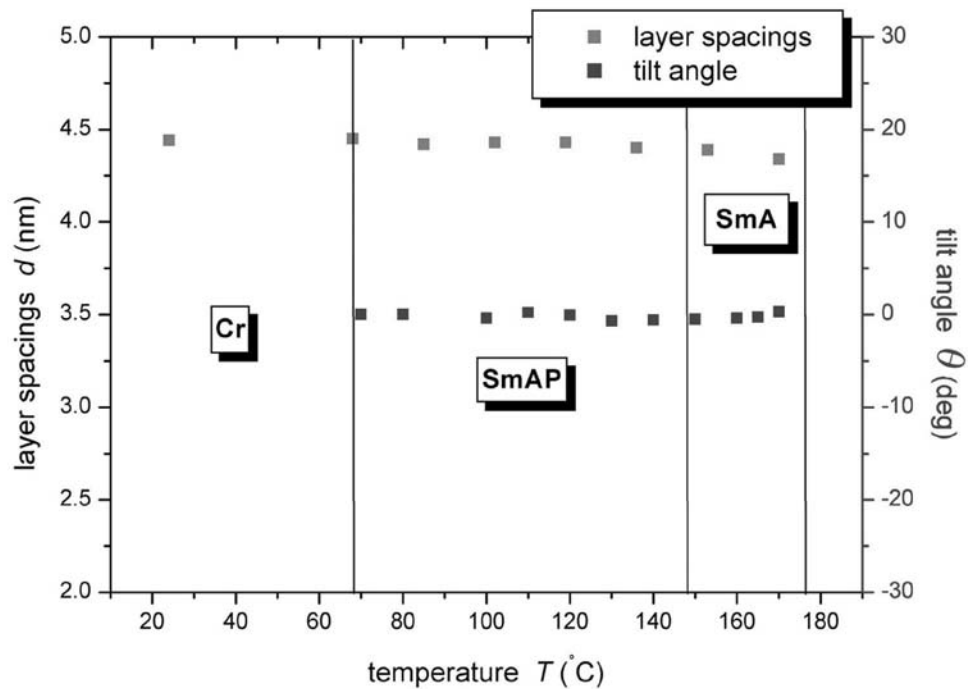


Fig. 3.17 Temperature dependence of the layer spacing d and the tilt angle θ [17]

The X-ray diffraction pattern exhibits an outer diffuse scattering, the maxima of which are clearly positioned on the equator, also in the phase below the SmA phase. No

change in the patterns appears down to 45 °C, where the layer reflections become more crescent-like and the outer diffuse scattering splits into a few peaks resulting from the appearance of an in-plane order. It is clearly seen that these wide-angle reflections still remain diffuse. The derived tilt angle obtained from the analysis of the diffuse outer scattering as well as the layer spacing versus temperature is illustrated in Fig. 3.17.

NMR measurements

Since the molecule is substituted in position 4 on the central ring, the long axis is different from the symmetry axis of a non-substituted molecule. It could be proved from the anisotropic shift of the CN carbon that the deviation is around 5 degrees. The order parameter was derived from the shift anisotropy of the central ring protons and carbons. The dependence of the order parameter is shown in Fig. 3.18. The bending angle α was found to be around 142 degrees in the SmA, and 132 degrees in the SmAP phase.

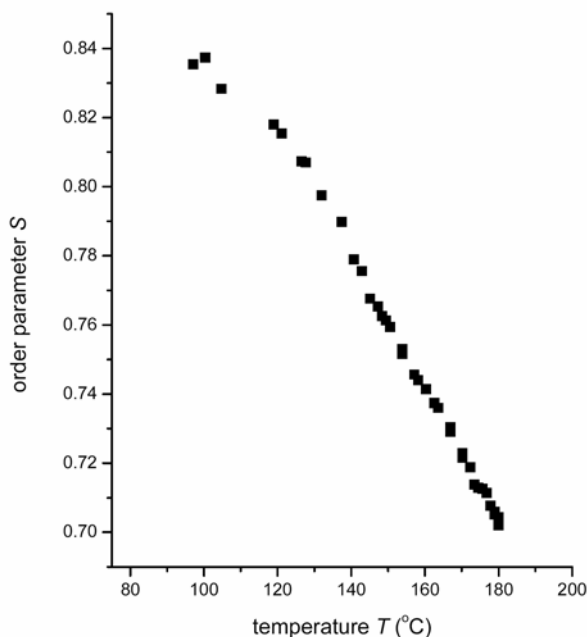
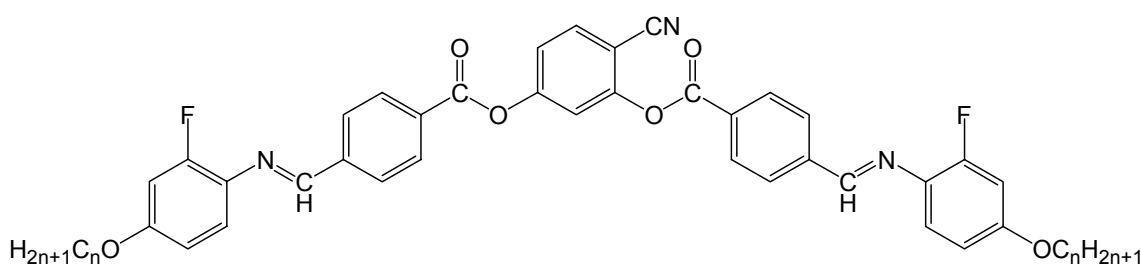


Fig. 3.18 The temperature dependence of the order parameter in compound **15.1** [17]

3.3.4.2 4-Cyano-1,3-phenylene bis[4-(4-n-alkoxy-2-fluoro-phenyliminomethyl) benzoates] (**16**)

These compounds exhibit high-temperature nematic and/or SmA and low-temperature SmCP mesophases. The mesophase behavior was observed only by polarizing microscopy. The grainy texture of the low-temperature phase gives a hint that it is a SmCP and not only a SmC phase. Preliminary electro-optical studies have shown that the low-temperature mesophase is switchable.



Sign.	n	Cr	SmCP	SmA	N	I
16.1	8	• 93 [27.7]	• 99 [2.9]	• 102 #	• 129 [0.8]	•
16.2	12	• 94 [38.5]	• 125 [3.0]	• 142 [0.4]	-	•

not observable on DSC

Table 3.11 Transition temperature (°C) and enthalpy [kJ/mol] values of compounds **16.1** and **16.2**

Comparing the non-fluorinated* [65] and both series of fluorinated 4-cyanoresorcinol derivatives (**15.1-15.5**, **16.1** and **16.2**) the following conclusions can be drawn:

- the clearing point decreases in substances **16.1** and **16.2**, does not change considerably in compounds **15.1-15.5**,
- the difference between the melting points (m. p.) of the octyloxy and the dodecyloxy derivatives do not change more than 2°C in the case of the fluorinated

materials (**15.1-15.5**, **16.1**, **16.2**), while the m. p. of the non-fluorinated dodecyloxy derivative is 32°C below the m. p. of the short-chain (n=8) homologue,

- each compound exhibits SmA, **16.1** an additional nematic phase. It enhances the chance to orient the low-temperature SmCP phase in weak magnetic field.
- each compound exhibits switchable mesophase: in compounds **15.1-15.5** SmAP phase appears, whilst the other substances exhibit SmCP phase,
- the switchable mesophase range is very wide (45-73°C) except for the compounds **16.1** where it takes only 2°C and compound **16.2** where it is moderately wide (31°C),
- all in all fluorination on the outer ring in position 2 (**16.1** and **16.2**) unfavorably influences the phase behavior, while in position 3 (**15.1-15.5**) considerably changes the structure of the switchable mesophase. It converts tilted SmCP into orthogonal SmAP mesophase.

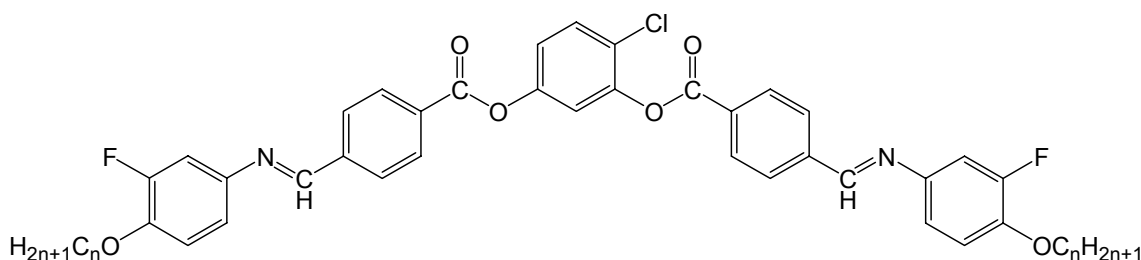
* The phase behavior of the 4-cyano-1,3-phenylene bis[4-(4-n-alkyloxyphenyliminomethyl)benzoates], the non-fluorinated compounds [65]: n=8 Cr 97 SmCP 142 SmC 146 SmA 175 I and if n=12 Cr 65 SmCP 122 SmC 141 SmA 188 I.

3.3.5 4-Chlororesorcinol derivatives

In this section you will read about compounds exhibiting SmCP (B_2) mesophase. There are few examples when this mesophase appears on cooling conventional smectic mesophases (SmC or SmA) [64]. Here you can find the first instance of SmCP emerging from nematic phase.

3.3.5.1 4-Chloro-1,3-phenylene bis[4-(4-*n*-alkoxy-3-fluorophenyliminomethyl)benzoates] (17)*Phase behavior (DSC)*

The short-chain homologue **17.1** exhibit SmCP, the long-chain homologue ($n=12$) SmCP and an additional SmA high-temperature mesophase. It is a rare phenomenon that the long-chain homologue exhibits an additional less-ordered high-temperature mesophase. The melting point marginally decreases, the clearing point subtly increases with chain-lengthening. The SmCP phase exists in wide range, while the SmA phase has six-degree-temperature range. Electro-optical and XRD studies were carried out on the substance **17.1**. The results will be introduced in the following.



Sign.	n	Cr	SmCP	SmA	I
17.1	8	• 90 [14.1]	• 133 [11.0]	-	•
17.2	12	• 82 [16.4]	• 133 [3.6]	• 139 [7.1]	•

Table 3.12 Transition temperature ($^{\circ}\text{C}$) and enthalpy [kJ/mol] values of compounds **17.1** and **17.2**

Texture observations and electro-optical measurements

On cooling the isotropic liquid, the SmCP phase appears with grainy fan-shaped texture. Applying electric field stripes parallel to the smectic layers appear. In this phase the field induced texture is independent of the polarity of the field. The switching polarization does not show any temperature dependence. Applying sufficiently high triangular voltage antiferroelectric switching could be observed (Fig. 3.19).

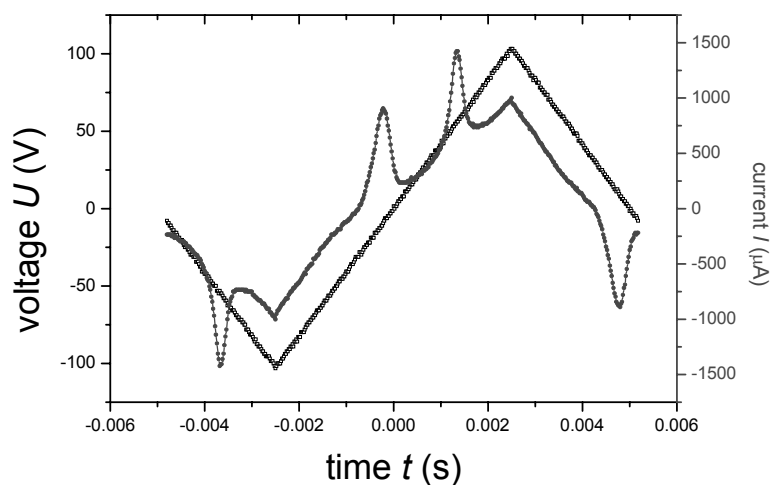


Fig. 3.19 Current response of compound 17.1

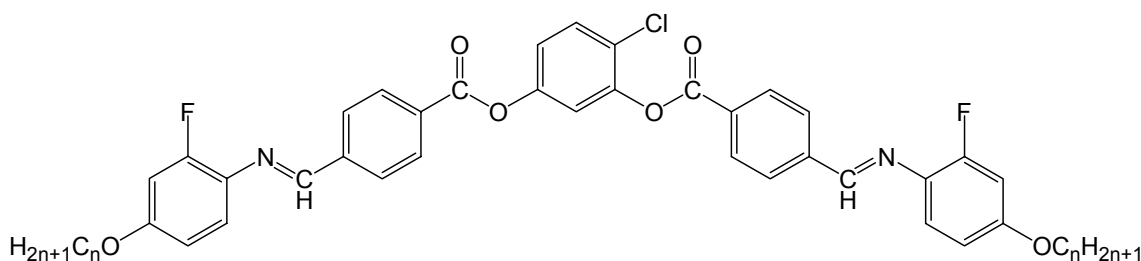
X-ray studies

The X-ray pattern without in-plane order is typical of SmCP phase: the layer reflections are observed on the meridian of the pattern; the maxima of the broad outer diffuse scattering are situated out of the equator indicating an inclination of the molecules and the absence of the long-range positional order within the layers. From the χ -scan the tilt angle of about 19 degrees has been derived.

3.3.5.2 4-Chloro-1,3-phenylene bis[4-(4-n-alkoxy-2-fluoro-phenyliminomethyl) benzoates] (18)

Phase behavior

These compounds exhibit SmCP, the short-chain homologue ($n=8$) an additional nematic phase. The melting point decreases, the clearing point increases with chain lengthening. Compound **17.1** was investigated in details, and will be described in this section.



Sign.	n	Cr	SmCP	N	I
18.1	8	• 71 [7.3]	• 99 [8.9]	• 103 [0.5]	•
18.2	12	• 64 [12.0]	• 112 [16.1]	-	•

Table 3.13 Transition temperature ($^{\circ}\text{C}$) and enthalpy [kJ/mol] values of compounds **18.1** and **18.2**

Polarizing microscopy and electro-optical measurements

The high-temperature nematic phase in the compound **18.1** exists in a short temperature interval of 4°C and shows characteristic schlieren or marble textures (Fig. 3.20). On cooling the schlieren texture transforms into a fine-grainy one. The compound **18.1** shows the electro-optical switching at high threshold field of about $100 \text{ V}/\mu\text{m}$. The switching polarization does not show any temperature dependence in the SmCP phase. The polarization value in SmCP mesophase is around 250 nCcm^{-2} .

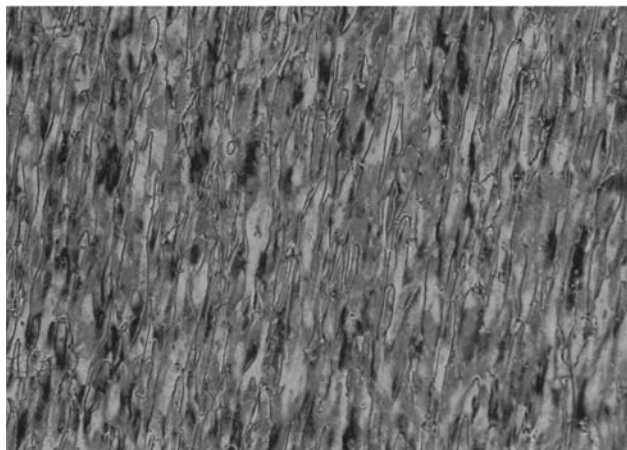


Fig. 3.20 Marble texture of the nematic phase in compound **18.1**

X-ray investigations

X-ray measurements on non-oriented samples showed the layer reflections up to the second order and broad diffuse scattering in the wide-angle region. The d -value is about 35 Å and temperature independent.

Experiments on oriented samples proved the existence of the SmCP phase as well as the high-temperature nematic phase. The splitting of the outer diffuse maxima indicates a tilted arrangement of the molecules in the smectic layers what is compatible with the SmCP phase. The splitting does not show any temperature dependence. In case of surface oriented samples the analysis of the wide-angle scattering shows a change of the molecular orientation upon the N→SmCP transition: the molecules lay parallel to the surface in the nematic phase, while the smectic layers are perpendicular to it in the smectic C phase. From the χ -scan the tilt angle in SmCP phase is approximately 35 degrees, which is close to the value could be estimated from the layer spacing.

Comparison the non-fluorinated* [64] and both fluorinated 4-chlororesorcinol derivatives (**17.1**, **17.2**, **18.1** and **18.2**) has the following outcome:

- the clearing point decreases by 30°C only in case of compounds **18.1** and **18.2**, fluorination in position 3 does not effect on the clearing point,
- fluorination significantly decreases the melting point: in **17.1** and **17.2** $\Delta T \sim 30^\circ\text{C}$, in **18.1** and **18.2** $\Delta T \sim 40^\circ\text{C}$,

- all substances exhibit SmCP mesophase, fluorination positively influences the width of the mesophase range,
- in compound **17.2** a high-temperature SmA, in compound **18.1** a nematic mesophase appears,
- altogether fluorination on the outer rings in any position positively influences the phase behavior of 4-chlororesorcinol derivatives: the temperature range of the switchable mesophase has become wider, and SmA-SmCP as well as N-SmCP polymorphism occur.

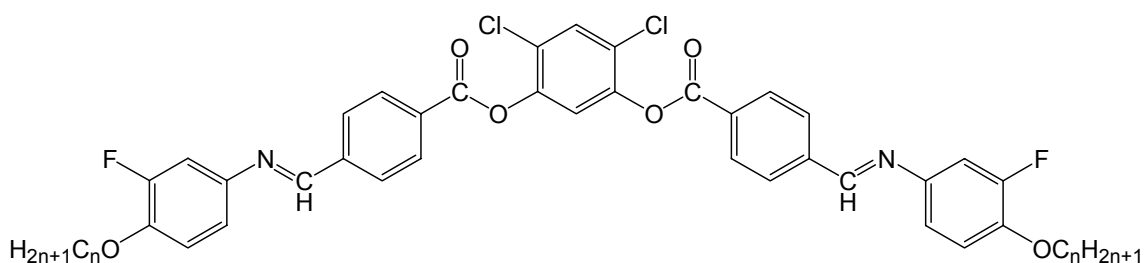
* The non-fluorinated substances, 4-chloro-1,3-phenylene bis[4-(4-n-alkyloxyphenyliminomethyl)benzoates] show the following mesophase behavior [64]: n=8 Cr 120 SmCP 133 I; n=12 Cr 115 SmCP 142 I.

3.3.6 4,6-Dichlororesorcinol derivatives

In this section you will read about bent-core mesogens with unusually wide bending angle between the wings. It results in rich polymorphism of mesophases more typical of calamitic compounds.

3.3.6.1 4,6-Dichloro-1,3-phenylene bis[4-(4-n-alkyloxy-3-fluoro-phenylimino-methyl)benzoates] (19)

Phase behavior



Sign.	n	Cr	SmCP	SmC	SmA	N	I
19.1	8	• 127 [49.0]	(• 95)	-	• 129.8	• 130.5	•
			-		*	*	
19.2	9	• 113 [44.4]	(• 100)	-	• 133	-	•
			[0.5]		[4.2]		
19.3	10	• 108 [50.5]	(• 103)	-	• 137	-	•
			[0.5]		[5.1]		
19.4	11	• 107 [52.8]	(• 102)	• 116	• 139	-	•
			[0.3]	~	[5.7]		
19.5	12	• 103 [57.1]	(• 100)	• 125	• 139	-	•
			[0.2]	~	[6.1]		

* The calorimetric peaks of SmA-N and N-I transition could not be resolved. The sum of these transition enthalpies: $\Delta H(\text{SmA-N}) + \Delta H(\text{N-I}) = 2.0 \text{ kJ/mol}$

~The transition is not observable on the DSC

Table 3.14 Transition temperature (°C) and enthalpy values [kJ/mol] of **19.1-19.5** provided by DSC measurements

These compounds exhibit “conventional” nematic and smectic as well as banana mesophases. The latent heat of SmC-SmCP transition is very small and strongly depends on the cooling rate. Such behavior implies the transition be of weakly first order. Furthermore SmCP mesophase appears only on cooling. The melting point slightly decreases, whilst the clearing point marginally increases with increasing chain length.

Texture observations and electro-optical investigations

Upon cooling of the isotropic liquid, SmA phase appears either as black homeotropic texture or as fan-shaped texture.

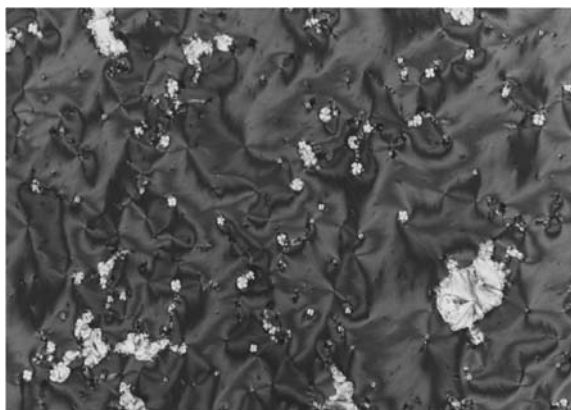


Fig. 3.21 Weakly birefringent texture of the SmC phase at 130°C (compound **19.5**)

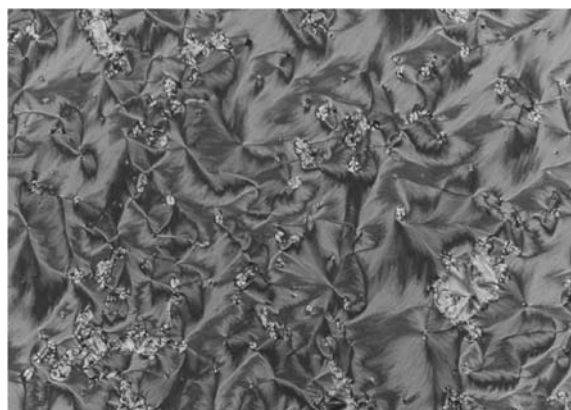


Fig. 3.22 Frozen schlieren texture of the SmCP phase at 95°C in compound **19.5**

In the SmC phase the fan-shaped texture becomes broken and characteristic pattern caused by long-wave director fluctuations is visible. When the phase is formed by homeotropic texture of the SmA phase, schlieren texture with very weak birefringence appears what indicates that the tilt angle in the SmC phase might be quite small (Fig. 3.21).

During the transition from the SmC into the SmCP phase the fluctuation of the c director (projection of the molecular long axis on the smectic layer) becomes less intensive resulting in a “frozen” schlieren pattern of SmCP phase. Meanwhile the contrast of the texture increases (Fig. 3.22). At the same time switching appears in respond to the external electric field. The extinction brushes of the fan-shaped texture experience small turns clock- and anticlockwise depending on the polarity of the external field. When the external field goes off the switched state relaxes in the initial state. These findings stand for antiferroelectric nature of the low-temperature mesophase and the anticlinic SmC_AP_A ground state. These compounds show a pronounced temperature dependence of the spontaneous polarization in the SmCP phase (Fig. 3.23).

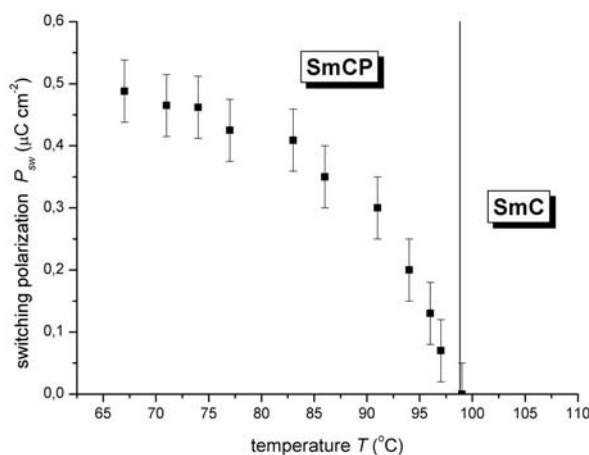


Fig. 3.23 Temperature dependence of the spontaneous polarization in compound 19.5

NMR measurements

There is just a slight temperature dependence of the order parameter $S=0.57-0.66$ in the SmA and SmC phases, however, during the transition from the SmC into the SmCP phase the orientational order parameter is essentially constant. The bending angle

α has been estimated on the base of ^{19}F -NMR measurements. The temperature dependence of the bending angle is illustrated in Fig. 3.24. In the SmA phase the molecule is, actually, stretched: the bending angle is close to 160 deg. There is just a slight decrease of the angle α in the SmC phase and the bending angle decreases considerably in the SmCP phase. This decrease is continuous and over a large temperature interval. In the meantime, the minimum value of the bending angle is just around 145 deg, considerably deviating from the temperature independent α of 120 – 115 deg of the other fluorinated compounds **13.1**, **21.1** and **21.2** with the I \rightarrow SmCP polymorphism.

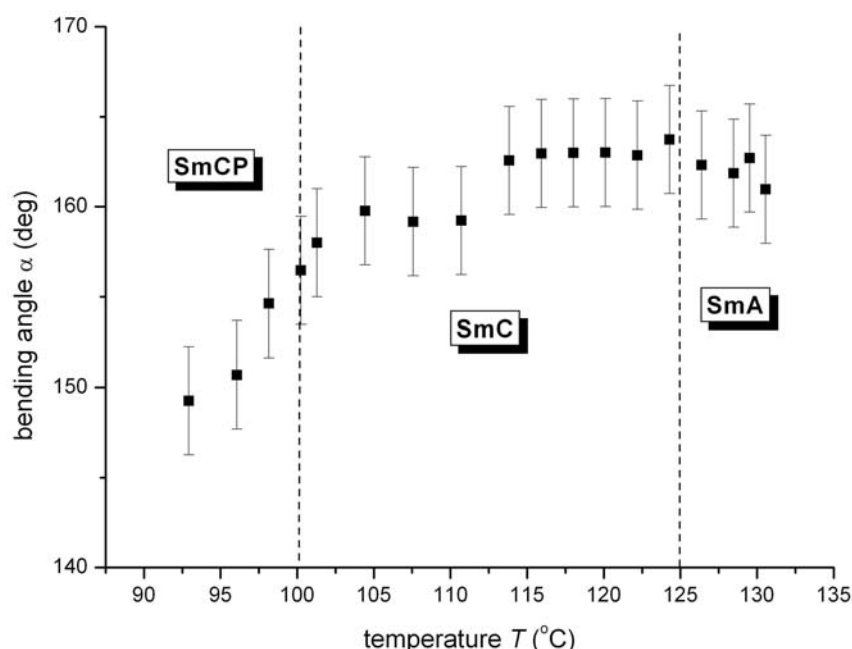


Fig. 3.24 Temperature dependence of the bending angle in compound **19.5**

X-ray measurements

All three mesophases (except for the nematic) show quasi-Bragg reflections from a layer structure as well as a wide-angle diffuse scattering appearing from the liquid-like order within the smectic layers. The layer spacing exhibit very weak temperature dependence for all compounds. In the SmA phase the d -values are smaller than the molecular length (Table 3.15). The experimental data can be well fitted by linear func-

tion giving the following dependence of the layer spacing on the length of the terminal chain n : $d = 36.08 + 1.12n$ (Å). Normally, the layer spacing d is proportional to the two-fold value of terminal chain length n . This implies that the molecules in the SmA phase are intercalated.

Sign	layer spacing d (Å)	molecular length L_{str} (Å)	length of the aliphatic chain L_{al} (Å)
19.1	44.8	52.0	11.2
19.2	46.1	52.6	12.6
19.3	47.9	58.0	14.1
19.4	48.3	60.8	15.4
19.5	49.3	62.8	16.8

Table 3.15 Layer spacing d , molecular length L_{str} , and the length of the aliphatic chains L_{al} in compounds **19.1-19.5** in SmA phase

In the SmC phase the layer spacing slightly decreases by 0.5 – 1 Å depending on the homologue. X-ray measurements performed on the oriented samples show that the patterns of all three mesophases SmA, SmC and SmCP look very similar. The χ -scan in the SmC phase is just slightly broader than in the SmA phase, which means that the molecular tilt should not exceed 2–4 degrees. In the SmCP phase the broadening is larger, however, no splitting is observed and the corresponding tilt angle is smaller than 5–7 degrees in agreement with results of the electro-optical measurements.

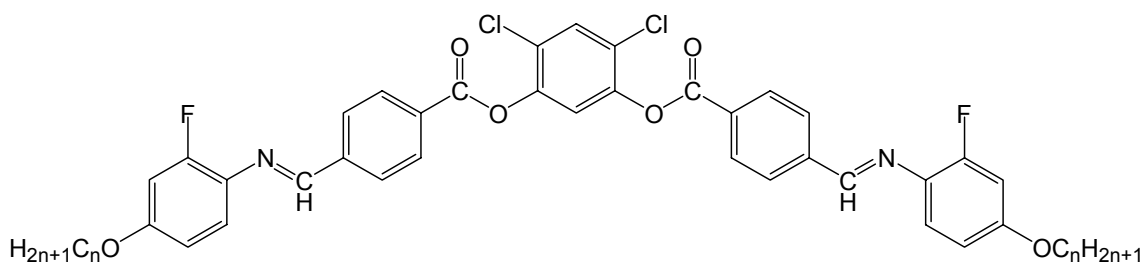
Dielectric measurements

In both types of compounds, with SmA-SmCP and SmC-SmCP transitions one relaxation process was observed in the paraelectric phases (SmA, SmC) and two relaxation processes were found in the antiferroelectric SmCP phase. The relaxation process in the paraelectric phases can be attributed to the rotations about the long molecular axis. The dielectric strength of this process shows a critical-like behavior in vicinity of

the transition into the antiferroelectric phase. Such behavior can be explained with the help of Landau-Ginsburg theory of paraelectric-ferroelectric transitions.

In the antiferroelectric phase there are two relaxation processes from 100 to 1 kHz and from 10 to 0.1 Hz. The dispersion curve of the high-frequency process in the paraelectric phase seems to proceed as the high-frequency process of the antiferroelectric phase. However, the two curves have discontinuity at the transition point. Therefore the high frequency process in the antiferroelectric SmCP phase does not have to correspond to the rotation about the long molecular axis. The low-frequency process corresponds to the relaxation time equal to the switching time provided by electro-optical measurements. Hence, one possible explanation is that these processes are attributed to the ferro- and antiferroelectric modes of the polarization fluctuations [94, 98].

3.3.6.2 4,6-Dichloro-1,3-phenylene bis[4-(4-*n*-alkyloxy-2-fluorophenylimino-methyl)benzoates] (20)



Sign.	n	Cr	SmC	N	I
20.1	8	•	-	(129 [1.5])	• 141 [6.4]
20.2	12	•	103 [53.0]	• (86 [2.3])	• 116 [1.6]

Table 3.16 Transition temperature (°C) and enthalpy values [kJ/mol] of **20.1** and **20.2** provided by DSC measurements

These compounds exhibit a monotropic nematic and the long chain homologue an additional enantiotropic SmC mesophase. The mesophases are typical of rod-like

molecules again what means that the molecules are conceivably stretched. As expected, all transitions are observable on the DSC curves (Table 3.16).

The following comparison can be made between the non-fluorinated* [40] and the fluorinated substances **19.1-19.5** and **20.1, 20.2**:

- all compounds exhibit high-temperature mesophases in which the molecules have stretched conformation (the bending angle is alike to rod-like molecules),
- the long-chain non-fluorinated compound exhibit a $\text{Sm}\tilde{\text{C}}$, a SmC and a nematic phase (with increasing temperature) [40],
- in compounds **19.1-19.5** an additional monotropic switchable low-temperature SmCP mesophase emerges,
- in **20.1** the nematic phase becomes monotropic, and only the long-chain homologue **20.2** exhibits SmC mesophase,
- in conclusion the fluorination in position of X favorably influences the polymorphism of 4,6-dichlororesorcinol bananas.

* The 4,6-dichloro-1,3-phenylene bis[4-(4-n-alkyloxyphenyliminomethyl)benzoates], the non-fluorinated mesogens have the following phase behavior [40]: if n=8 Cr 126 N 148 I and if n=12 Cr 148 $\text{Sm}\tilde{\text{C}}$ 113 SmC 121 N 137 I.

3.3.7 5-Fluororesorcinol derivatives

In this section you will read about bent-core mesogens exhibiting unique polymorphism of B₅ mesophases [99]. Additionally, these compounds are the first mesogenic 5-substituted-resorcinol derivatives with non-perfluorinated terminal chain.

3.3.7.1 5-Fluoro-1,3-phenylene bis[4-(4-*n*-alkyloxy-3-fluorophenyl)iminomethyl]benzoates] (21)

From the homologue serie ($n=8-12$) the compound **21.1** and **21.5** were thoroughly investigated. Since identification of the mesophases requires long electro-optical and NMR studies, the mesophases exhibited by the compounds $n=9-11$ cannot be unambiguously provided. Furthermore, the difference between SmCP (B₂) and B₅ mesophases can be seen only on cooling in polarizing microscope, the XRD measurements on powder sample were also made on cooling. Thus, the transition temperature and enthalpy values obtained on cooling are given. The phase sequence except for the octyloxy and dodecyloxy homologues is a preliminary.

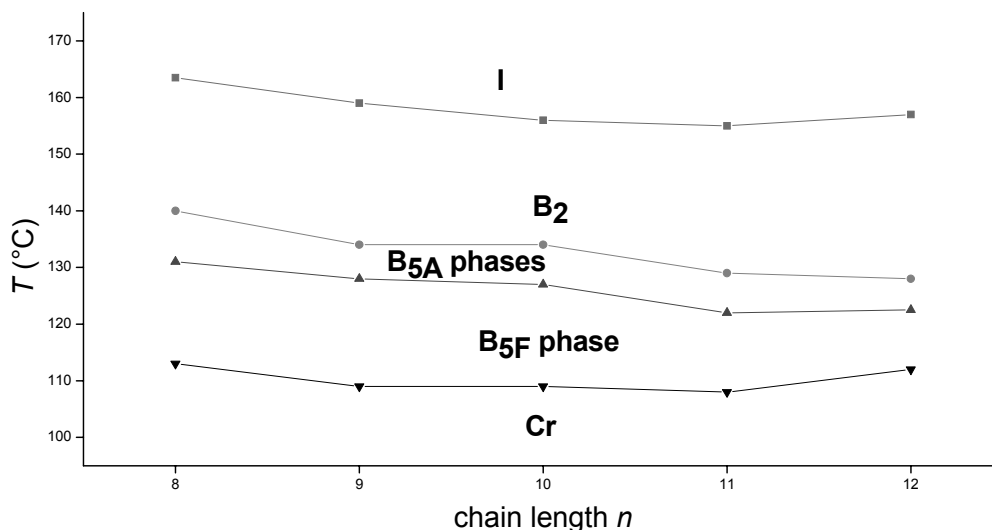
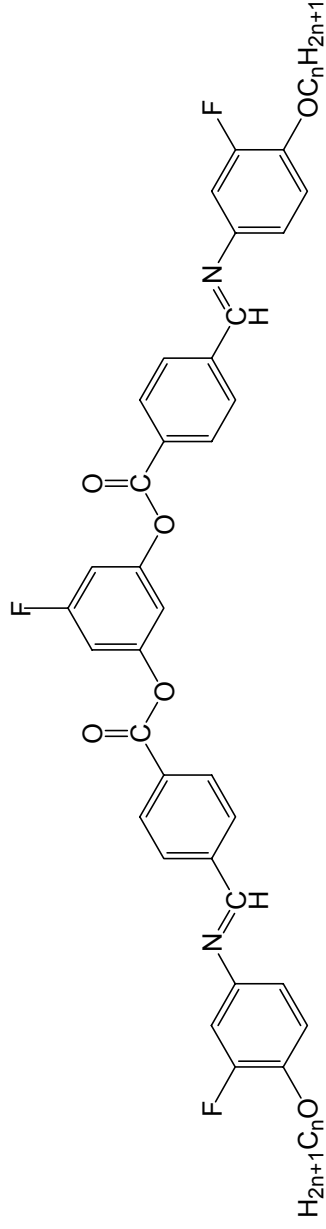


Fig. 3.25 The phase behavior of substances **21.1-21.5**. The phase assignment is a preliminary for the substances **21.2-21.4**. The B_{5A} subphases could not be distinguished by means of DSC.



Sign.	n	Cr	B _{5F}	B _{5A''''}	B _{5A'''}	B _{5A''}	B _{5A'}	B _{5A}	B ₂	I
21.1	8	• 113 [2.7]	• 131 [1.3]	• 135.5 [1.6]	• 137 [0.2]	• 138.9 [0.2]	•	-	139.8 • [0.5]	163.5 • [23]
21.2	9	• 109 [2.5]	*				128	* 134	* 159	•
21.3	10	• 109 [2.2]	*				127	* 134	* 156	•
							[0.9]	[1.3]	[23.2]	
21.4	11	• 108 [1.8]	*				122	* 129	* 155	•
21.5	12	• 112 [1.0]	•	-	-	-	-	122.5 • [2.5]	128 • [0.9]	157 • [24.6]

Table 3.17 Transition temperature (°C) and enthalpy values [kJ/mol] of compounds 21.1-21.5 on cooling; * means supposed phase.

Polarizing microscopy and electro-optical investigations

On cooling the isotropic liquid the SmCP (B_2) mesophase appears as a non-specific grainy texture. A kind of schlieren texture could be obtained by shearing the sample. At the transitions into the low-temperature phases the texture does not markedly change. Nevertheless for a fast heating or cooling rate these phase transitions have also been recognized by a minor change of the paramorphic textures.

Fan-shaped domains have been obtained using a sufficiently high electric field. At the transition $B_2 \rightarrow B_{5A}$ the fan-shaped texture becomes more flat. A considerable change has been observed at the transition into B_{5F} when a constriction of the texture has been seen and the fans become broken, but there is no change in texture at the transition into the solid state.

Above the threshold the initial bright birefringent ribbon texture of the B_2 phase transforms into a smooth SmA-like fan-shaped texture. When the field is removed, the texture switches back into the initial state. The textures of the switched state are independent of the sign of the applied field what points to a racemic ground state. At the transition from the B_2 into the B_{5A} phase the threshold slightly increases from $0.6 \text{ V}/\mu\text{m}$ until $1.3 \text{ V}/\mu\text{m}$, however, the change of the textures on switching looks similar to the case of the B_2 phase (Fig. 3.26).

In the B_{5F} phase the texture of the switched states does not relax or change anyway when the external field is removed. The switching into another polarized state takes place only when the field of opposite polarity (higher than the threshold field) is applied. In contrast to the B_2 and B_{5A} phases, the textures of the switched states are different for opposite signs of the electric field, that means, dark domains became bright and vice versa.

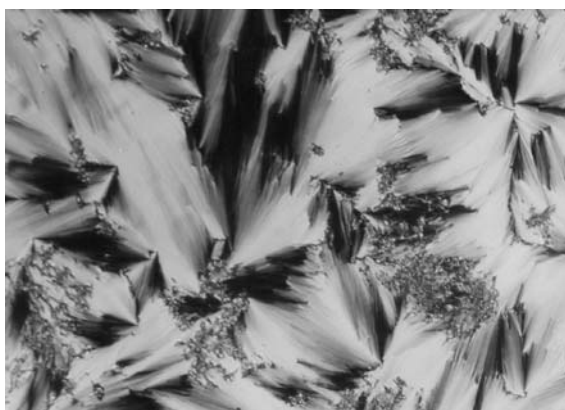
There is a remarkable difference between the appearance of the antiferroelectric B_{5A} phase on cooling and heating. On heating from the B_{5F} phase, some homochiral domains remain, where the texture is different for an opposite sign of the applied field. In contrast, on cooling from B_2 the B_{5A} phase appears as a racemic one. In the B_2 phase only a racemic ground state has been observed. The hysteresis curves of the B_{5A} and B_{5F} phases are illustrated in Fig. 3.27. The value of spontaneous polarization slightly changes between the mesophases.



a)



b)



c)

Fig 3.26 Optical textures of the B_{5A} phase in compound **21.5** at 125°C a) $E=0 \text{ V}\mu\text{m}^{-1}$ b) $E=0.6 \text{ V}\mu\text{m}^{-1}$ c) $E=1.6 \text{ V}\mu\text{m}^{-1}$

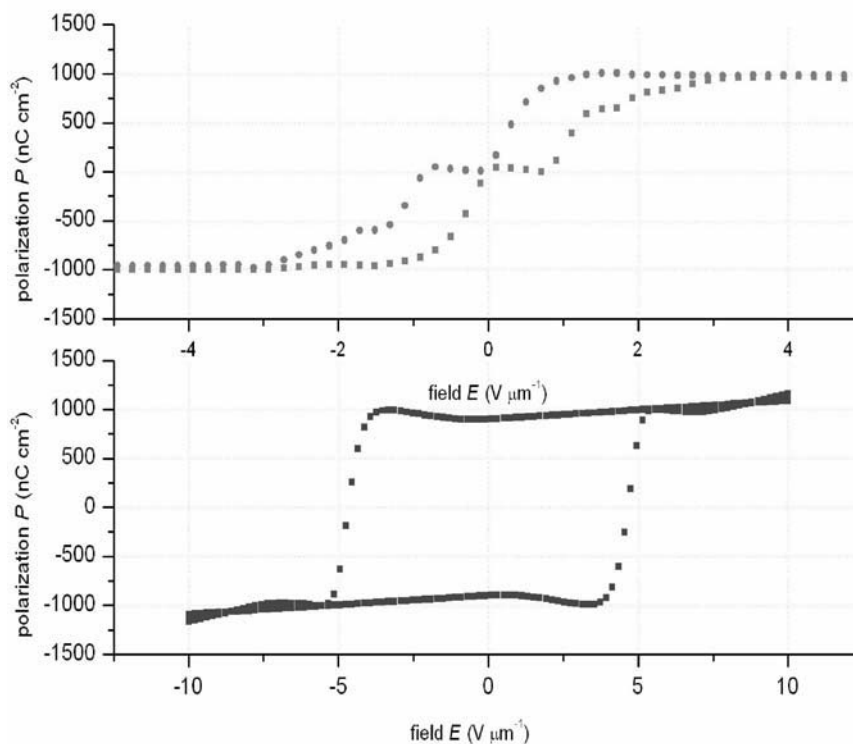


Fig. 3.27 Hysteresis curves of the B_{5A} (red) and the B_{5F} (blue) mesophases

X-ray investigations

Although the compounds under investigation possess quite a large number of mesophases, only two kinds of X-ray patterns could be observed: one typical of the SmC or B_2 and the other one typical of the B_5 phases. The high temperature phase exhibits a pattern without in-plane order, typical for SmCP: the layer reflections are observed on the meridian of the pattern; the maxima of the broad outer diffuse scattering are situated out of the equator indicating an inclination of the molecules and the absence of the long-range positional order within the layers. There are two kinds of scattering centers in the low-temperature phases: ordered in a rectangular two-dimensional lattice (the molecules from different layers are not correlated) and disordered centers that give a broad diffuse halo. Such behavior is characteristic for B_5 phases. No discontinuous change has been seen at the phase transition temperatures observed in the DSC below the B_2 phase. The layer spacing d , obtained from the powder samples is nearly independent of the temperature for the short-chain homologue **21.1**, whereas in the long-

chain homologue **21.5** a slight temperature dependence of the d -values has been observed.

NMR studies

In these compounds there are fluoro-substituents on the central as well as on the outer rings. Therefore order parameter and the bending angle α could be obtained from ^{19}F -NMR measurements. The fluoro-substituent on the central ring provides a triplet representing the dipole interaction between the fluorine and the neighboring protons, the fluoro-substituents on the outer rings produce a doublet as a result of the dipole splitting of these fluorines. The splitting of the triplet can be written as

$$\Delta\nu_{\xi\xi}^F = \Delta\nu_C^F S \quad (3.1)$$

where $\Delta\nu_C^F = -15.08$ ppm is an interaction constant defined by the geometry of the central ring.

The splitting of the fluorines on the outer rings can be written as

$$\Delta\nu_{\xi\xi}^F = \Delta\nu_A^F S \left(\frac{3}{2} \cos^2(\varepsilon) - \frac{1}{2} \right) \quad (3.2)$$

where the splitting constant $\Delta\nu_A^F = -28.0$ ppm.

This tendency of splitting could be observed in all phases. Therefore it was assumed that the angle ε (the angle between the molecular and the para axis of the molecule) in low temperature phases has similar values to those in the high temperature phase. However, poor orientation in the B_5 phases resulted in broadening of the peaks. The bending angle α ($\alpha = 180 - 2\varepsilon$) was found to be around 116-118 deg. The order parameter S is nearly temperature independent in the B_2 phase, and slightly decreases in the B_{5A} phase reaching its maximum of 0.9 in the B_{5F} phase (Fig. 3.28).

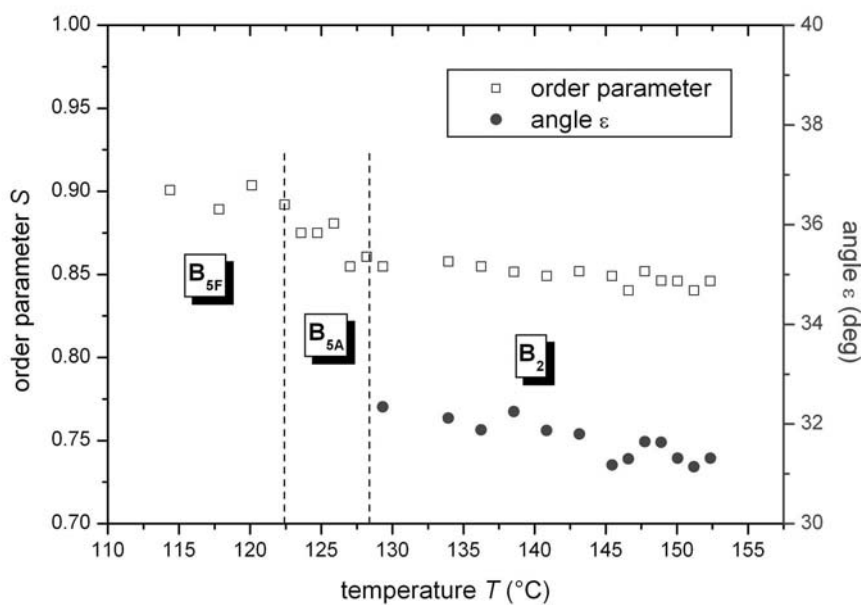
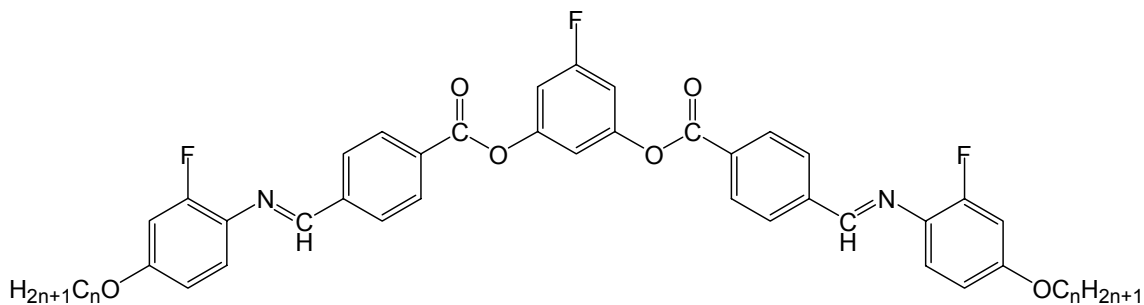


Fig 3.28 Temperature dependence of the order parameter S and the angle ε in compound 21.5

3.3.7.2 5-Fluoro-1,3-phenylene bis[4-(4- n -alkoxy-2-fluoro-phenyliminomethyl) benzoates] (22)



Sign.	n	Cr	SmCP	I
22.1	8	•	- 139 [39.3]	•
22.2	12	•	135 • 137 - [38.8]*	•

* summ of ΔH value of both transitions, the peaks could not be separated

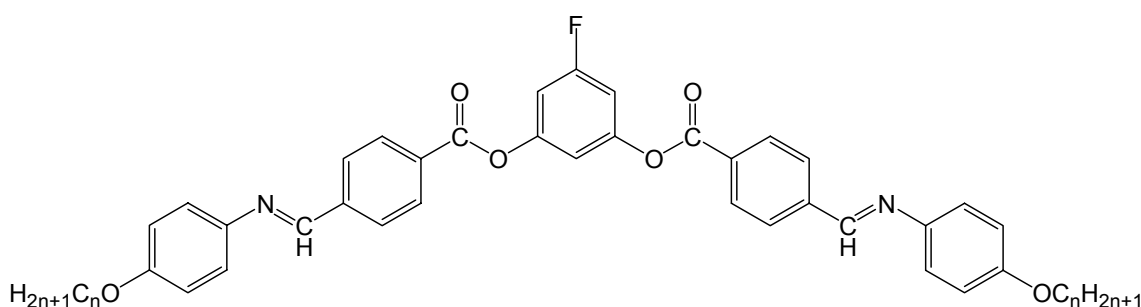
Table 3.18 Transition temperature (°C) and enthalpy values [kJ/mol] of compounds 22.1 and 22.2

3.3.7.3 5-Fluoro-1,3-phenylene bis[4-(4-n-alkoxyphenyliminomethyl)benzoates] (23)

5-fluororesorcinol derivative bananas had not been prepared before the beginning of this work. Therefore not only should the compounds **21** and **22** have been synthesized but also the substances without fluoro-substituents on the outer rings.

Phase behavior (DSC)

These compounds exhibit enantiotropic SmCP (B_2) mesophase. Chain lengthening decreases the melting and clearing points. Accordingly, the mesophase range becomes narrower with increasing chain length. Compound **23.1** was studied in detail and will be described below.



Sign.	n	Cr	SmCP	I
23.1	8	• 158 [12.3]	• 179 [23.8]	•
23.2	12	• 149 [15.6]	• 169 [27.9]	•

Table 3.19 Transition temperature ($^{\circ}\text{C}$) and enthalpy values [kJ/mol] of compounds **23.1** and **23.2**

Texture observations and electro-optic measurements

The SmCP phase appears from the isotropic phase as a fine grainy texture (Fig. 3.24). When the cooling rate is slow (0.1 K/min) a fan-shaped texture can be observed.

Application of an electric field leads to electro-optical switching. This process has a threshold of about ~ 1.5 V/ μm . The switched state is independent of the polarity of the external field. The switching polarization does not show any temperature dependence. The polarization values are quite high (~ 640 nCcm⁻²).

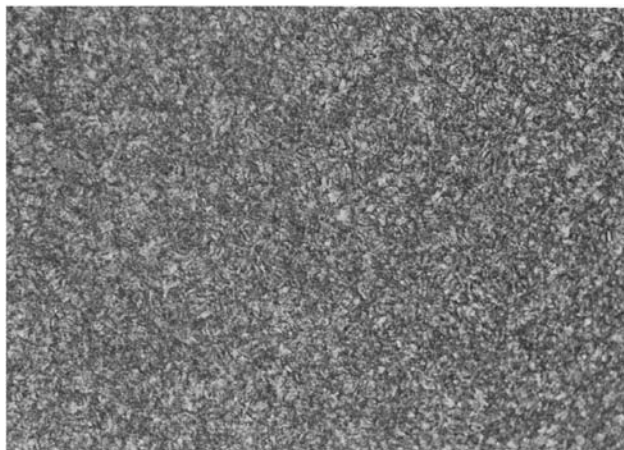


Fig. 3.29 The grainy texture of SmCP phase in compound **23.2**

X-ray investigation

X-ray measurements on non-oriented samples showed the layer reflections up to the second order and broad diffuse scattering in the wide-angle region. The d -values are temperature independent ($d=37.5$ Å). Experiments on oriented samples provided some more information about the structure of the mesophases. The splitting of the outer diffuse maxima indicates a tilted arrangement of the molecules in the smectic layers, which is compatible with the SmCP phase. The splitting does not show any temperature dependence.

NMR studies

The symmetry of the molecule defines the molecular axis perpendicular to the C-F bond in the central ring. The ¹³C-NMR spectra of the central ring provide us with eight parameters: four shift anisotropies and four C-F dipolar couplings. These data are enough to estimate both a transversal order parameter S and the longitudinal order pa-

parameter D . However, poor resolution of the central ring carbons complicates experimental realization.

The splitting observed in ^{19}F -NMR spectra is governed by the dipolar interactions between the fluorine and the neighboring protons. The spectrum consists of a triplet of (overlapped) doublets. This additional splitting between the two peaks of a doublet gives another way to estimate the transversal order parameter. The longitudinal order parameter was found to be $S=0.875$, the transversal order parameter $D=0.006$.

Comparing the fluorinated (**21** and **22**) and non-fluorinated (**23**) substances described above the following can be outlined:

- substances **23.1** and **23.2** exhibit SmCP mesophase,
- fluorination on the outer rings in position 2 drastically reduces (**22.2**), even vanishes (**22.1**) the phase existence,
- fluorination on the outer rings in position 3 (**21.1-21.5**) has a completely different influence: not only do SmCP phase exist, but low-temperature B_5 mesophases appear, too.

Furthermore 5-chloro-1,3-phenylene bis[4-(4-n-octyloxyphenyliminomethyl) benzoate] (**24**) was prepared. This compound is not liquid crystalline: it melts at 150°C and freezes at 136°C .

Chapter 4 *m*-Phenylenediamine derivatives (28, 29)

In this section you will read about bent-core substances substituted on the central ring and/or with fluoro-substituents on the middle rings. The molecules are symmetric, the benzene rings are connected with azomethine and carboxylic groups. The position and the direction of the linking groups have been changed, though. As you will see it leads to drastic consequences.

4.1 The synthetic work

m-Phenylenediamine derivatives with or without substituents on the central ring with and without fluoro-substituent on the middle rings were synthesized.

The first step of the synthesis is demethylation of 2-fluoro-4-methoxybenzaldehyde with borontribromide in dichloromethane. The product (**25**) [100] was esterified with 4-*n*-octyloxy-benzoic acid. The synthesis of the fluorinated two-core mesogen **26** is illustrated in Fig. 4.1.

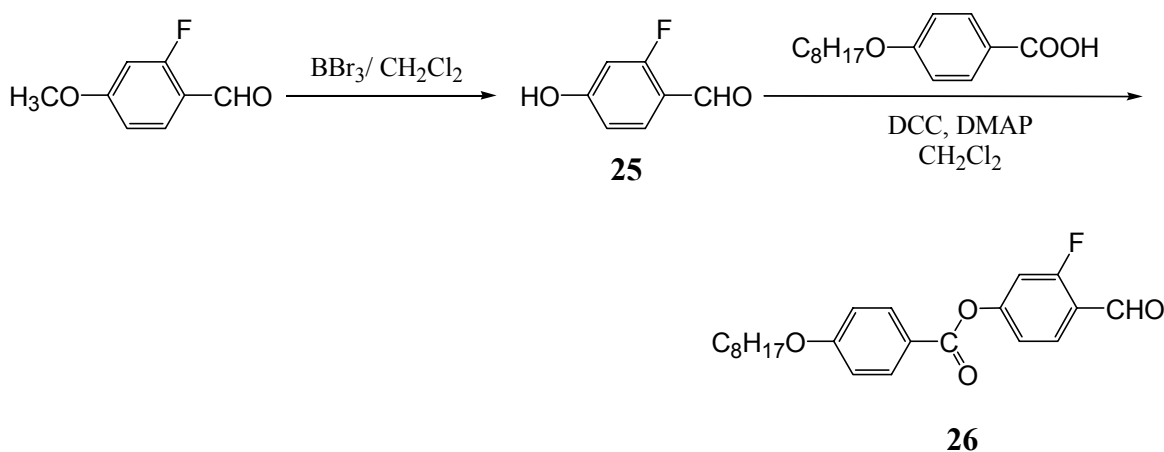


Fig. 4.1 Synthesis of 4-*n*-octyloxybenzoic acid 3-fluoro-4-formylphenyl ester (**26**)

The 4-*n*-octyloxybenzoic acid 3-fluoro-4-formylphenyl ester (**26**) possesses liquid crystalline properties: Cr 41 SmA 50 I. The non-fluorinated two-core mesogen was available in the laboratory.

The *m*-phenylenediamines are commercially available except of 2,4-diaminofluorobenzene. 2,4-Dinitrofluorobenzene was reduced using catalytic hydrogenation (Fig. 4.2). Since compound **27** is sensitive to air, light and heat the reduction was carried out in methanol so that before the next synthesis step only Pd/C catalyst had to be removed from the solution of **27**. Thereby the product (**27**) was not exposed to the elevated temperature necessary to concentrate its solution.

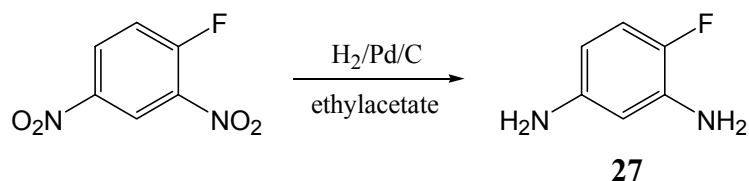
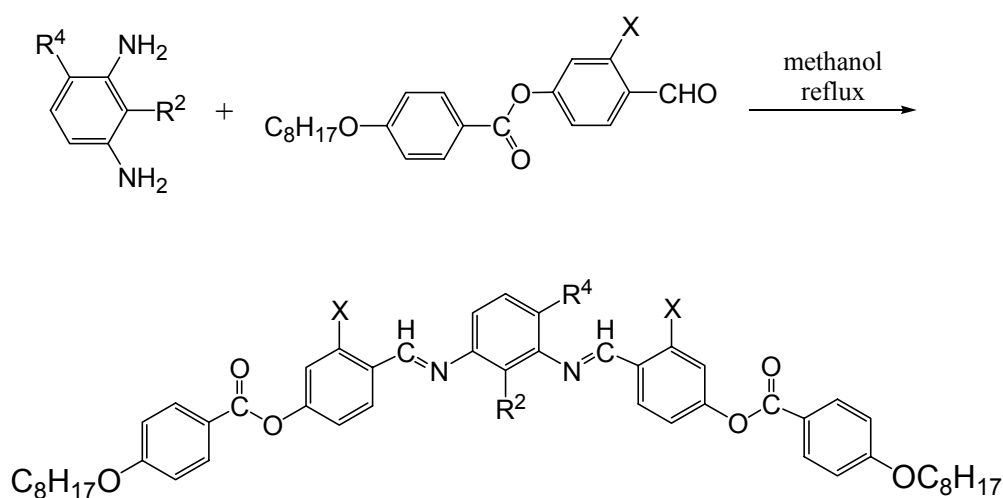


Fig. 4.2 Catalytic hydrogenation of 2,4-dinitrofluorobenzene (**27**)

The final step of the synthesis is condensation of the central core and the mesogenic wing units (Fig. 4.3).



Sign.	28.1 ^[27]	28.2	28.3	28.4	28.5	29.1	29.2	29.3	29.4	29.5
R²	H	CH ₃	H	H	H	H	CH ₃	H	H	H
R⁴	H	H	CH ₃	NO ₂	F	H	H	CH ₃	NO ₂	F
X	H	H	H	H	H	F	F	F	F	F

Fig. 4.3 Synthesis of *N,N'*-bis[4-(4-*n*-octyloxybenzoyloxy)benzylidene]phenylene-1,3-diamines (**28, 29**)

4.2 Characterization

The following substituents have been introduced on the central core: methyl group in position 2 and 4, nitro-group and fluorine in position 4. All compounds were prepared with and without fluoro-substituents on the middle rings (X=H or F). All substances have octyloxy terminal chains. Most of the substances exhibit B₁ mesophase.

Sign.	X	R	Cr	B ₁	I
28.1 ^[27]	H	H	• 114 [20.8]	• 135 [16.9]	•
28.2	H	2-CH ₃	• 140 [37.2]	(• 128.5) *	•
28.3	H	4-CH ₃	• 104 [38.9]	(• 102) [12.6]	•
28.4	H	4-NO ₂	• 109 [7.9]	-	•
28.5	H	4-F	• 111 [14.1]	• 142 [18.9]	•
29.1	F	H	• 88 [43.3]	• 116 [16.1]	•
29.2	F	2-CH ₃	• 145 [87.5]	-	•
29.3	F	4-CH ₃	• 93 [29.7]	• 95 [5.9]	•
29.4	F	4-NO ₂	• 126 [5.6]	-	•
29.5	F	4-F	• 95 [19.0]	• 117 [16.7]	•

* The transition peaks of the melting and clearing points overlap

Table 4.1 Transition temperature (°C) and enthalpy values [kJ/mol] of **28.1-28.5** and **29.1-29.5** provided by DSC measurements

The nitro-substituted compounds (**28.4** and **29.4**) do not have liquid crystalline properties. The methyl-substituted non-fluorinated materials (**28.2** and **28.3**) have a monotropic B₁ phase which recrystallizes very fast, while the non-substituted (**28.1**) and 4-fluoro-substituted (**28.5**) compounds exhibit moderately wide enantiotropic B₁ mesophase.

Fluorination of **28.1** and **28.5** decreases the melting and clearing points as well as the temperature range of the mesophase. The 4-methyl derivative fluorinated substance (**29.3**) exhibit a short-range enantiotropic B₁ mesophase. Fluorination produces a negative effect on the 2-methyl-derivative (**29.2**): the compound has no liquid crystalline properties: it crystallizes at 132°C on cooling.

To sum up, this kind of directing and positioning of the connecting groups in bent-core molecules does not seem to be very fruitful. Moreover, substitution of the central ring does not bring about changes in the phase behavior. Therefore this study on the influence of the fluorination on the middle rings is not really informative. However, it is a modest contribution to the science of bent-core materials. Unfortunately, the substances are thermally instable, therefore proper characterization cannot be given about these substances. For the same reason NMR investigations to obtain the bending angle α could not be carried out on these materials. Because of the thermal instability of these materials we have not prepared further compounds of this substance class. It might be possible, though, that the long-chain homologues like other bent-core substances (see e.g. compounds **14**) exhibit SmCP phase.

Chapter 5 Isophthalaldehyde bis[4-(4-subst.-phenyloxycarbonyl)anilines] (30)

In this section symmetrical bananas with azomethine linking groups between the central and the middle rings and carboxylic connections between the middle and outer rings will be introduced. Since substituted isophthalaldehydes are not easily available, we decided to investigate the influence of the terminal chain on the mesophase behavior. As you will see, only compounds with alkyl- and alkyloxy terminal chains [2] show mesomorphic behavior: most of them exhibit B₄ and SmCP (B₂) mesophases. Note that in case of calamitic compounds terminal chain dependence of the mesophase behavior found for bananas is atypical.

5.1 Synthetic work

Isophthalaldehyde derivatives with varied terminal chains were synthesized. 1,3-Phenylene bis(4-methyliminobenzoic acid) (non-liquid crystal) was available in the laboratory. It was reacted with the corresponding 4-substituted phenol providing the isophthalaldehyde bis[4-(4-subst.-phenyloxycarbonyl)anilines] (Fig. 5.1).

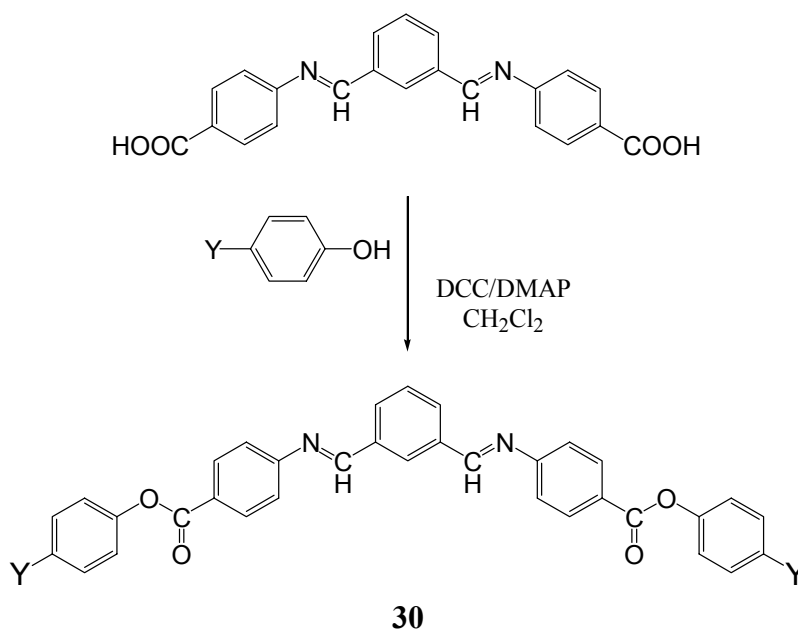
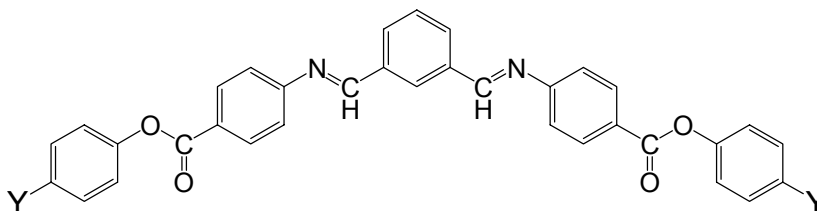


Fig. 5.1 Synthesis of isophthalaldehyde bis[4-(4-substituted-phenyloxycarbonyl)anilines]

5.2 Characterization

Phase behavior (DSC)

Sign	Y	Cr	B ₄	SmCP	I
30.1	OC ₅ H ₁₁	• 156 [53.0]	-	-	•
30.2	OC ₆ H ₁₃	• 156 [54.4]	-	-	•
30.3	OC ₇ H ₁₅	• 132 [33.3]	• 154 [53.5]	(• 146) [14.5]	•
30.4	OC ₈ H ₁₇	• 126 [31.7]	• 148 [13.4]	• 152 [54.1]	•
W1[□]	OC ₉ H ₁₉	• 132 [45.8]	• 145 [37.2]	• 149 [12.0]	•
30.5	OC ₁₀ H ₂₁	• 131 [43.5]	• 148 [39.4]	• 153 [15.8]	•
30.6	OC ₁₂ H ₂₅	• 136 [53.5]	• 145 [38.1]	• 154 [15.4]	•
30.7	C ₈ H ₁₇	• 127 [31.8]	-	(• 114)*	•
30.8	C ₁₂ H ₂₅	• 123 [35.1]	-	(• 121) [12.6]	•

Sign	Y	Cr	B ₄	SmCP	I
30.9	COC ₆ H ₁₃	• 176 [89.9]	-	-	•
30.10	COC ₇ H ₁₅	• 173 [74.7]	-	-	•
30.11	COC ₉ H ₁₉	• 167 [70.6]	-	-	•
30.12	CN	• 243 [51.8]	-	-	•
30.13	C ₂ H ₄ CN	• 189 [61.2]	-	-	•
30.14	COOC ₆ H ₁₃	• 158 [66.5]	-	-	•
30.15	COOC ₁₀ H ₂₁	• 151 [78.3]	-	-	•

* This transition could be observed only by polarizing microscopy

□ This material was available in the laboratory [91]

Table 5.1 Transition temperature (°C) and enthalpy [kJ/mol] values of compounds **30.1-30.15**

Materials with several kinds of terminal chains were prepared, but compounds with terminal alkanoyl- or alkyloxycarbonyl- or cyanoethyl- or cyano-substituents do not display liquid crystalline properties. Substances with alkyl- and alkyloxy chains exhibit mesophases. Liquid crystalline phase emerges only on cooling in the case of materials with terminal alkyl chains independently of the chain length. Compounds with alkyloxy chains exhibit enantiotropic SmCP (B₂) and soft crystalline B₄ mesophases. The short-alkyloxy-chain homologues (**30.1** and **30.2**) do not show liquid crystalline properties, the heptyloxy homologue (**30.3**) exhibits B₄ and monotropic SmCP phases. Compounds with octyloxy or longer chains (**30.4-30.6**) emerge with B₄ and SmCP phases on cooling and heating, too.

The longer chain length the wider SmCP and the narrower B₄ phase exist. The transition temperatures (including the melting and clearing points) do not differ much from each other and show no tendency on the part of chain lengthening.

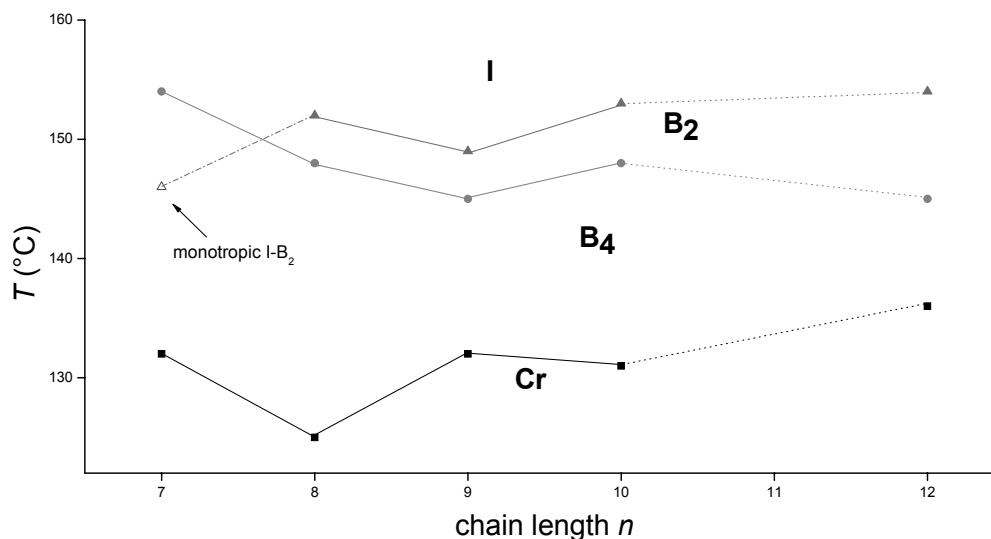


Fig. 5.2 The phase behavior of compounds 30.3-30.6 and W1

Polarizing microscopy

The transition between the crystalline and B₄ phase could be well observed only at the first heating of virgin crystals: the B₄ phase remains crystalline-like, although, birefringence disappears. The SmCP phase shows up with grainy fan-shaped texture. The SmCP phase can be supercooled in most cases and the B₄ phase appears at 10-15°C below the transition temperature on heating. Owing to the supercooling isotropic SmCP phase transition could be found in **30.3**. The B₄ phase arises with pattern reminding of annual rings (Fig. 5.3). Another characteristic is transparent blue color. On further cooling very slow (several-week long) crystallization takes place.



Fig. 5.3 Annual rings in B₄ texture of **W1** at 139°C

X-ray measurements

The measurements were made on compound **W1**. In the B₄ phase the wide-angle reflections are strongly broadened comparing with those of the crystalline state what may be indicative of a crystalline phase with strong lattice distortions [34]. However, dielectric measurements point to a low-frequency relaxation process in B₄ phase. In other words, B₄ phase is certainly not a classical crystalline phase. In the SmCP phase layer reflections up to the second order and broad diffuse scattering in the wide-angle region have been observed. It implies liquid-like order in smectic layers. The *d*-values are smaller than the molecular length *L* for a molecule with bending angle 120 degrees. It suggests that the molecules are tilted in the smectic layers by around 35 degrees.

Electro-optical investigations

The observations were made on compound **W1**. The SmCP phase appears from the isotropic liquid with pattern consisting of batonnets with irregular stripes perpendicular to the fans. Applying an electric field above the threshold, this pattern turns into a SmA-like fan-shaped texture. The repolarization current response exhibits two peaks per half period of the applied triangular voltage indicating an antiferroelectric (AFE) ground state. The spontaneous polarization was found to be about 150 nCcm⁻².

As you can see, terminal chains strongly influence the phase behavior. The substances with electron-donating alkyl- and alkoxy chains possess liquid crystalline properties while compounds with electron-withdrawing alkanoyl, alkoxy-carbonyl, cyano and propionitrile terminal groups do not. On the one hand, in the knowledge of the facts about calamitic mesogens this tendency is very surprising. On the other hand, these compounds represent extensive five-ring bent-shaped aromatic systems very different from rod-like mesogens whereby we cannot count on the same effect of terminal moieties on the mesophase behavior.

Chapter 6 Conclusion

6.1 The role of the linking groups

Several bent-shaped mesogens with varied linking groups have been synthesized: azomethine and carboxylic groups join five benzene rings together. The compounds differ in the position and the direction of the linking groups. Several examples known from the literature [2, 27, 75] show that bent-core molecules made up from five benzene rings joined only by carboxylic groups do not show such a rich variety of mesophases as those connected by carboxylic and azomethine groups as in the first banana presented by Niori et al. [1]. In Fig. 6.1 you can see the general formula of some symmetric five-ring bananas.

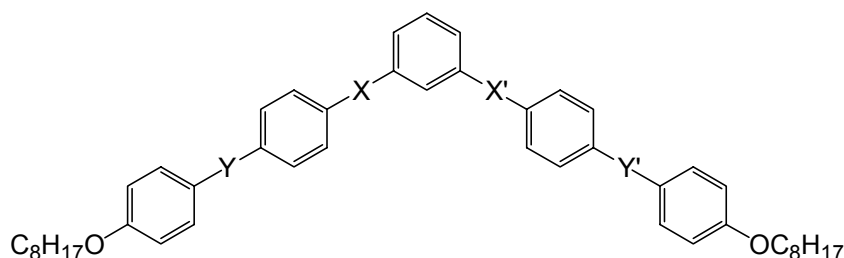


Fig. 6.1 General formula of symmetric five-ring bent-core molecules with octyloxy terminal chains

Sign.	Y	X	X'	Y'	Cr	B ₄	B ₃	B ₂	B ₁	I
L1 ^[1]	N=CH	COO	OOC	CH=N	-	• 139.7	• 151.9	• 173.9	-	•
30.4	OOC	N=CH	CH=N	COO	• 126	• 148	-	• 152	-	•
28.1 ^[27]	COO	CH=N	N=CH	OOC	• 114	-	-	-	• 135	•

Table 6.1 Phase behavior of five-ring bent-shaped isomers

As you can see compounds **L1** and **29.4** exhibit switchable B₂ mesophase and crystalline-like B₄, while compound **28.1** shows up with columnar B₁ phase. As it has already been mentioned in section 2.3, compounds only with carboxylic connections exhibit B₁ phase. It is worthy noting that in ester-type molecules conjugation between the benzene rings is not completed.

Bedel et al. [53] suggest that formation of liquid crystalline phases by bent-core compounds might be determined by the partial charges of the aromatic cores: if the donor or acceptor nature of the four linking groups leads to an alternate sequence of positive and negative charges on the five benzene rings mesomorphic properties will emerge. If you consider compound **30.4** and **28.1**, the above-mentioned theory does not seem to work. Very clear tendency of alternating partial charges can be displayed only in the case of substance **L1**. The middle rings in compounds **30.4** and **28.1** are exposed to electronic effects of opposite sign. There is another basic difference between compounds **L1** and **30.4**, **28.1**. Rotation around the single bond of ester linking group is possible in the central part of the molecule in the case of substance **L1**. It means there might be numerous conformers influencing the bent of the molecules: in other words, the bent is more flexible. The wings are completely different: extensive conjugation through the azomethine groups is established. Additionally, the double bond of azomethine connection hinders free rotation. NMR studies have shown that the rings take part in a kind of flip-flop motion: the benzene-ring planes are either parallel or perpendicular to each other [40].

In the case of compound **30.4** and **28.1** the bent is more rigid, and the wings are flexible. The central and the middle rings are conjugated, and the conjugation does not expand over the whole wing. It is worthy noting that compounds **30.4** and **28.1** exhibit only banana phases, whilst laterally substituted substances from the class of compound **L1** exhibit classical nematic and smectic phases, too. Unfortunately, comparison of the substituent effect on these three substance classes could not be drawn. The *m*-phenylenediamines are air- and heat sensitive, in other words to unstable to investigate them. Lateral substitution of the isophthalaldehyde derivatives is a hard nut to crack.

Bent-core molecules embody a very complex chemical system. Calculations and theoretical predictions about such systems cannot be made without limitations and simplifications. Therefore more facts need to be collected and worked up to render more exact calculations and complete our knowledge.

6.2 The role of lateral fluoro-substituents

The commonest used lateral substituent is fluoro-substituent. It is the smallest possible substituent, yet it has the highest electronegativity (EN= 4.0) among the chemical elements. Therefore it brings about drastic change in the electron distribution of the aromatic core: fluoro-substitution electronically impoverishes the ring as well as the connecting group or the alkyloxy chain situated next to the substituted position [74].

Lateral fluoro-substitution brings about a lot of change in resorcinol derivative bananas. Substitution on the outer rings in position 2 (X=H, Y=F) usually negatively influences the mesophase behavior: switchable mesophase disappears (**14**), the mesophase stability undermines. Introducing lateral substituent on the outer rings in position 3 (X=F, Y=H) brings about favorable changes: wider scale of mesophases could be observed (**13**, **21**), new mesophases appeared (**9**, **13**, **15**). The banana mesophase(s) appears in the case of non-fluorinated bent-shaped resorcinol derivative (X=H, Y=H) always emerges in the fluoro-substituted compound if X=F. Moreover, new mesophases and subphases show up. Fluorination usually brings about lower clearing points: the most considerable changes could be observed in the case of 2-methylresorcinol ($R^2=CH_3$) (**14.1** and **14.2**, **13.1-13.5**), 2-nitroresorcinol ($R^2=NO_2$) (**11.1** and **11.2**) and 4-chloro-resorcinol derivatives (**18.1** and **18.2**). If $R^4=Cl$ fluoro-substitution independently of the position of the fluorine decreases the melting point (**18.1**, **18.2**, **17.1**, and **17.2**).

Fluorination of 5-fluororesorcinol derivatives ($R^5=F$) results in drastic changes independently of the position. If X=F (**21.1-21.5**) several B_5 phases appear, if Y=F (**22.1** and **22.2**) only the long-chain homologue (**22.2**) exhibits SmCP phase over a strongly reduced temperature interval comparing with the non-fluorinated compound.

Concerning the character of mesophases the following observations have been made. Fluorination of 2-methylresorcinol ($R^2=CH_3$) similarly influences the mesophase character. If X=F (**13.1-13.5**) several SmCP phases appear, if Y=F only the dodecyloxy homologue (**14.2**) exhibits SmCP mesophase and there is no low-temperature B_5 phase. The mesophase character of substituted resorcinol derivative bent-shaped compounds with octyloxy terminal chains can be seen in Table 6.2.

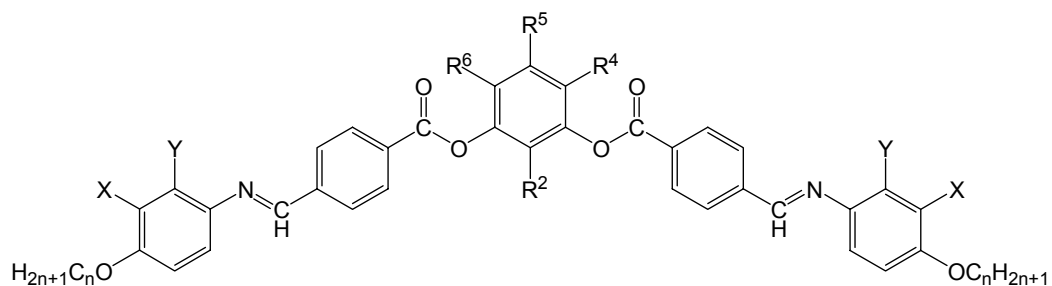


Fig. 6.2 The general formula of resorcinol derivatives

central ring		X=Y=H		X=F, Y=H		X=H, Y=F
resorcinol	[1]	B ₄ , B ₃ , B ₂	9.1	B ₄ , B ₂ , SmC _G	10.1	B ₂
2-nitroresorcinol	[30]	B ₇	11.1	B _x , B ₇	12.1	B ₇
2-methylresorcinol	[55]	B ₅ , B ₂	13.1	B ₅ , B ₂ '', B ₂ ', B ₂	14.1	B ₁
4-cyanoresorcinol	[65]	B ₂ , SmC, SmA	15.1	C _{PA} , SmA	16.1	B ₂ , SmA, N
4-chlororesorcinol	[64]	B ₂	17.1	B ₂	18.1	B ₂ , N
4,6-dichlororesorcinol	[40]	SmC̃, SmC, SmA	19.1	B ₂ , SmA, N	20.1	N
5-fluoresorcinol	23.1	B ₂	21.1	B _{5F} , B _{5A} '', B _{5A} '', B _{5A} ', B _{5A} ', B ₂	22.1	-*

* The long chain homologue exhibits B₂ phase.

Table 6.2 Comparison of fluorinated and non-fluorinated substituted resorcinol derivatives with octyloxy terminal chains. The phase sequence follows increasing temperature.

Fluorination of the m-phenylenediamine derivatives on the middle ring (**29**) does not effect strongly on the phase behavior. The mesophase character does not change at

all: the mesogens exhibit B₁ mesophase (in some cases only monotropic). In the case of these compounds substitution on the central ring either does not influence the mesophase character (**28.1**, **28.3**, **28.5**) or the substance is not liquid crystalline at all (**28.4**). However, the compounds are thermally not stable what makes difficult to determine the phase behavior.

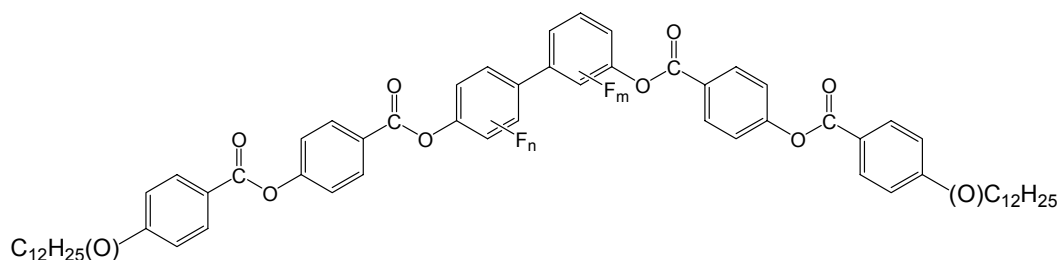


Fig. 6.3 Fluorinated biphenyl derivatives $n=1, 2$, $m=1, 2, 3$ [59]

Investigating the effect of lateral fluoro-substitution on the central unit of 3,4'-disubstituted biphenyl derivative bent-shaped molecules Dantlgraber et al. found that fluorination decreases the clearing point of the biphenyl derivatives [59]. Furthermore they pointed out that the more fluoro-substituents on the biphenyl ring the narrower mesophase range occur. Even loss of liquid crystalline character happens.

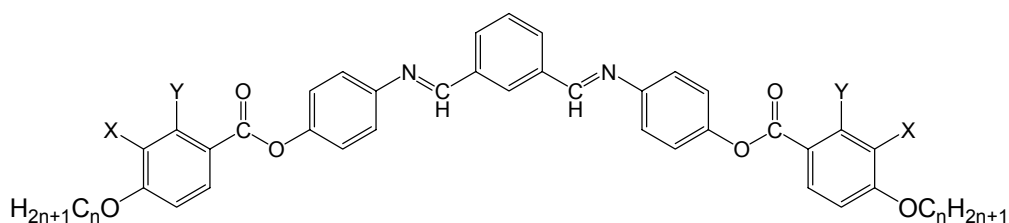


Fig. 6.4 General scheme of isophthalaldene bis[4-(4- n -alkoxybenzoyloxy)anilines] investigated by Bedel et al. [74]

Bedel et al. studied the effect of lateral fluoro-substitution on 1,3-bis [4-(4- n -alkoxybenzoyloxy) phenyliminomethyl] benzene (Fig. 6.4) [74]. They found that the position of the fluoro-substituent essentially influences the mesophase character. If the outer rings are substituted in position 3 ($X=F$) the mesophase character changes. If $Y=F$

the materials exhibit the same kind of mesophase as the non-fluorinated ones. The same tendency was found for the resorcinol derivatives presented in this work. They prepared the difluorinated compounds ($X=Y=F$) and showed that these substances display the same mesophase as the compounds where $X=F$. They calculated the charge distribution over the molecules, but it does not seem to have any connection with the phase character. Conversely there is a significant difference between the charge distributions of the molecules exhibiting the same mesophase.

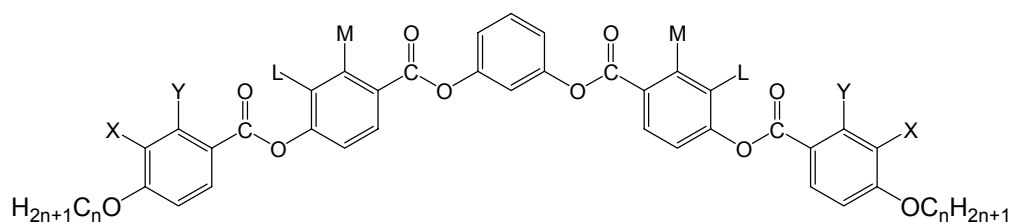


Fig. 6.5 General scheme of 1,3-phenylene bis[4-(4-n-alkoxybenzoyloxy)benzoate] [75]

Another extensive study of fluoro substitution was made on ester-type (containing only ester connecting groups) bent-shaped mesogens (Fig. 6.5) [75]. These ester-type bent mesogens do not have rich variety of mesophases: the short-chain homologue ($n=6$) exhibit B_1 , the long-chain homologue ($n=14$) SmCP (B_2) mesophase. Fluoro-substitution influenced adversely the mesophase behavior. Either the same kind of mesophase appears as in the non-fluorinated substance and the mesophase stability undermines (e.g. $M=F$, $Y=F$, $M=Y=F$) or the substance is not liquid crystal (e.g. $L=F$, $X=L=F$, $Y=L=F$). Additionally in most of the cases increasing the number of fluoro-substituents leads to the loss of liquid crystalline character ($X=L=F$, $Y=L=F$).

It is worthy noting that bent-shaped compounds with azomethine connecting group could provide a more favorable phase behavior through fluoro-substitution than ester-type bananas.

By and large, the influence of fluorination on bent-shaped compounds crucially depends on the position and the number of the fluoro-substituents. In addition it is not predictable how substitution of the central ring and lateral fluorination together affect on the phase behavior. That is why investigation of the influence of lateral substitution of bent-core molecules on liquid crystalline properties is of keen interest.

All in all resorcinol derivatives introduced in this work show unique mesomorphic character, there is no other substance class of bananas with such varied mesophase behavior. Fluorination on the outer rings of resorcinol bananas, further enrich the spectrum of banana mesophases: theoretically predicted mesophases have been discovered, subphases of switchable mesophases have been found.

Regrettably, we could not investigate the effect of lateral substitution on *m*-phenylenediamine derivatives (**28**, **29**) because these materials are unstable. According to the microscopic observations, some of the compounds (**28.1**, **28.2**, **28.3**, **28.5**, **29.1**, **29.3** and **29.5**) exhibit B₁ phase.

Studying the influence of terminal chains on isophthalydene derivatives novel observations could be made. If the terminal chains have electron donating effect (**30.1-30.8** and **W1**) the substances are mesogenic: new B₄-B₂ polymorphism occurs. At the same time, compounds with electron withdrawal terminal moieties are not liquid crystalline. In the meantime, Bedel et al. reported about mesogenic five-ring bent-shaped compounds with electron withdrawal alkyloxycarbonyl terminal chains [76]. However, those bananas differ from our isophthalydene derivatives in the position and directing of the linking groups, too. Broadly speaking, we ought to consider the bent molecules as a whole; the effect of the building stones – connecting groups, terminal chains, etc. – cannot be sharply distinguished.

Chapter 7 Summary

Bent-shaped liquid crystals represent a challenging field of condensed matter. Up to the discovery of the unique mesophase character of bent-shaped compounds only chiral mesogens exhibited ferro- and antiferroelectric switchable mesophases suitable for application. On the other hand, bent-core molecules, consisting of at least five, usually aromatic, rings, create a very complex system. Calculation and modeling of such systems can be made with limitations and simplifications. Therefore to obtain reliable predictions concerning structure-property relationship our factual knowledge need to be broadened. Numerous bent-core substances were prepared to make a better understanding on the connection between the structure and mesomorphic character of banana-shaped molecules.

Symmetrical bent-core materials derived from resorcinol and substituted resorcinols fluorinated on the outer rings in different positions were synthesized. Fluoro-substituents were introduced for two reasons: to investigate the influence of fluoro-substitution on the mesophase behavior in “bananas”, and to make it possible to apply ^{19}F -NMR technique for characterization of bent-core substances. Similarly, deuterated banana compounds were synthesized to get more information about banana mesophases with the help of ^2H -NMR.

Even the fluorinated 4-(4-*n*-alkyloxyphenyliminomethyl)benzoic acid intermediates (Fig. 7.1) have interesting liquid crystalline properties.

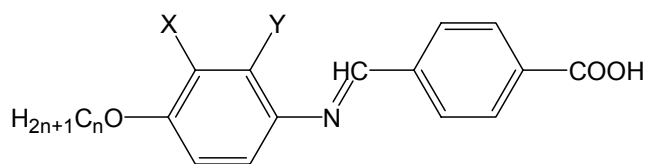


Fig. 7.1 General scheme of fluorinated 4-(4-*n*-alkyloxyphenyliminomethyl)benzoic acids (5, 6)

The compounds where $X=\text{F}$ (**5.1-5.5**), by contrast to the non-fluorinated analogues [40], exhibit two smectic mesophases: SmC and SmX. The latter is a new smectic mesophase not found in other substances before.

In the final step of the synthesis resorcinol derivatives fluorinated on the outer rings (Fig. 7.2) have been obtained.

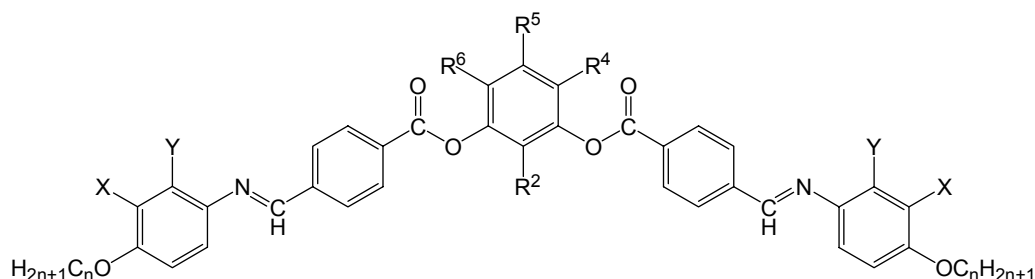


Fig. 7.2 General formula of substituted 1,3-phenylene bis[4-(4-n-alkyloxy-2/3-fluoro-phenyliminomethyl) benzoates] (9-24)

The liquid crystalline character of these compounds is mostly determined by the substituent(s) on the central ring. For this reason the mesophase behavior of the substances will be marshaled regarding this fact.

Both kinds of fluorinated resorcinol derivative substances ($R^n=H$) [89, 90] exhibit switchable SmCP (B_2) phase as the non-fluorinated compounds [1, 2]. If $X=F$ (9.1-9.5) additional low-temperature B_4 and high-temperature SmC_G phases appear.

The 2-nitroresorcinol derivatives ($R^2=NO_2$) independently of the position of the fluoro-substituent ($X=F$: 11.1 and 11.2; $Y=F$: 12.1 and 12.2) exhibit B_7 phase as the non-fluorinated substances [30]. Fluorination in position 2 on the outer rings decreases the clearing point what eases the performance of physical investigations.

Fluorination radically effects on the phase behavior of 2-methylresorcinol derivative bananas ($R^2=CH_3$). The octyloxy homologue of the non-fluorinated substance [26] exhibit B_5 and SmCP (B_2) mesophases, the long-chain homologue ($n=12$) SmCP (B_2) phase [2]. Fluorination in position 2 ($Y=F$) on the outer rings negatively affects the mesophase character: the octyloxy homologue (14.1) appears with B_1 phase only on cooling, the dodecyloxy homologue (14.2) exhibit SmCP (B_2) phase. As poor the compounds 14.1 and 14.2 are in phase transitions as rich polymorphism occurs if fluorine is introduced in position 3 ($X=F$) on the outer rings (13.1-13.5). These compounds exhibit a low-temperature B_5 and polymorphic SmCP (B_2 , B_2'' , B_2''' , B_2'''') mesophases. The latter differ in d-values from each other.

Both kinds of fluorinated 4-cyanoresorcinol derivative ($R^4=CN$) exhibit a high-temperature SmA (**16.1** an additional nematic) and a low-temperature switchable smectic phase. If the outer rings are fluorinated in position 2 ($Y=F$, **16.1** and **16.2**), tilted smectic i.e. SmCP (B_2) phase emerges, while if $X=F$ (**15.1-15.5**) orthogonal smectic i.e. SmAP (C_{PA}) phase appears. These are the first substances proved to exhibit SmAP mesophase.

The fluorinated 4-chlororesorcinol derivatives ($R^4=Cl$) (**17.1**, **17.2**, **18.1** and **18.2**) exhibit SmCP mesophase as well as the non-fluorinated ones [64]. Fluorination in any position on the outer rings undermines the stability of SmCP phase. If $X=F$ the dodecyloxy homologue (**17.2**) exhibit high-temperature SmA, if $Y=F$ the octyl-oxy homologue (**18.1**) nematic mesophase. This is the first instance for a nematic SmCP phase transition. Note that here the mesophase behavior of substances where $Y=F$ (**18**) is more unique than in case of the compounds where $X=F$ (**17**).

The 4,6-dichlororesorcinol derivatives ($R^4=R^6=Cl$) fluorinated on the outer rings in position 2 ($Y=F$, **20.1** and **20.2**) exhibit only mesophases typical for calamitic compounds: nematic and smectic C phases. This kind of mesophase character was found for the non-fluorinated substances [40], too. At the same time if fluoro-substituent is introduced in position 3 ($X=F$, **19.1-19.5**) low-temperature SmCP (B_2) phase arises on cooling. However, the bending angle α between the wings of the molecules in this mesophase is still much wider (145 degrees) than usually in SmCP phase (115-120 degrees) in the case of other compounds.

Also the first mesogenic 5-substituted-resorcinol derivatives with alkyloxy terminal chains have been introduced in this work. The 5-fluoresorcinol derivatives ($R^5=F$, **23.1** and **23.2**) exhibit SmCP (B_2) mesophase. The compounds fluorinated on the outer rings in position 3 ($X=F$, **21.1-21.5**) arise with additional polymorphic B_5 phases: one of them is ferroelectric (B_{5F}), the other is antiferroelectric (B_{5AF}). Fluorination on the outer rings in position 2 ($Y=F$) drastically decreases ($n=12$, **22.2**) the mesophase stability. Liquid crystalline properties even vanish in the case of the octyloxy homologue ($n=8$, **22.1**). Resorcinol derivatives sensitively respond to substitution in position 5: the 5-chloro-resorcinol derivative **24** ($R^5=Cl$, $X=Y=H$) is not liquid crystalline. If R^5 is different from H or F, in other words the substituent is more voluminous than H or F

the compound is not liquid crystalline anymore in case of five-ring bent-shaped compounds.

The structure of the central ring in resorcinol derivative bent-core substances determines the mesophase character (Table 7.1). Fluorination on the outer rings brings about changes as follows:

- the clearing points decrease or does not change remarkably ,
- new switchable mesophases appear if X=F: either subphases arise ($R^2=CH_3$, $R^5=F$) or SmCP phase emerges ($R^4=R^6=Cl$),
- except for 4-chloro-resorcinol derivatives ($R^4=Cl$) fluorination on the outer rings in position 2 ($Y=F$) unfavorably while in position 3 ($X=F$) favorably influences the mesophase behavior.

Sign.	R ⁿ	mesophase	α (deg)	S
10.1	H	SmCP	118-120	0.82
13.1d	2-CH ₃	B ₅ , SmCP*	117	0.84-0.88
15.1	4-CN	SmA	142	0.70-0.76
		SmAP	132	0.76-0.84
17.1	4-Cl	SmCP	131	0.77-0.83
19.5	4,6-Cl,Cl	SmA	~180	0.57-0.60
		SmC	>175	0.60-0.66
		SmCP	142-172	0.66
21.5	5-F	B ₅ [#] , SmCP	116-118	0.85-0.90

* polymorphic SmCP phases

[#] polymorphic B₅ phases

Table 7.1 Mesophases, bending angle and order parameter of selected fluorinated compounds

NMR studies elucidated that substituents in positions R², R⁴, R⁵ and R⁶ have an effect on the bending angle between the two wings of the bent-shaped molecules. NMR investigations highlighted an additional relation between the bending angle and the order parameter in SmCP phase: the smaller the bending angle α the higher ordered the

mesophase is. We should take into consideration that smaller bending angle means larger sterical moment what results in a stronger inhibition in the rotation about the long molecular axis and this net effect produces a higher order in the phase.

Materials derived from *m*-phenylenediamine substituted on the central ring with and without fluoro-substituent in position Q on the middle rings have been synthesized (Fig. 7.3).

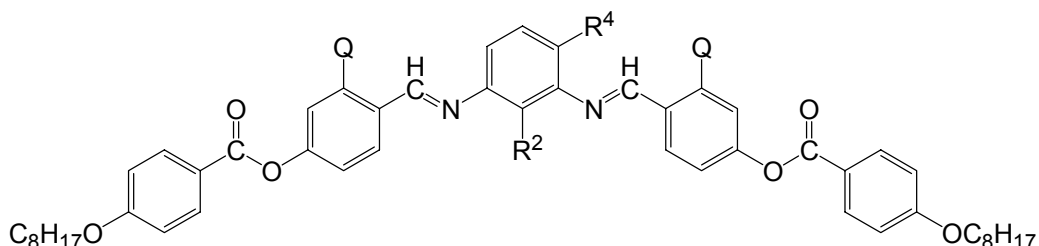


Fig. 7.3 General formula of *N,N'*-bis[4-(4-*n*-octyloxybenzoyloxy)benzylidene] phenylene-1,3-diamines (**28**, **29**)

This combination of the connecting groups does not seem to be very promising. The substances either exhibit B_1 mesophase or do not show mesophase behavior at all ($R^4 = \text{NO}_2$, **28.4** and **29.4**). Unfortunately, these substances are instable and therefore not suitable for further investigations.

Symmetrical bent-core substances derived from isophthalaldehyde (Fig. 7.4) have been synthesized with varied terminal chains.

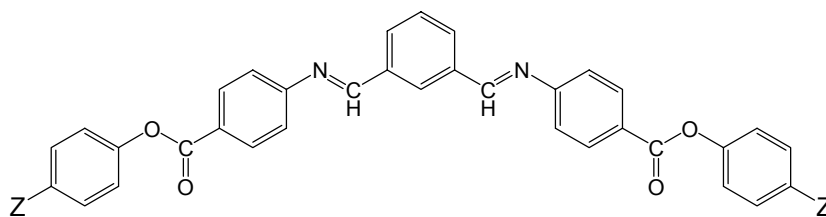


Fig. 7.4 General formula of isophthalaldehyde bis[4-(4-subst.-phenyloxycarbonyl)anilines] (**30**)

Mesogenic character (SmCP and B_4 phases) occurs only if the terminal chains have electron donating effect (alkyl- and alkyloxy chains), whilst materials with electron withdrawing terminal chains (alkanoyl- or alkyloxycarbonyl- or cyanoethyl- or cyano terminal substituents) do not exhibit liquid crystalline mesophases.

Among others, the following new compounds with especially interesting mesophase behavior have been presented in this work:

- the first compounds (**15.1-15.5**) with SmAP phase,
- substances exhibit SmC_G phase (**9.1-9.5**),
- the first mesogens have polymorphic SmCP phases (**13.1-13.5**),
- the first liquid crystalline materials display ferro- and polymorphic antiferroelectric B₅ phases (**21.1-21.5**),
- the first compound undergoes nematic SmCP transition (**18.1**).

To sum up introduction of fluoro-substituent on subst.-1,3-phenylene bis[4-(4-n-alkyloxyphenyliminomethyl)benzoates] has been a remarkably successful project. Accordingly, bent-core substances substituted on the central as well as on the outer rings have been maintaining interest.

Zusammenfassung

Bananen-förmige Flüssigkristalle stellen eine neue Herausforderung auf dem Gebiet der kondensierten Materie dar. Einige der von gebogenen Molekülen gebildeten Mesophasen besitzen ferroelektrische Eigenschaften, ein Verhalten, welches bisher nur an chiralen Verbindungen beobachtet wurde. Zusammenhänge zwischen der chemischen Struktur und den resultierenden physikalischen Eigenschaften sind von grundlegendem Interesse. Da die aus fünf oder mehr aromatischen Ringen bestehenden, gebogenen Mesogene recht komplizierte Systeme darstellen, können Berechnung und Modellierung nur mit erheblichen Vereinfachungen durchgeführt werden. Um weiterreichende Aussagen über die Beziehungen zwischen der Struktur und den flüssigkristallinen Eigenschaften bananen-förmiger Flüssigkristalle zu ermöglichen, ist die Synthese und Untersuchung zahlreicher neuer Verbindungen unumgänglich.

In der vorliegenden Arbeit wurden gebogene Mesogene synthetisiert, die sich im wesentlichen von Resorcin bzw. substituierten Resorcinen ableiten und an den äußeren Phenylringen in verschiedenen Positionen mit Fluor substituiert sind. Die Auswahl von Fluoratomen als laterale Substituenten erfolgte aus zwei Gründen. Zum einen sollte deren Einfluss auf das Mesophasenverhalten untersucht werden. Zum anderen ermöglicht dieses Halogen eine Charakterisierung der Mesophasen durch die ^{19}F -NMR Spektroskopie im kristallin-flüssigen Zustand. Mit der gleichen Zielstellung wurden auch deuterierte Verbindungen synthetisiert.

Bereits die als Zwischenprodukte hergestellten fluorierten 4-(4-n-Alkyloxyphenyliminomethyl)benzoesäuren (Fig. 7.1) weisen interessante kristallin-flüssige Eigenschaften auf.

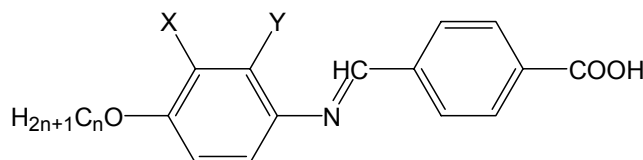


Fig. 7.1 Fluorierte 4-(4-n-Alkyloxyphenyliminomethyl)benzoesäuren

Die Verbindungen (**5.1-5.5**) mit $X = F$ besitzen zwei smektische Mesophasen: SmC und SmX und unterscheiden sich damit deutlich von den nicht-fluorierten Substanzen [40]. Die SmX-Phase ist neu, konnte jedoch noch nicht umfassend charakterisiert werden.

Die Umsetzung dieser Benzoesäuren mit entsprechend substituierten Resorcinen führte zu Verbindungen der folgenden allgemeinen Struktur:

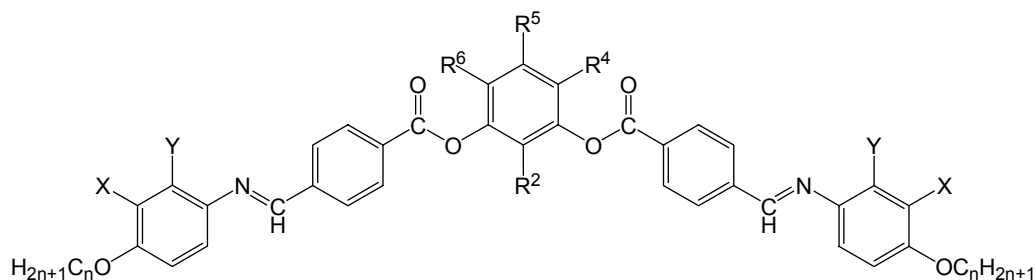


Fig. 7.2 Allgemeine Formel der substituierten 1,3-Phenylen-bis[4-(4-n-alkoxy-2/3-fluorophenyliminomethyl)benzoate] (**9-24**)

Die kristallin-flüssigen Eigenschaften werden wesentlich vom Substituentenmuster am zentralen Ring bestimmt, weshalb nachfolgend das Mesophasenverhalten unter diesem Aspekt zusammengefasst werden soll.

Ausgehend vom Resorcin ($R^n = H$) [89, 90] zeigen beide Serien (X bzw. $Y = F$) eine schaltbare SmCP (B_2) Phase wie die nicht-fluorierten Substanzen [1, 2]. Befindet sich jeweils ein Fluoratom in Position $X = F$ (**9.1-9.5**), so treten zusätzlich eine B_4 -Phase bei tieferen Temperaturen sowie eine Hochtemperatur SmC_G Phase auf. Die Eigenschaften und Phasenstruktur der letztgenannten Phase sind derzeit von besonderem Interesse.

Die 2-Nitroresorcinderivate ($R^2 = NO_2$) zeigen unabhängig von der Position der Fluoratome ($X = F$: **11.1** und **11.2**; $Y = F$: **12.1** und **12.2**) B_7 Phasen ebenso wie die entsprechenden nicht-fluorierten Verbindungen [30]. Einführung von Fluor in Position 2 der äußeren Ringe ($Y = F$) erniedrigt die Klärtemperaturen, was die Durchführung physikalischer Messungen erleichtert.

Das Mesophasenverhalten der 2-Methylderivate ($R^2 = CH_3$) wird durch die Einführung von Fluoratomen deutlich verändert. Während für das unfluorierte Octyloxy-Homologe erstmals eine B_5 - SmCP (B_2) Polymorphie beschrieben wurde [26], bewir-

ken Fluorsubstituenten in Position 2 der äußeren Ringe ($Y=F$) ein Verschwinden der B_5 Phase. Für das Octyloxy-Homologe (**14.1**) konnte lediglich eine B_1 Phase beim Abkühlen beobachtet werden, die Dodecyloxy-Verbindung (**14.2**) zeigt eine SmCP (B_2) Phase. Falls jedoch Fluor in Position 3 ($X=F$) eingeführt wird (**13.1-13.5**), so treten bisher unbekannte, einzigartige Polymorphie-Varianten auf. Die Verbindungen zeigen eine Niedrigtemperatur B_5 Phase und mehrere polymorphe SmCP (B_2 , B_2'' , B_2''' , B_2'''') Phasen. Die Phasenstrukturen der verschiedenen B_2 Phasen sind im Detail unbekannt. Gefunden wurde u.a., dass die Schichtdicke (d-Werte) unterschiedlich sind.

Beide Serien von fluorierten 4-Cyanoresorcinderivaten ($R^4=CN$) weisen eine Hochtemperatur SmA Phase (**16.1** zusätzlich eine nematische) sowie eine schaltbare smektische Tieftemperaturphase auf. Falls die äußeren Ringe in Position 2 ($Y=H$) fluoriert wurden (**16.1** und **16.2**), erscheint eine „geneigte“ SmCP Phase, während im Falle von $X=F$ (**15.1-15.5**) eine orthogonal smektisch Phase beobachtet wurde. Letztgenannte konnte als SmAP (C_{PA}) Phase zugeordnet werden, womit die Existenz dieser theoretisch vorhergesagten Phase erstmals bewiesen werden konnte.

Die fluorierten 4-Chlorresorcinderivate ($R^4=Cl$) (**17.1**, **17.2**, **18.1** and **18.2**) zeigen SmCP Mesophasen in Analogie zu den fluorfreien Verbindungen [64]. Die Einführung von Fluor in die äußeren Ringe erhöht die Mesophasenstabilität der SmCP Phase. Falls $X=F$, so zeigt das Dodecyloxy-Homologe (**17.2**) zusätzlich ein Hochtemperatur SmA Phase. Falls $Y=F$, so tritt beim Octyloxy-Derivate zusätzlich eine nematische Mesophase auf. Dies war das erste Beispiel für eine nematisch-SmCP Phasenumwandlung. Damit besitzen ausnahmsweise die in Position 2 fluorierten Verbindungen interessantere Phasensequenzen als die in Position 3 fluorierten Substanzen.

Die 4,6-Dichlorresorcinderivate ($R^4=R^6=Cl$), fluoriert in Position 2 ($Y=F$) der äußeren Ringe, zeigen ebenso wie die unfluorierten Verbindungen [40] ein für calamitische Flüssigkristalle typisches Verhalten, d.h. nematische und smektische C Phasen. Eine SmCP Phase wurde beim Unterkühlen der Verbindungen mit $X=F$ (**19.1-19.5**) beobachtet.

Mit den 5-Fluorresorcinderivaten **21-23** werden die ersten kristallin-flüssigen Fünfkern-Mesogene vorgestellt, die lediglich Alkyloxygruppen in den terminalen Positionen haben und an der Spitze der gebogenen Moleküle substituiert sind.. Die Verbindungen **23.1** and **23.2** ($R^5=F$) besitzen keine Halogenatome an den äußeren Ringen und

weisen eine SmCP Mesophase auf. Die Substanzen **21.1-21.5**, fluoriert an den äußeren Ringe in Position 3 ($X=F$), zeigen zusätzlich zur SmCP Phase weitere polymorphe B_5 Phasen. Davon ist eine ferroelektrisch (B_{5F}), die anderen sind antiferroelektrisch (B_{5A}). Fluorierung in Position 2 ($Y=F$) verringert drastisch die Mesophasenstabilität. Das Octyloxy-Homologe ($n=8$, **22.1**) ist z.B. gar nicht flüssig-kristallin. Wie empfindlich gebogene Fünfkern-Mesogene auf Substituenten in Position R^5 reagieren, wird durch die Tatsache belegt, dass für das 5-Chlorresorcinderivat **24** ($R^5=Cl$, $X=Y=H$) keine flüssig-kristallinen Eigenschaften nachgewiesen werden konnten.

In den von uns untersuchten Resorcinderivaten wird das kristallin-flüssige Verhalten ganz wesentlich vom Substituentenmuster am zentralen Ring bestimmt, wie an ausgewählten Beispielen in Tabelle 7.1 gezeigt wird. Eine Substitution der äußeren Ringe mit Fluoratomen bewirkt die folgenden Änderungen:

- Die Klärtemperaturen werden meist erniedrigt, können aber auch nahezu unverändert bleiben.
- In den meisten Fällen führte die Substitution der 3-Position der äußeren Ringe mit Fluoratomen zu neuen Phasen bzw. interessanteren Phasensequenzen als eine Substitution in 2-Position.
- Schaltbare B_2 bzw. B_5 Subphasen können auftreten wenn $R^2=CH_3$ bzw. $R^5=F$ und $X = F$ ist
- Hingegen ist eine Fluorsubstitution der Position 2 der äußeren Ringe ($Y=F$) nicht so attraktiv, abgesehen von den 4-Chlorresorcinderivaten ($R^4=Cl$), welche eine nematisch- B_2 Phasensequenz aufweisen können.

NMR Untersuchungen belegen, dass der Biegungswinkel zwischen den beiden Schenkeln der bananen-förmigen Moleküle durch Substituenten in den Positionen R^2 , R^4 und R^6 beeinflusst wird. Weiterhin gibt es einen interessanten Zusammenhang zwischen dem Biegungswinkel und Ordnungsgrad, wie aus Tab. 7.1 zu ersehen ist. Je kleiner der Biegungswinkel α , desto höher ist der Ordnungsgrad in den smektischen Phasen. Demnach kann man annehmen, dass bei Molekülen mit kleinerem Biegungswinkel die sterischen Effekte an Bedeutung gewinnen. Es wird eine Rotation um die Molekül-längsachse behindert und eine dichtere polare Packung begünstigt.

Sign.	R ⁿ	Mesophase	α (deg)	S
10.1	H	SmCP	118-120	0.82
13.1d	2-CH ₃	B ₅ , SmCP*	117	0.84-0.88
15.1	4-CN	SmA	142	0.70-0.76
		SmAP	132	0.76-0.84
17.1	4-Cl	SmCP	131	0.77-0.83
19.5	4,6-Cl,Cl	SmA	~180	0.57-0.60
		SmC	>175	0.60-0.66
		SmCP	142-172	0.66
21.5	5-F	B ₅ [#] , SmCP	116-118	0.85-0.90

* polymorphe SmCP Phasen

polymorphe B₅ Phasen

Table 7.1 Mesophasen, Biegungswinkel und Ordnungsgrade ausgewählter fluorierter Verbindungen

m-Phenylenediaminderivate, substituiert am zentralen Ring und mit bzw. ohne Fluorsubstituent in Position Q der mittleren Ringe wurden ebenfalls hergestellt (Fig. 7.3).

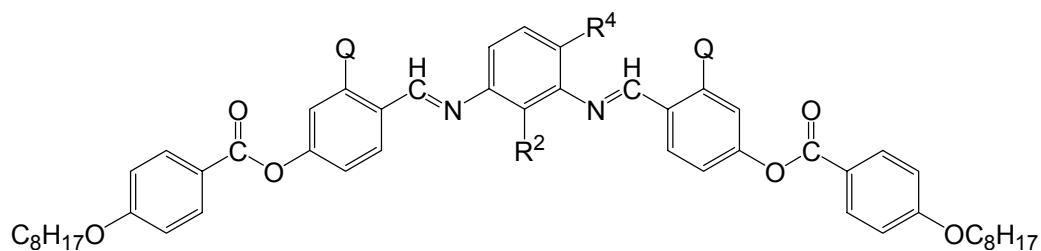


Fig. 7.3 N,N'-bis[4-(4-n-Octyloxybenzoyloxy)benzylidene] phenylene-1,3-diamine (**28**, **29**)

Diese Kombination der Verknüpfungsgruppen ist jedoch wenig Erfolg versprechend. Die Substanzen, die entweder B₁ Phase zeigen oder nicht flüssigkristallin sind (R⁴=NO₂, **28.4** and **29.4**), sind auf Grund mangelnder Stabilität für weitere Untersuchungen ungeeignet.

Symmetrische Isophthalaldehydderivate **30** (Fig. 7.4) enthalten die gleichen Verknüpfungsgruppen, jedoch in umgekehrter Richtung. Es wurde der Einfluss verschiedener Flügelgruppen untersucht.

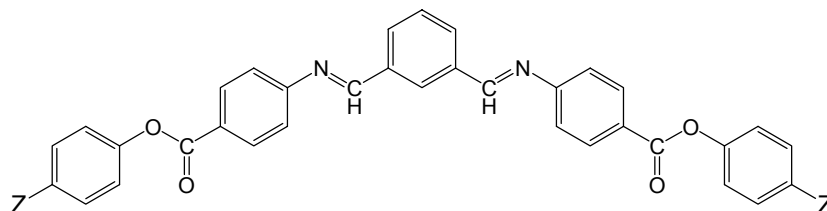


Fig. 7.4 Isophthalaldehyde bis[4-(4-subst.-phenoxy)benzoate] (**30**)

Die Verbindungen, in denen die Flügelgruppen Elektronendonator-Eigenschaften aufweisen (Alkyl- und Alkyloxy-Ketten), sind flüssig-kristallin, während Substanzen mit elektronenziehenden terminalen Substituenten (Alkanoyl- und Alkyloxycarbonyl-, Cyanoethyl- bzw Cyan-Gruppen) nicht flüssig-kristallin sind.

Im Rahmen der vorliegenden Arbeit wurden erstmalig gefunden

- Verbindungen (**15.1-15.5**) mit einer SmAP Phase,
- Substanzen (**9.1-9.5**) mit einer SmC_G Phase,
- Verbindungen mit polymorphen SmCP (B₂) Phasen (**13.1-13.5**),
- Flüssigkristalle mit polymorphen B₅ Phasen sowie einem Phasenübergang zwischen einer ferro- und einer antiferroelektrischen B₅ Phase (**21.1-21.5**),
- eine Substanz mit einem SmCP-nematisch Übergang (**18.1**).

Zusammenfassend kann festgestellt werden, dass sich die Einführung von Fluoratomen in die äußeren Phenylringe von substituierten 1,3-Phenyl-bis[4-(4-n-alkyloxyphenyliminomethyl)benzoaten] als ein sehr erfolgreiches Konzept erwiesen hat. Somit werden bananen-förmige Verbindungen, die sowohl am zentralen Ring als auch an den äußeren Ringen substituiert sind, auch weiterhin von großem Interesse sein.

Chapter 8 Experimental part

The following substances were available in the laboratory:

4-cyanoresorcinol	3-(4-hydroxyphenyl)propionitrile
4-n-alkyloxyphenols	4-n-octyloxybenzoic acid 4-
4-n-alkylphenols	formylphenylester
4-n-alkanoylphenols	1,3-phenylene bis(4-methylimino-
4-n-octyloxybenzoic acid	benzoic acid)
4-hydroxybenzoic acid n-alkylester	

The following substances were commercially available:

n-alkanols (Acros)	boron tribromide in 1M CH ₂ Cl ₂ solution (Aldrich)
n-octylbromide (Lancaster)	sodium chloride (Merck)
4-hydroxybenzonitrile (Aldrich)	resorcinol (Aldrich)
2-fluoro-4-nitrophenol (Acros)	2-nitroresorcinol (Aldrich)
3-fluoro-4-nitrophenol (Acros)	2-methylresorcinol (Aldrich)
formylbenzoic acid (Merck)	4-chlororesorcinol (Aldrich)
triphenylphosphine (Acros)	4,6-dichlororesorcinol (Aldrich)
diethyl azodicarboxylate (Lancaster)	N,N'-dicyclohexylcarbodiimide (Fluka)
silica gel 0.063- 0.200 mm (J. T. Baker)	4-dimethylaminopyridine (Ferak)
potassium carbonate (Merck)	2-fluoro-4-methoxybenzaldehyde (Lancaster)
sodium hydroxide (Merck)	2,4-dinitro-fluorobenzene (Aldrich)
chloroform-d (Chemotrade)	2,4-diaminotoluene (Lancaster)
dimethylsulfoxide-d ₆ (Chemotrade)	2,6-diaminotoluene (Lancaster)
sodium sulfate (Merck)	m-phenylenediamine (Reachim)
Pd on activated carbon (Aldrich)	4-nitro-m-phenylenediamine (Lancaster)
1-fluoro-3,5-dimethoxybenzene (Aldrich)	
1-chloro-3,5-dimethoxybenzene (Acros)	

Physical measurements were performed on the instruments given in the following. The microscopic observations were made using polarizing microscope Nikon Labophot-2A

equipped with Linkam TP 92 heating stage. Photos were taken with the help of a Nikon F-601 camera.

The calorimetric measurements were performed on a Perkin-Elmer Pyris 1 differential scanning calorimeter.

The NMR spectra were taken on Varian VXR 400 and Varian Unity 500.

The mass spectra were taken on the instrument AMD 402 (Intectra GmbH).

The elemental analysis was made by the instrument CHNS-932 (Leco Co.).

Thin layer chromatography was made on aluminium sheets covered by silica gel 60 F₂₅₄ (Merck).

You will find analytical data given for one instance of each serie below. The rest is available in the working group of Professor Weissflog.

8.1 Substituted fluorinated 1,3-phenylene bis[4-(4-n-alkyloxy-phenylimino-methyl)benzoates] (9-24)

8.1.1 4-n-Alkyloxy-2/3-fluoro-nitrobenzene (1, 2)

8.1.1.1 Mitsunobu etherification

32 mmol (5 g) 2/3-Fluoro-4-nitrophenol, 39 mmol n-alkanol and 39 mmol (9.8 g) triphenylphosphine (PPh₃) were dissolved in abs. tetrahydrofuran (THF). The reaction mixture was cooled down to 0°C (ice-water bath) and 50.5 mmol (8.0 ml) diethyl azodicarboxylate (DEAD) diluted with 32 ml THF was dripped to it. After giving all DEAD to the reaction mixture it was stirred at room temperature for about twenty four hours. The solvent was evaporated, and diethylether was given to the crude product. White precipitation (triphenylphosphine oxide, O=PPh₃) forms after two days. It was filtered out, the solvent was evaporated. The crude product was purified by column chromatography: silica gel, eluent: ethylacetate:heptane=1:2.5. Yield: 61-70%.

8.1.1.2. Williamson etherification

32 mmol (5 g) 2/3-Fluoro-4-nitrophenol was dissolved in dry dimethylformamid (DMF) or dry acetone. 34 mmol n-alkylbromide, pulverized potassium carbonate and catalytic

amount potassium iodide were given to it. The reaction mixture was heated under reflux for 40-50 hours. The cold reaction mixture was poured into water. It was extracted with ether twice. The unified ether phases were extracted with 0.1 N sodium hydroxide (NaOH) solution so many times that the inorganic layer is not yellow anymore. Afterward, it was extracted with water and dried over sodium sulphate (Na₂SO₄) overnight. The crude product was purified by column chromatography (octyl and nonyloxy derivatives) or recrystallized from ethanol. Yield: 53-90%.

Sign.	Name	Melting point (°C)	Yield (g/%) [§]
1.1	3-fluoro-4-n-octyloxy-nitrobenzene	yellow oil [#]	7.76/90
1.2	3-fluoro-4-n-nonyloxy-nitrobenzene	yellow oil [~]	*
1.3	4-n-decyloxy-3-fluoro-nitrobenzene	25.4	5.80/61
1.4	3-fluoro-4-n-undecyloxy-nitrobenzene	26	5.68/57
1.5	4-n-dodecyloxy-3-fluoro-nitrobenzene	38	5.52/53

[§] The yields are given for the Williamson etherification.

[#] purified by chromatography (ethylacetate:heptane= 1:2.5, silica gel) *R_f*: 0.50

[~] *R_f*: 0.49 in ethylacetate:heptane= 1:2.5 on silica sheet

* According to the NMR spectra the crude product was pure, therefore the raw product was used in the next step.

4-n-Dodecyloxy-3-fluoro-nitrobenzene (1.5)

¹H-NMR (400 MHz, CDCl₃) δ (ppm) / *J*(Hz) 8.01 (dd-dd, 1H, ³*J*= 8.9, ⁴*J*= 2.7, ⁵*J*_{H-F}= 1.6, Ar-H), 7.94 (dd, 1H, ⁴*J*= 2.7, ³*J*_{H-F}= 10.6, Ar-H), 6.99 (dd, 1H, ³*J*= 8.9, ⁴*J*_{H-F}= 8.1, Ar-H), 4.10 (t, 2H, ³*J*= 6.5, OCH₂), 1.81-1.88 (m, 2H, OCH₂CH₂), 1.20-1.56 (m, 18H, (CH₂)₉CH₃), 0.84-0.87 (m, 3H, CH₃)

¹³C-NMR (100 MHz, CDCl₃) δ (ppm) / *J*(Hz) 152.99 (d, ^o*J*_{C-F}= 10.7), 151.30 (d, ⁱ*J*_{C-F}= 251.6), 140.58 (d, ^m*J*_{C-F}= 7.7), 120.78 (d, ^p*J*_{C-F}= 3.7), 112.9 (d, ^m*J*_{C-F}= 2.2), 112.19 (d, ^o*J*_{C-F}= 22.8), 69.96 (AlkC1), 31.91 (AlkC2), 29.63 (AlkC3), 29.62 (AlkC4), 29.55 (AlkC5), 29.50 (AlkC6), 29.33 (AlkC7), 29.26 (AlkC8), 28.90 (AlkC9), 25.81 (AlkC10), 22.68 (AlkC11), 14.08 (AlkC12)

EIMS m/z (rel. int) 325 (20), 168 (40), 157 (9), 141 (14), 125 (7), 111 (21), 97 (24), 85 (41), 71 (56), 57 (100)

Elemental analysis: calcd C 66.44; H 8.67; N 4.30 found C 66.5; H 8.5; N 4.3

4-n-Dodecyloxy-2-fluoro-nitrobenzene (2.5)

$^1\text{H-NMR}$ (400 MHz, CDCl_3) δ (ppm) / J (Hz) 8.02-8.08 (m, 1H, $^3J=9.3$, $^4J_{\text{H-F}}=10.8$, Ar-H), 6.67-6.73 (m, 2H, $^3J=9.3$, $^4J=2.7$, $^5J_{\text{H-F}}=0.8$, $^3J_{\text{H-F}}=13.0$, Ar-H), 3.99-4.02 (m, 2H, OCH_2), 1.76-1.83 (m, 2H, OCH_2CH_2), 1.24-1.57 (m, 18H, $(\text{CH}_2)_9\text{CH}_3$), 0.84-0.87 (m, 3H, CH_3)

$^{13}\text{C-NMR}$ (100 MHz, CDCl_3) δ (ppm) / J (Hz) 164.85 (d, $^{\circ}J_{\text{C-F}}=11.0$), 157.43 (d, $^iJ_{\text{C-F}}=264.8$), 130.50 (d, $^{\circ}J_{\text{C-F}}=5.9$), 120.76 (d, $^mJ_{\text{C-F}}=1.5$), 110.67 (d, $^pJ_{\text{C-F}}=2.9$), 103.43 (d, $^{\circ}J_{\text{C-F}}=23.9$), 69.42 (AlkC1), 31.90 (AlkC2), 29.63 (AlkC3), 29.61 (AlkC4), 29.55 (AlkC5), 29.50 (AlkC6), 29.33 (AlkC7), 29.25 (AlkC8), 28.83 (AlkC9), 25.84 (AlkC10), 22.67 (AlkC11), 14.07 (AlkC12)

EIMS m/z (rel. int) 325 (9), 309 (21), 168 (6), 157 (6), 141 (22), 127 (14), 111 (16), 97 (19), 85 (37), 71 (62), 57 (100)

Elemental analysis: calcd C 66.4; H 8.7; N 4.3 found C 66.7; H 8.5; N 4.2

Sign.	Name	Melting point ($^{\circ}\text{C}$)	Yield (g/%) [§]
2.1	2-fluoro-4-n-octyloxy-nitrobenzene	oil [#]	5.27/61
2.2	4-n-dodecyloxy-2-fluoro-nitrobenzene	26.5	5.52/70

[§] The yields are given for the Mitsunobu etherification.

[#] purified by column chromatography (ethylacetate:heptane= 1:1, silica gel) R_f : 0.55

8.1.2 4-n-Alkyloxy-2/3-fluoro-anilines (3, 4)

The nitrobenzene (**1**, **2**) was dissolved in ethylacetate, and 10 m/m% Pd/C (5%) was given to it. After purging the solution with nitrogen, hydrogen was led into it. After two or three hours the reaction is completed. The Pd/C was filtered out and the solvent was

evaporated. The crude product was recrystallized from chloroform with heptane. Yield: 41-66%.

4-n-Dodecyloxy-3-fluoro-aniline (3.5)

$^1\text{H-NMR}$ (500 MHz, DMSO) $\delta(\text{ppm}) / J(\text{Hz})$ 6.79 (dd, 1H, $^3J = 8.7$, $^4J_{\text{H-F}} = 9.6$, Ar-H), 6.37 (dd, 1H, $^4J = 2.5$, $^3J_{\text{H-F}} = 13.8$, Ar-H), 6.26 (dd-dd, 1H, $^3J = 8.7$, $^4J = 2.5$, $^5J_{\text{H-F}} = 1.2$, Ar-H), 4.88 (s, 2H, NH₂), 3.82 (t, 2H, $^3J = 6.5$, OCH₂), 1.60-1.63 (m, 2H, OCH₂CH₂), 1.23-1.37 (m, 18H, (CH₂)₉CH₃), 0.83-0.86 (m, 3H, CH₃).

Sign.	Name	Melting point (°C)	Yield (%)
3.1	3-fluoro-4-n-octyloxy-aniline	54	41
3.2	3-fluoro-4-n-nonyloxy-aniline	55	46
3.3	4-n-decyloxy-3-fluoro-aniline	57.5	66
3.4	3-fluoro-4-n-undecyloxy-aniline	58	60
3.5	4-n-dodecyloxy-3-fluoro-aniline	63	65

4-n-Dodecyloxy-2-fluoro-aniline (4.2)

$^1\text{H-NMR}$ (500 MHz, CDCl₃) $\delta(\text{ppm}) / J(\text{Hz})$ 6.78 (t, 1H, $^3J = 9.0$, $^4J_{\text{H-F}} = 9.5$, Ar-H), 6.61 (dd, 1H, $^4J = 2.5$, $^3J_{\text{H-F}} = 12.5$, Ar-H), 6.53 (dd, 1H, $^3J = 9.0$, $^4J = 2.5$, Ar-H), 3.84 (t, 2H, $^3J = 6.7$, OCH₂), 1.69-1.74 (m, 2H, OCH₂CH₂), 1.25-1.43 (m, 18H, (CH₂)₉CH₃), 0.85-0.88 (m, 3H, CH₃)

EIMS m/z (rel. int) 295 (26), 127 (100)

Sign.	Name	Melting point (°C)	Yield (%)
4.1	2-fluoro-4-n-octyloxy-aniline	oil	*
4.2	4-n-dodecyloxy-2-fluoro-aniline	37.4	60

8.1.3 4-(4-n-Alkyloxy-2/3-fluoro-phenyliminomethyl)benzoic acids (**5**, **6**)

32 mmol (4.8 g) 4-Formylbenzoic acid was dissolved in hot ethanol and 32 mmol 4-n-alkyloxy-2/3-fluoro-aniline (**3**, **4**) was given to it. It was heated under reflux for four hours. The product precipitates cooling down the reaction mixture. The precipitation was filtered out and recrystallized from ethanol at least twice. Yield: 53-85%. Mesogenic behavior see in Table 3.1 and 3.2 in section 3.2.

4-(4-n-Dodecyloxy-3-fluoro-phenyliminomethyl)benzoic acid (5.5)

4.8 g Formylbenzoic acid, 9.4 g 4-n-dodecyloxy-3-fluoro-aniline (**3.5**). The product is white powder. Yield: 7.25 g (53%).

Mesogenic behavior: Cr 114 SmX 169 SmC 146 I

¹H-NMR (500 MHz, DMSO, 70°C) δ (ppm) / J (Hz) 8.72 (s, 1H, CH=N), 8.05 (d, 2H, ³ J = 8.1, Ar-H), 8.00 (d, 2H, ³ J = 8.1, Ar-H), 7.27 (dd, 1H, ³ $J_{\text{H-F}}$ = 12.6, ⁴ J = 2.3, Ar-H), 7.18 (t, 1H, ³ J = 8.8, Ar-H), 7.14 (dd, 1H, ³ J = 8.8, ⁴ $J_{\text{H-F}}$ = 1.6, Ar-H), 4.07 (t, 2H, ³ J = 6.4, OCH₂), 1.71-1.76 (m, 2H, OCH₂CH₂), 1.25-1.45 (m, 18H, (CH₂)₉CH₃), 0.84-0.86 (m, 3H, CH₃)

EIMS m/z (rel. int) 427 (26), 259 (100)

Elemental analysis: calcd C 73.0; H 8.0; N 3.3 found C 72.7; H 8.2; N 3.4

4-(4-n-Dodecyloxy-2-fluoro-phenyliminomethyl)benzoic acid (6.2)

4.2 g Formylbenzoic acid, 8.3 g 4-n-dodecyloxy-2-fluoro-aniline (**4.2**). The product is white powder. Yield: 7.60 g (64%).

Mesogenic behavior: Cr 165 N 237 I

¹H-NMR (500 MHz, DMSO, 50°C) δ (ppm) / J (Hz) 8.76 (s, 1H, CH=N), 8.05 (d, 2H, ³ J = 8.4, Ar-H), 8.01 (d, 2H, ³ J = 8.4, Ar-H), 7.37 (t, 1H, ³ J = 9.1, ⁴ $J_{\text{H-F}}$ = 9.1, Ar-H), 6.89 (dd, 1H, ⁴ J = 2.8, ³ $J_{\text{H-F}}$ = 12.8, Ar-H), 6.80 (dd, 1H, ³ J = 9.1, ⁴ J = 2.8, Ar-H), 3.99 (t, 2H, ³ J = 6.4, OCH₂), 1.67-1.73 (m, 2H, OCH₂CH₂), 1.24-1.43 (m, 18H, (CH₂)₉CH₃), 0.83-0.86 (m, 3H, CH₃)

EIMS m/z (rel. int) 427 (46), 371 (32), 259 (100)

Elemental analysis: calcd C 73.0; H 8.0; N 3.3 found C 72.9; H 8.3; N 3.2

Sign.	Yield (g/%)
5.1	10.10/85
5.2	9.37/76
5.3	8.95/70
5.4	7.01/53
5.5	7.25/59
6.1	7.49/63
6.2	7.60/64

8.1.4 5-Fluororesorcinol (**7a**) and 5-chlororesorcinol (**7b**)

9.6 mmol 1-Halogeno-3,5-dimethoxybenzene was dissolved in dry dichloromethane in a three-neck flask and purged with nitrogen. 29 mmol (29 ml of 1M solution in DCM) boron tribromide was added to the solution under nitrogen atmosphere at room temperature. It was stirred at room temperature in the closed flask for two days. The reaction was quenched with water given drop wise to the reaction mixture stirred for an additional thirty minutes. The mixture was extracted with diethylether twice. The combined organic layer was extracted with brine and water. It was dried over Na_2SO_4 overnight. The solvent was evaporated, and the crude product was recrystallized from toluene.

5-Fluororesorcinol (7a) [84, 85]

1.50 g 1-Fluoro-3,5-dimethoxybenzene, 29 ml 1M solution of BBr_3 . The product is brown crystalline solid. Yield 1.8 g (87.5%). R_f : 0.13 (ethylacetate:heptane= 1:2.5). Melting point: 145°C.

$^1\text{H-NMR}$ (400 MHz, DMSO) δ (ppm) / J (Hz) 5.97 (dd, 2H, $^3J_{\text{H-F}} = 8.8$, $^4J = 2.2$, Ar-H), 6.04 (m, 1H, $^4J = 2.2$, $^5J_{\text{H-F}} = 0.8$, Ar-H), 9.61 (s, 2H, OH)

5-Chlororesorcinol (7b)

1.65 g 1-Chloro-3,5-dimethoxybenzene, 29 ml 1M solution of BBr₃. The product is brown crystalline solid. Yield 1.11 g (80%).

¹H-NMR (400 MHz, DMSO) δ (ppm) / J (Hz) 6.15 (t, 1H, ⁴ J = 2.2, Ar-H), 6.22 (d, 2H, ⁴ J =2.2, Ar-H), 9.65 (s, 2H, OH)

**8.1.5 Substituted 1,3-phenylene bis[4-(4-n-alkoxy-2/3-fluorophenyl-
iminomethyl)benzoates] (9-22)**

1 mmol (Substituted) resorcinol (**7**, **8**), 2 mmol 4-(4-n-alkoxy-2/3-fluorophenyliminomethyl)benzoic acid (**5**, **6**), and 2.4 mmol (0.5 g) N,N'-dicyclohexylcarbodiimide (DCC) were dissolved in dry dichloromethane (DCM). Catalytic amount of 4-dimethylaminopyridine (DMAP) was given to it. It was stirred at room temperature for two days. The precipitation (N,N'-dicyclohexylurea, DCU) was filtered out and the solvent was evaporated. The crude product was recrystallized from dimethylformamid with ethanol, afterward, from toluene with methanol. Yield: 30-72%.

1,3-Phenylene bis[4-(3-fluoro-4-n-octyloxyphenyliminomethyl)benzoate] (9.1)

0.13 g Resorcinol (**8a**), 0.85 g 4-(3-fluoro-4-n-octyloxyphenyliminomethyl)benzoic acid (**5.1**), 0.30 g DCC. The product is yellow powder. Yield 0.45 g (55%).

Mesogenic behavior: Cr 129 (B₄ 98) SmCP 164 SmC_G 166 I

¹H-NMR (400 MHz, CDCl₃) δ (ppm) / J (Hz) 8.52 (s, 2H, CH=N), 8.27 (d, 4H, ³ J = 8.4, Ar-H), 8.01 (d, 4H, ³ J = 8.4, Ar-H), 7.48 (dd, 1H, ³ J = 8.0, Ar-H), 7.22 (dd, 2H, ³ J = 8.0, ⁴ J = 2.2, Ar-H), 7.18 (d, 1H, ⁴ J = 2.2, Ar-H), 7.11 (dd, 2H, ³ J_{H-F} = 12.2, ⁴ J = 2.5, Ar-H), 7.05 (tt, 2H, ³ J = 8.8, ⁴ J = 2.5, ⁵ J_{H-F} = 0.8, Ar-H), 6.98 (t, 2H, ³ J = 8.8, ⁴ J_{H-F} = 8.8, Ar-H), 4.05 (t, 4H, ³ J = 6.6, OCH₂), 1.79-1.86 (m, 4H, OCH₂CH₂), 1.24-1.51 (m, 20H, (CH₂)₅CH₃), 0.86-0.90 (m, 6H, CH₃)

EIMS m/z (rel. int) 816 (16), 354 (100), 213 (24)

Elemental analysis: calcd C 73.5; H 6.7; N 3.4 found C 73.7; H 7.0; N 3.0

1,3-Phenylene bis[4-(2-fluoro-4-n-octyloxyphenyliminomethyl)benzoate] (10.1)

0.11 g Resorcinol (**8a**), 0.85 g 4-(2-fluoro-4-n-octyloxyphenyliminomethyl)benzoic acid (**6.1**), 0.5 g DCC. The product is yellow powder. Yield 0.42 g (52%).

Mesogenic behavior: Cr 127 SmCP 142 I

¹H-NMR (400 MHz, CDCl₃) δ (ppm) / J (Hz) 8.66 (s, 2H, CH=N), 8.27 (d, 4H, ³ J = 8.0, Ar-H), 8.03 (d, 4H, ³ J = 8.0, Ar-H), 6.70-7.52 (m, 10H, Ar-H), 3.95 (t, 4H, ³ J = 6.5, OCH₂), 1.71-1.85 (m, 4H, OCH₂CH₂), 1.24-1.44 (m, 20H, (CH₂)₅CH₃), 0.85-0.90 (m, 6H, CH₃)

EIMS m/z (rel. int) 816 (8), 354 (100), 213 (10)

2-Nitro-1,3-phenylene bis[4-(3-fluoro-4-n-octyloxyphenyliminomethyl)benzoate] (11.1)

0.31 g 2-Nitroresorcinol (**8b**), 1.71 g 4-(3-fluoro-4-n-octyloxyphenyliminomethyl)benzoic acid (**5.1**), 0.30 g DCC. The product is yellow powder. Yield 0.40 g (46.5%).

Mesogenic behavior: Cr (142 B_x) 147 B₇ 169 I

¹H-NMR (400 MHz, CDCl₃) δ (ppm) / J (Hz) 8.52 (s, 2H, CH=N), 8.22 (d, 4H, ³ J = 8.4, Ar-H), 8.01 (d, 4H, ³ J = 8.4, Ar-H), 7.67 (d, 1H, ³ J = 8.3, Ar-H), 7.43 (d, 2H, ³ J = 8.3, Ar-H), 7.11 (dd, 2H, ³ J _{H-F}= 12.1, ⁴ J = 2.4, Ar-H), 7.05 (tt, 2H, ³ J = 8.6, ⁴ J = 2.4, ⁵ J _{H-F}= 1.2, Ar-H), 6.97 (t, 2H, ³ J = 8.6, ⁴ J _{H-F}= 8.8, Ar-H), 4.04 (t, 4H, ³ J = 6.6, OCH₂), 1.78-1.85 (m, 4H, OCH₂CH₂), 1.25-1.50 (m, 20H, (CH₂)₅CH₃), 0.86-0.89 (m, 6H, CH₃)

EIMS m/z (rel. int) 861 (0.7), 508 (12), 371 (25), 354 (43), 259 (100), 242 (31), 213 (19)

2-Nitro-1,3-phenylene bis[4-(2-fluoro-4-n-octyloxyphenyliminomethyl)benzoate] (12.1)

0.19 g 2-Nitroresorcinol (**8b**), 0.85 g 4-(2-fluoro-4-n-octyloxyphenyliminomethyl)benzoic acid (**6.1**), 0.30 g DCC. The product is yellow powder. Yield 0.26 g (30%).

Mesogenic behavior: Cr 81 B₇ 157 I

¹H-NMR (500 MHz, CDCl₃) δ (ppm) / J (Hz) 8.66 (s, 2H, CH=N), 8.22 (d, 4H, ³ J = 8.4, Ar-H), 8.03 (d, 4H, ³ J = 8.4, Ar-H), 6.70-7.43 (m, 9H, Ar-H), 3.95 (t, 4H, ³ J = 6.5,

OCH₂), 1.73-1.76 (m, 4H, OCH₂CH₂), 1.24-1.71 (m, 20H, (CH₂)₅CH₃), 0.84-0.89 (m, 6H, CH₃)

EIMS *m/z* (rel. int) 508 (8), 463 (12), 371 (49), 354 (62), 336 (28), 259 (100), 242 (12), 213 (11), 195 (11), 138 (12), 69 (13)

2-Methyl-1,3-phenylene bis[4-(3-fluoro-4-n-octyloxyphenyliminomethyl)benzoate]
(13.1)

0.3 g 2-Methylresorcinol (**8c**), 1.8 g 4-(3-fluoro-4-n-octyloxyphenyliminomethyl)benzoic acid (**5.1**), 1.2 g DCC. The product is yellow powder. Yield 0.41 g (50%).

Mesogenic behavior on cooling: Cr 103 B_x 112 B₅ 136 B₂' 142 B₂' 147 B₂ 153 I

¹H-NMR (500 MHz, CDCl₃) δ(ppm) / *J*(Hz) 8.66 (s, 2H, CH=N), 8.30 (d, 4H, ³*J* = 8.4, Ar-H), 8.02 (d, 4H, ³*J* = 8.4, Ar-H), 7.32 (d, 1H, ³*J* = 8.1, Ar-H), 7.14 (d, 2H, ³*J* = 8.1, Ar-H), 7.11 (dd, 2H, ³*J*_{H-F} = 12.2, ⁴*J* = 2.5, Ar-H), 7.05 (tt, 2H, ³*J* = 8.7, ⁴*J* = 2.5, ⁵*J*_{H-F} = 1.0, Ar-H), 6.98 (t, 2H, ³*J* = 8.7, ⁴*J*_{H-F} = 8.8, Ar-H), 4.05 (t, 4H, ³*J* = 6.6, OCH₂), 2.13 (s, 3H, Ar-CH₃), 1.79-1.86 (m, 4H, OCH₂CH₂), 1.24-1.51 (m, 20H, (CH₂)₅CH₃), 0.86-0.90 (m, 6H, CH₃)

EIMS *m/z* (rel. int) 830 (12), 354 (100), 242 (31), 213 (34), 69 (12)

2-Methyl-1,3-phenylene bis[4-(2-fluoro-4-n-octyloxyphenyliminomethyl)benzoate]
(14.1)

0.15 g 2-Methylresorcinol (**8c**), 0.85 g 4-(2-fluoro-4-n-octyloxyphenyliminomethyl)benzoic acid (**6.1**), 0.30 g DCC. The product is yellow powder. Yield 0.32 g (39%).

Mesogenic behavior: Cr (131 B₁) 135 I

¹H-NMR (500 MHz, CDCl₃) δ(ppm) / *J*(Hz) 8.66 (s, 2H, CH=N), 8.30 (d, 4H, ³*J* = 8.4, Ar-H), 8.05 (d, 4H, ³*J* = 8.4, Ar-H), 6.70-7.35 (m, 9H, Ar-H), 3.95 (t, 4H, ³*J* = 6.5, OCH₂), 2.12 (s, 3H, Ar-CH₃), 1.72-1.81 (m, 4H, OCH₂CH₂), 1.24-1.47 (m, 20H, (CH₂)₅CH₃), 0.86-0.89 (m, 6H, CH₃)

EIMS *m/z* (rel. int) 830 (6), 354 (100), 242 (6), 213 (7), 69 (6)

4-Cyano-1,3-phenylene bis[4-(3-fluoro-4-n-octyloxyphenyliminomethyl)benzoate]
(15.1)

0.14 g 4-Cyanoresorcinol (**8d**), 1.71 g 4-(3-fluoro-4-n-octyloxyphenyliminomethyl)benzoic acid (**5.1**), 1.1 g DCC. The product is yellow powder. Yield 0.59 g (70%).

Mesogenic behavior: Cr 73 SmAP 145 SmA 180 I

¹H-NMR (500 MHz, CDCl₃) δ(ppm) / J(Hz) 8.53 (s, 2H, CH=N), 8.32 (d, 2H, ³J= 8.4, Ar-H), 8.25 (d, 2H, ³J= 8.4, Ar-H), 8.03 (d, 2H, ³J= 8.4, Ar-H), 8.02 (d, 2H, ³J= 8.4, Ar-H), 7.79 (d, 1H, ³J= 8.5, Ar-H), 7.56 (d, 1H, ⁴J= 2.2, Ar-H), 7.33 (dd, 1H, ³J= 8.5, ⁴J= 2.2, Ar-H), 7.11 (tt, 2H, ³J_{H-F}= 12.2, ⁴J= 2.3, Ar-H), 7.05 (d, 2H, ³J= 8.8, Ar-H), 6.98 (t, 2H, ³J= 8.8, Ar-H), 4.04 (t, 4H, ³J= 6.5, OCH₂), 1.79-1.85 (m, 4H, OCH₂CH₂), 1.28-1.50 (m, 20H, (CH₂)₅CH₃), 0.86-0.89 (m, 6H, CH₃)

EIMS *m/z* (rel. int.): 841 (8), 592 (4), 488 (8), 354 (100), 259 (11), 242 (78), 213 (36), 127 (6), 69 (11)

4-Cyano-1,3-phenylene bis[4-(2-fluoro-4-n-octyloxyphenyliminomethyl)benzoate]
(16.1)

0.14 g 4-Cyanoresorcinol (**8d**), 1.71 g 4-(2-fluoro-4-n-octyloxyphenyliminomethyl)benzoic acid (**6.1**), 1.1 g DCC. The product is yellow powder. Yield 0.25g (30%).

Mesogenic behavior: Cr 93 SmCP 99 SmA 102 N 129 I

¹H-NMR (400 MHz, CDCl₃) δ(ppm) / J(Hz) 8.66 (s, 1H, CH=N), 8.65 (s, 1H, CH=N), 8.30 (d, 2H, ³J= 8.2, Ar-H), 8.25 (d, 2H, ³J= 8.2, Ar-H), 8.04 (m, 4H, Ar-H), 6.70-7.56 (m, 9H, ³J= 8.9, ⁴J= 2.5, Ar-H), 3.94-3.96 (m, 4H, OCH₂), 1.75-1.81 (m, 4H, OCH₂CH₂) 1.25-1.47 (m, 20H, (CH₂)₅CH₃), 0.85-0.88 (m, 6H, CH₃)

EIMS *m/z* (rel. int.): 841 (14), 592 (6), 354 (100), 259 (7), 242 (22), 213 (13), 127 (9), 69 (11)

4-Chloro-1,3-phenylene bis[4-(3-fluoro-4-n-octyloxyphenyliminomethyl)benzoate]
(17.1)

0.33 g 4-Chlororesorcinol (**8e**), 1.71 g 4-(3-fluoro-4-n-octyloxyphenyliminomethyl)benzoic acid (**5.1**), 1.1 g DCC. The product is yellow powder. Yield 0.43 g (50%).

Mesogenic behavior: Cr 90 SmCP 133 I

¹H-NMR (400 MHz, CDCl₃) δ (ppm) / J (Hz) 8.53 (s, 1H, CH=N), 8.52 (s, 1H, CH=N), 8.30 (d, 4H, ³ J = 8.2, Ar-H), 8.25 (d, 4H, ³ J = 8.2, Ar-H), 7.54 (d, 1H, ³ J = 8.8, Ar-H), 7.32 (d, 1H, ⁴ J = 2.5, Ar-H), 7.18 (dd, 1H, ³ J = 8.8, ⁴ J = 2.5, Ar-H), 7.04-7.13 (m, 4H, ³ J_{H-F} = 12.1, ³ J = 8.8, ⁴ J = 2.1, Ar-H), 6.98 (t, 2H, ³ J = 8.8, ⁴ J_{H-F} = 8.6, Ar-H), 4.03-4.06 (m, 4H, OCH₂), 1.24-1.86 (m, 24H, (CH₂)₆CH₃), 0.86-0.90 (m, 6H, CH₃)

EIMS m/z (rel. int) 354 (100), 242 (50), 213 (50)

4-Chloro-1,3-phenylene bis[4-(2-fluoro-4-n-octyloxyphenyliminomethyl)benzoate]
(18.1)

0.18 g 4-Chlororesorcinol (**8e**), 0.85 g 4-(2-fluoro-4-n-octyloxyphenyliminomethyl)benzoic acid (**6.1**), 0.30 g DCC. The product is yellow powder. Yield 0.30 g (35%).

Mesogenic behavior: Cr 71 SmCP 99 N 103 I

¹H-NMR (400 MHz, CDCl₃) δ (ppm) / J (Hz) 8.66 (s, 1H, CH=N), 8.65 (s, 1H, CH=N), 8.30 (d, 2H, ³ J = 8.2, Ar-H), 8.25 (d, 2H, ³ J = 8.2, Ar-H), 8.04 (m, 4H, Ar-H), 6.70-7.56 (m, 9H, ³ J = 8.9, ⁴ J = 2.5, Ar-H), 3.94-3.96 (m, 4H, OCH₂), 1.75-1.81 (m, 4H, OCH₂CH₂), 1.25-1.47 (m, 20H, (CH₂)₅CH₃), 0.85-0.88 (m, 6H, CH₃)

EIMS m/z (rel. int) 354 (100), 242 (23), 213 (21)

4,6-Dichloro-1,3-phenylene bis[4-(3-fluoro-4-n-octyloxyphenyliminomethyl)benzoate]
(19.1)

0.39 g 4-Chlororesorcinol (**8f**), 1.63 g 3-fluoro-4-(4-n-octyloxyphenyliminomethyl)benzoic acid (**5.1**), 1.1 g DCC. The product is yellow powder. Yield 0.49 g (55%).

Mesogenic behavior: Cr 127 (SmCP 95) SmA 129.8 N 130.5 I

$^1\text{H-NMR}$ (400 MHz, CDCl_3) $\delta(\text{ppm}) / J(\text{Hz})$ 8.53 (s, 2H, CH=N), 8.29 (d, 4H, $^3J = 8.5$, Ar-H), 8.02 (d, 4H, $^3J = 8.5$, Ar-H), 7.65 (s, 1H, Ar-H), 7.41 (s, 1H, Ar-H), 7.11 (dd, 2H, $^3J_{\text{H-F}} = 12.2$, $^4J = 2.5$, Ar-H), 7.05 (tt, 2H, $^3J = 8.5$, $^4J = 2.5$, $^5J_{\text{H-F}} = 1.3$, Ar-H), 6.98 (t, 2H, $^3J = 8.5$, $^4J_{\text{H-F}} = 8.7$, Ar-H), 4.04 (t, 4H, $^3J = 6.5$, OCH_2), 1.78-1.85 (m, 4H, OCH_2CH_2), 1.25-1.50 (m, 20H, $(\text{CH}_2)_5\text{CH}_3$), 0.86-0.89 (m, 6H, CH_3)

EIMS m/z (rel. int.): 884 (10), 354 (100), 242 (18), 216 (20)

Elemental analysis: calcd C 67.8; H 5.9; N 3.2; Cl 8.0 found C 67.9; H 5.9; N 3.0; Cl 9.8

4,6-Dichloro-1,3-phenylene bis[4-(2-fluoro-4-n-octyloxy-phenyliminomethyl)benzoate]
(20.1)

0.20 g 4-Chlororesorcinol (**8f**), 0.85 g 2-fluoro-4-(4-n-octyloxyphenyliminomethyl)benzoic acid (**5.1**), 0.3 g DCC. The product is yellow powder. Yield 0.43 g (48%).

Mesogenic behavior: Cr (129 N) 141 I

$^1\text{H-NMR}$ (400 MHz, CDCl_3) $\delta(\text{ppm}) / J(\text{Hz})$ 8.53 (s, 2H, CH=N), 8.29 (d, 4H, $^3J = 8.5$, Ar-H), 8.02 (d, 4H, $^3J = 8.5$, Ar-H), 7.64 (s, 1H, Ar-H), 7.40 (s, 1H, Ar-H), 7.20-7.23 (m, 2H, Ar-H), 6.70-6.73 (m, 4H, Ar-H), 3.95 (t, 4H, $^3J = 6.5$, OCH_2), 1.69-1.81 (m, 4H, OCH_2CH_2), 1.24-1.48 (m, 20H, $(\text{CH}_2)_5\text{CH}_3$), 0.86-0.89 (m, 6H, CH_3)

EIMS m/z (rel. int.): 884 (2), 354 (100), 242 (9), 213 (9)

5-Fluoro-1,3-phenylene bis[4-(3-fluoro-4-n-octyloxy-phenyliminomethyl)benzoate]
(21.1)

0.15 g 5-Fluororesorcinol (**7a**), 0.85 g 3-fluoro-4-(4-n-octyloxyphenyliminomethyl)benzoic acid (**5.1**), 0.3 g DCC. The product is yellow powder. Yield 0.46 g (55%).

Mesogenic behavior on cooling: Cr 113 B_{5F} 131 B_{5A}'''' 135.5 B_{5A}'''' 137 B_{5A}'' 138.9 B_{5A}'' 139.8 B₂ 163.5 I

$^1\text{H-NMR}$ (400 MHz, CDCl_3) $\delta(\text{ppm}) / J(\text{Hz})$ 8.53 (s, 2H, CH=N), 8.25 (d, 4H, $^3J = 8.4$, Ar-H), 8.01 (d, 4H, $^3J = 8.4$, Ar-H), 7.11 (dd, 2H, $^3J_{\text{H-F}} = 12.0$, $^4J = 2.4$, Ar-H), 7.04-7.07 (m, 5H, $^4J = 2.4$, Ar-H), 6.9-7.00 (m, 4H, Ar-H), 4.05 (t, 4H, $^3J = 6.7$, OCH_2), 1.79-1.84 (m, 4H, OCH_2CH_2), 1.24-1.49 (m, 20H, $(\text{CH}_2)_5\text{CH}_3$), 0.86-0.89 (m, 6H, CH_3)

EIMS m/z (rel. int.) 834 (22), 722 (4), 611 (1), 368 (2), 354 (100), 259 (2), 242 (46), 213 (34), 138 (2), 105 (1), 69 (11)

5-Fluoro-1,3-phenylene bis[4-(2-fluoro-4-n-octyloxy-phenyliminomethyl)benzoate]
(22.1)

0.44 g 5-Fluororesorcinol (**7a**), 1.42 g 2-fluoro-4-(4-n-octyloxyphenyliminomethyl)benzoic acid (**6.1**), 1.0 g DCC. The product is yellow powder. Yield 0.54 g (65%). Melting point: 139°C.

$^1\text{H-NMR}$ (400 MHz, CDCl_3) δ (ppm) / J (Hz) 8.66 (s, 2H, CH=N), 8.25 (d, 4H, $^3J= 8.2$, Ar-H), 8.03 (d, 4H, $^3J= 8.2$, Ar-H), 6.70-7.23 (m, 9H, Ar-H), 3.95 (t, 4H, $^3J= 6.5$, OCH_2), 1.75-1.81 (m, 4H, OCH_2CH_2), 1.28-1.46 (m, 20H, $(\text{CH}_2)_5\text{CH}_3$), 0.85-0.87 (m, 6H, CH_3)

EIMS m/z (rel. int.) 834 (11), 354 (100), 259 (11), 242 (46), 213 (10), 69 (13)

5-Fluoro-1,3-phenylene bis[4-(4-n-octyloxyphenyliminomethyl)benzoate] (**23.1**)

The compound was prepared as it is described in section 8.1.5. 0.15 g 5-fluororesorcinol (**7a**), 0.78 g 4-(4-n-octyloxyphenyliminomethyl)benzoic acid, 0.54 g DCC. The product is yellow powder. Yield 0.52 g (65%).

Mesogenic behavior: Cr 158 SmCP 179 I

$^1\text{H-NMR}$ (400 MHz, CDCl_3) δ (ppm) / J (Hz) 8.56 (s, 2H, CH=N), 8.25 (d, 4H, $^3J= 8.4$, Ar-H), 8.01 (d, 4H, $^3J= 8.4$, Ar-H), 7.27 (d, 4H, $^3J= 8.9$, Ar-H), 7.06 (d, 1H, $^5J_{\text{H-F}}= 1.2$, Ar-H), 6.98 (dd, 2H, $^3J_{\text{H-F}}= 9.0$, $^4J= 2.1$, Ar-H), 6.93 (d, 4H, $^3J= 8.9$, Ar-H), 3.97 (t, 4H, $^3J= 6.5$, OCH_2), 1.75-1.82 (m, 4H, OCH_2CH_2), 1.26-1.49 (m, 20H, $(\text{CH}_2)_5\text{CH}_3$), 0.85-0.89 (m, 6H, CH_3)

EIMS m/z (rel. int.) 798 (6), 463 (16), 336 (100), 224 (16), 195 (23), 69 (9)

8.2 N,N'-bis[4-(4-n-Octyloxybenzoyloxy)benzylidene]phenylene-1,3-diamines (28, 29)

8.2.1 2-Fluoro-4-hydroxy-benzaldehyde (25) [100]

19 mmol (3.0 g) 2-Fluoro-4-methoxy benzaldehyde was dissolved in dry dichloromethane in a three-neck flask and purged with nitrogen. 31 mmol (31 ml of 1M solution in DCM) boron tribromide was added to the solution under nitrogen atmosphere at room temperature. It was stirred at room temperature in the closed flask for six days. The reaction was quenched with water given drop wise to the reaction mixture stirred for an additional thirty minutes. Afterward, about 3 ml 31.8%-os HCl solution was given to the solution, and it was stirred for additional half an hour. The mixture was extracted with diethylether twice. The combined organic layer was extracted with brine and water. It was dried over Na₂SO₄ overnight. The solvent was evaporated, and the crude product was recrystallized from acetic acid. The product is red powder. Yield: 1.73 g (65%). *R_f*: 0.10 (ethylacetate:heptane=1:2.5). Melting point: 173°C.

8.2.2 4-n-Octyloxybenzoic acid 3-fluoro-4-formylphenyl ester (26)

10 mmol (2.5 g) 4-n-Octyloxy-benzoic acid, 10 mmol (1.4 g) 2-fluoro-4-hydroxy benzaldehyde (25) and 12 mmol (2.5 g) DCC were dissolved in dry dichloromethane. Catalytic amount of DMAP was given to it. It was stirred for a day at room temperature. The precipitation (N,N'-dicyclohexylurea, DCU) was filtered out and the solvent was evaporated. The crude product was recrystallized from ethanol twice. The product is white powder. Yield: 2.23 g (60%). *R_f*: 0.50 (ethylacetate:heptane=1:2.5).

Mesogenic behavior: Cr 41 SmA 50 I

¹H-NMR (400 MHz, CDCl₃) δ(ppm) / *J*(Hz) 10.315 (s, 1H, CH=O), 8.09 (dd, 2H, ³*J*= 9.2, Ar-H), 7.93 (d, 1H, ³*J*= 8.4, Ar-H), 7.12-7.16 (m, 1H, Ar-H), 7.10-7.11 (m, 1H, Ar-H), 6.96 (m, 2H, ³*J*= 9.2, Ar-H), 4.03 (t, 2H, ³*J*= 6.6, OCH₂), 3.65-3.75 (m, 2H, OCH₂CH₂), 1.19-1.88 (m, 20H, (CH₂)₅CH₃), 0.84-0.91 (m, 3H, CH₃)

8.2.3 4-Fluoro-m-phenylenediamine (27)

2,4-Dinitrofluorobenzene was dissolved in methanol, and 10 m/m% Pd/C (5%) was given to it. After purging the solution with nitrogen, hydrogen was led into it. After two or three hours the reaction is completed. The Pd/C was filtered out. Since the product decomposes very fast, this solution was used up immediately to get **28.5** and **29.5**. The yield was considered 100% in order to obtain completely substituted product.

8.2.4 N,N'-bis[4-(4-n-octyloxybenzoyloxy)benzylidene]phenylene-1,3-diamines (28, 29)

1.3 mmol Diamine and 2.6 mmol 4-n-octyloxybenzoic acid 4-formylphenyl ester or 4-n-octyloxybenzoic acid 3-fluoro-4-formylphenyl ester was dissolved in hot methanol. It was stirred for two days at room temperature. The precipitation was filtered out and washed with methanol. The crude product was recrystallized from DMF with ethanol at least twice. Yield: 25-80%.

N,N'-bis[4-(4-n-octyloxybenzoyloxy)benzylidene] 2-methylphenylene-1,3-diamine (28.2)

0.16 g 2,6-Diamino-toluene, 0.92 g 4-n-octyloxybenzoic acid 4-formyl-phenyl ester. The product is yellow powder. Yield: 0.68 g (66%).

Mesogenic behavior: Cr 140 (B₁ 127.5) I

¹H-NMR (500 MHz, CDCl₃) δ(ppm) / J(Hz) 8.39 (s, 2H, CH=N), 8.14 (tt, 4H, ³J= 8.9, ⁴J= 4.6, Ar-H), 7.99 (d, 4H, ³J= 8.5, Ar-H), 7.32 (d, 4H, ³J= 8.5, Ar-H), 7.21 (t, 1H, ³J= 7.8, Ar-H), 6.97 (tt, 4H, ³J= 8.9, Ar-H), 6.82 (d, 2H, ³J= 7.8, Ar-H), 4.04 (t, 4H, ³J= 6.5, OCH₂), 2.36 (s, 3H, Ar-CH₃), 1.78-1.84 (m, 4H, OCH₂CH₂), 1.44-1.51 (m, 4H, OCH₂CH₂CH₂), 1.26-1.37 (m, 16H, (CH₂)₄CH₃), 0.87-0.90 (m, 6H, CH₃)

EIMS *m/z* (rel. int.) 354 (1), 233 (100), 121 (71), 93 (4)

N,N'-bis[4-(4-*n*-octyloxybenzoyloxy)2-fluoro-benzylidene] 2-methylphenylene-1,3-diamine (**29.2**)

0.10 g 2,6-Diamino-toluene, 0.60 g 4-*n*-octyloxybenzoic acid 4-formyl-phenyl ester (**26**). The product is yellow powder. Yield: 0.49 g (70%). Melting point: 145°C.

¹H-NMR (500 MHz, CDCl₃) δ(ppm) / *J*(Hz) 8.67 (s, 2H, CH=N), 8.29 (t, 2H, ³*J*= 8.5, ⁴*J*_{H-F}= 8.2, Ar-H), 8.12 (tt, 4H, ³*J*= 8.9, Ar-H), 7.22 (d, 1H, ³*J*= 8.0, Ar-H), 7.13 (dd, 2H, ³*J*= 8.5, ⁴*J*= 2.3, Ar-H), 7.09 (dd, 2H, ³*J*_{H-F}= 10.8, ⁴*J*= 2.3, Ar-H), 6.97 (tt, 4H, ³*J*= 8.9, Ar-H), 6.85 (d, 2H, ³*J*= 8.0, Ar-H), 4.04 (t, 4H, ³*J*= 6.5, OCH₂), 2.37 (s, 3H, Ar-CH₃), 1.78-1.84 (m, 4H, OCH₂CH₂), 1.44-1.50 (m, 4H, OCH₂CH₂CH₂), 1.26-1.37 (m, 16H, (CH₂)₄CH₃), 0.87-0.90 (m, 6H, CH₃)

EIMS *m/z* (rel. int.) 830 (3), 233 (100), 121 (75), 93 (3)

8.3 Isophthalydene bis[4-(4-subst.-phenyloxycarbonyl)anilines] (30)

10 mmol (3.72 g) 1,3-Phenylene bis(4-methyliminobenzoic acid), 22 mmol of the corresponding 4-substituted phenol and 26 mmol (5.27 g) DCC was dissolved in dry dichloromethane. Catalytic amount of DMAP was given to it. It was stirred at RT for five to seven days. The precipitation (N,N'-dicyclohexylurea, DCU) was filtered out and the solvent was evaporated. The crude product was recrystallized from toluene at least three times. Yield: 30-40%.

Isophthalydene bis [4-(4-octyloxy-phenyloxycarbonyl)aniline] (30.4)

3.72 g 1,3-Phenylene bis(4-methyliminobenzoic acid), 5.5 g 4-*n*-octyloxybenzoic acid, 5.27 g DCC. The product is yellow powder. Yield: 3.12 g (40%).

Mesogenic behavior: Cr 126 B₄ 148 SmCP 152 I

¹H-NMR (400 MHz, CDCl₃) δ(ppm) / *J*(Hz) 8.54 (s, 2H, CH=N), 8.47 (s, 1H, Ar-H), 8.23 (dd, 4H, ³*J*= 8.5, Ar-H), 8.09 (d, 4H, ³*J*= 8.5, Ar-H), 7.63 (t, 1H, ³*J*= 7.8, Ar-H), 7.28 (dd, 4H, ³*J*= 8.5, Ar-H), 7.11 (tt, 4H, ³*J*= 9.0, Ar-H), 6.92 (tt, 4H, ³*J*=9.0, Ar-H),

3.95 (t, 4H, $^3J= 6.6$, OCH₂), 1.74-1.81 (m, 4H, OCH₂CH₂), 1.23-1.49 (m, 20H, (CH₂)₅CH₃), 0.86-0.89 (m, 6H, CH₃)

Bibliography

- [1] T. Niori, T. Sekine, J. Watanabe, T. Furukawa, H. Takezoe, *J. Mater. Chem.*, **6**, 1231 (1996)
- [2] G. Pelzl, S. Diele, W. Weissflog, *Adv. Mater.*, **11**, 707 (1999)
- [3] M. Barón, *Pure Appl. Chem.*, **73**, 845 (2001)
- [4] R. Amaranatha Reddy, B. K. Sadashiva, *Liq. Cryst.*, **27**, 1613 (2000)
- [5] T. J. Dingemans, E. T. Samulski, *Liq. Cryst.*, **27**, 131 (2000)
- [6] J. Thisayukta, Y. Nakayama, J. Watanabe, *Liq. Cryst.*, **27**, 1129 (2000)
- [7] Y. Matsunaga, T. Hosoda, *Mol. Cryst. Liq. Cryst.*, **326**, 369 (1999)
- [8] J. Watanabe, H. Komura, T. Niori, *Liq. Cryst.*, **13**, 455 (1993)
- [9] T. Niori, S. Adachi, J. Watanabe, *Liq. Cryst.*, **19**, 139 (1995)
- [10] J. Watanabe, T. Niori, S.-W. Choi, Y. Takanishi, H. Takezoe, *Jpn. Appl. Phys.*, **37**, 401 (1998)
- [11] S.-W. Choi, M. Zennoji, Y. Takanishi, H. Takezoe, T. Niori, J. Watanabe, *Mol. Cryst. Liq. Cryst. A*, **328**, 185 (1999)
- [12] K. Pelz, W. Weissflog, U. Baumeister, S. Diele, *Liq. Cryst.*, **30**, 1151 (2003)
- [13] M. W. Schröder, S. Diele, G. Pelzl, U. Dunemann, H. Kresse, W. Weissflog, *J. Mater. Chem.*, **13**, 1877 (2003)
- [14] D. Vorländer, A. Apel, *Ber. Dtsch. Chem. Ges.*, **65**, 1101 (1932)
- [15] T. Akutagawa, Y. Matsunaga, K. Yasuhara, *Liq. Cryst.*, **17**, 659 (1994)
- [16] P.E. Cladis, H.R. Brand, H. Pleiner, *Eur. Phys. J. B*, **6**, 347 (1998)
- [17] A. Eremin, *Dissertation*, Martin-Luther-University Halle-Wittenberg (2003)
- [18] J. Thisayukta, H. Niwano, H. Takezoe, J. Watanabe, *J. Mater. Chem.*, **11**, 1 (2001)
- [19] M. Nakata, D. R. Link, J. Thisayukta, Y. Takanishi, K. Ishikawa, J. Watanabe, H. Takezoe, *J. Mater. Chem.*, **11**, 2694 (2001)
- [20] A. Eremin, S. Diele, G. Pelzl, H. Nádasi, W. Weissflog, *Phys. Rev. E*, **67**, 021702 (2003)
- [21] D. R. Link, N. A. Clark, B. I. Ostrovskii, E. A. Soto Bustamante, *Phys. Rev. E*, **61**, R37 (2000)
- [22] A. Eremin, S. Diele, G. Pelzl, H. Nádasi, W. Weissflog, J. Salfetnikova, H. Kresse, *Phys. Rev. E*, **64**, 051707 (2001)

- [23] T. C. Lubensky, A. B. Harris, R. D. Kamien, G. Yan, *Ferroelectrics*, **212**, 1 (1998)
- [24] A. B. Harris, R. D. Kamien, T. C. Lubensky, *Rev. Mod. Phys.*, **71**, 1745 (1999)
- [25] R. Link, G. Natale, R. Shao, J. E. MacLennan, N. A. Clark, E. Körblova, D. M. Walba, *Science*, **278**, 1924 (1997)
- [26] S. Diele, S. Grande, H. Kruth, Ch. Lischka, G. Pelzl, W. Weissflog, I. Wirth, *Ferroelectrics*, **212**, 169 (1998)
- [27] W. Weissflog, I. Wirth, S. Diele, G. Pelzl, H. Schmalfluss, T. Schoss, A. Würflinger, *Liq. Cryst.*, **28**, 1603 (2001)
- [28] E. Mátyus, K. Fodor-Csorba, *Liq. Cryst.*, **30**, 445 (2003)
- [29] A. Jákli, D. Krüerke, H. Sawade, and G. Heppke, *Phys. Rev. Lett.*, **86**, 5715 (2001)
- [30] G. Pelzl, S. Diele, C. Lischka, I. Wirth, W. Weissflog, *Liq. Cryst.*, **26**, 135 (1999)
- [31] H. R. Brand, P. E. Cladis, H. Pleiner, *Europhys. Lett.*, **57**, 368 (2002)
- [32] D. A. Coleman, J. Fernsler, N. Chattham, M. Nakata, Y. Takanishi, E. Körblova, D. R. Link, R.-F. Shao, W. G. Jang, J. E. MacLennan, O. Mondainn-Monval, C. Boyer, W. Weissflog, G. Pelzl, L.-C. Chien, J. Zasadzinski, J. Watanabe, D. M. Walba, H. Takezoe, N. A. Clark, *Science*, **301**, 1204 (2003)
- [33] T. Sekine, T. Niori, M. Sone, J. Watanabe, S. Choi, Y. Takanishi, Takezoe, *Jpn. J. Appl. Phys.*, **36**, 6455 (1997)
- [34] J. Thisayukta, H. Takezoe, J. Watanabe, *Jpn. J. Appl. Phys.*, **40**, 3277 (2001)
- [35] H. Lippmann, *Ann. Phys.*, **2**, 287 (1958)
- [36] R. Blinc, *Liq. Cryst.*, **26**, 1295 (1999)
- [37] E. Ciampi, M. I. C. Furby, L. Brennan, J. W. Emsley, A. Lesage, L. Emsley, *Liq. Cryst.*, **26**, 109 (1999)
- [38] F. Roussel, J.-P. Bayle, M. A. Khan, B. M. Fung, O. Yokokohji, T. Shimizu, H. Koh, S. Kumai, *Liq. Cryst.*, **26**, 251 (1999)
- [39] D. W. Allender, G. P. Crawford, J. W. Doane, *Phys. Rev. Lett.*, **67**, 1442 (1991)
- [40] W. Weissflog, Ch. Lischka, S. Diele, G. Pelzl, I. Wirth, S. Grande, H. Kresse, H. Schmalfluss, H. Hartung, A. Stettler, *Mol. Cryst. Liq. Cryst.*, **333**, 203 (1999)
- [41] T. M. Duncan, *A Compilation of Chemical Shift Anisotropies*, The Farragut Press, Chicago, 1990
- [42] K. Miyazawa, T. Kato, M. Itoh, M. Ushioda, *Liq. Cryst.*, **29**, 1483 (2002)
- [43] H. Matsuzaki, Y. Matsunaga, *Liq. Cryst.*, **14**, 105 (1993)

- [44] V. Prasad, *Liq. Cryst.*, **28**, 145 (2001)
- [45] G. Heppke, D. D. Parghi, H. Sawade, *Liq. Cryst.*, **27**, 313 (2000)
- [46] D. M. Walba, E. Körblova, R. Shao, N. A. Clark, *J. Mater. Chem.*, **11**, 2743 (2001)
- [47] R. Amaranatha Reddy, B. K. Sadashiva, S. Dhara, *Chem. Commun.*, 1972 (2001)
- [48] D. Shen, S. Diele, G. Pelzl, I. Wirth, C. Tschierske, *J. Mater. Chem.*, **9**, 661, (1999)
- [49] J. Matraszek, J. Mieczkowski, J. Szydłowska, E. Górecka, *Liq. Cryst.*, **27**, 429 (2000)
- [50] J. Mieczkowski, J. Szydłowska, J. Matraszek, D. Pocięcha, E. Górecka, B. Donnio, D. Guillon, *Phys. Rev. E*, **67**, 031702 (2003)
- [51] H. T. Nguyen, J. C. Rouillon, J. P. Marcerou, J. P. Bedel, P. Barois, S. Sarmento, *Mol. Cryst. Liq. Cryst.*, **328**, 177 (1999)
- [52] B. K. Sadashiva, R. Amaranatha Reddy, R. Pratibha, N. V. Madhusudana, *Chem. Commun.*, 2140 (2001)
- [53] J. P. Bedel, J. C. Rouillon, J. P. Marcerou, M. Laguerre, M. F. Achard, H. T. Nguyen, *Liq. Cryst.*, **27**, 103 (2000)
- [54] M. Zennyoji, Y. Takanishi, K. Ishikawa, J. Thisayukta, J. Watanabe, H. Takezoe, *Mol. Cryst. Liq. Cryst.*, **366**, 2545 (2001)
- [55] S. Diele, S. Grande, H. Kruth, C. Lischka, G. Pelzl, W. Weissflog, I. Wirth, *Ferroelectrics*, **212**, 169 (1998)
- [56] A. Eremin, I. Wirth, S. Diele, G. Pelzl, H. Schmalfluss, H. Kresse, H. Nádasi, K. Fodor-Csorba, E. Gács-Baitz, W. Weissflog, *Liq. Cryst.*, **29**, 775 (2002)
- [57] D. Shen, S. Diele, I. Wirth, C. Tschierske, *Chem. Commun.*, 2573 (1998)
- [58] D. Shen, A. Pegenau, S. Diele, I. Wirth, C. Tschierske, *J. Am. Chem. Soc.*, **122**, 1593, (2000)
- [59] G. Dantlgraber, D. Chen, S. Diele, C. Tschierske, *Chem. Mater.*, **14**, 1149 (2002)
- [60] G. Dantlgraber, A. Eremin, S. Diele, A. Hauser, H. Kresse, G. Pelzl, C. Tschierske, *Angew. Chem.*, **114**, 2514 (2002)
- [61] W. Weissflog, H. Nádasi, U. Dunemann, G. Pelzl, S. Diele, A. Eremin, H. Kresse, *J. Mater. Chem.*, **11**, 2748 (2001)
- [62] L. Kovalenko, W. Weissflog, S. Grande, S. Diele, G. Pelzl, I. Wirth, *Liq. Cryst.*, **27**, 683 (2000)

- [63] A. Jákli, Ch. Lischka, W. Weissflog, G. Pelzl, A. Saupe, *Liq. Cryst.*, **27**, 1405 (2000)
- [64] G. Pelzl, S. Diele, S. Grande, A. Jákli, Ch. Lischka, H. Kresse, H. Schmalfuss, I. Wirth, W. Weissflog, *Liq. Cryst.*, **26**, 401 (1999)
- [65] I. Wirth, S. Diele, A. Eremin, G. Pelzl, S. Grande, L. Kovalenko, N. Pancenko, W. Weissflog, *J. Mater. Chem.*, **11**, 1642 (2001)
- [66] W. Weissflog, Ch. Lischka, S. Diele, G. Pelzl, I. Wirth, *Mol. Cryst. Liq. Cryst.*, **328**, 101 (1999)
- [67] A. Jákli, Ch. Lischka, W. Weissflog, G. Pelzl, S. Rauch, G. Heppke, *Ferroelectrics*, **243**, 239 (2000)
- [68] A. Jákli, Ch. Lischka, W. Weissflog, G. Pelzl, *Liq. Cryst.*, **27**, 715 (2000)
- [69] K. Fodor-Csorba, A. Vajda, G. Galli, A. Jákli, D. Demus, S. Holly, E. Gács-Baitz, *Macromol. Chem. Phys.*, **203**, 1556 (2002)
- [70] J. Mieczkowski, J. Szydłowska, J. Matraszek, D. Pocięcha, E. Górecka, B. Donnio, D. Guillon, *J. Mater. Chem.*, **12**, 3392 (2002)
- [71] S. Shubashree, B. K. Sadashiva, S. Dhara, *Liq. Cryst.*, **29**, 789 (2002)
- [72] R. Amaranatha Reddy, B. K. Sadashiva, *Liq. Cryst.*, **29**, 1365 (2002)
- [73] R. Amaranatha Reddy, B. K. Sadashiva, *Liq. Cryst.*, **30**, 273 (2003)
- [74] J. P. Bedel, J. C. Rouillon, J. P. Marcerou, M. Laguerre, H. T. Nguyen, M. F. Achard, *J. Mater. Chem.*, **12**, 2214 (2002)
- [75] R. Amaranatha Reddy, B. K. Sadashiva, *Liq. Cryst.*, **30**, 1031 (2003)
- [76] J. P. Bedel, J. C. Rouillon, J. P. Marcerou, M. Laguerre, H. T. Nguyen, M. F. Achard, *Liq. Cryst.*, **28**, 1285 (2001)
- [77] C.-K. Lee, S.-S. Kwon, S.-T. Shin, E.-J. Choi, S. Lee, L.-C. Chien, *Liq. Cryst.*, **29**, 1007 (2002)
- [78] D. M. Walba, E. Körblova, R. Shao, J. E. MacLennan, D. R. Link, N. A. Clark, *Science*, **288**, 2181 (2000)
- [79] D. Shen, *Dissertation*, Martin-Luther-University Halle-Wittenberg (2001)
- [80] L. Kovalenko, D. Lose, S. Diele, G. Pelzl, W. Weissflog, Proceedings of the 26th Arbeitstagung der Flüssigkristalle, p. 40 (1998)

- [81] L. Kovalenko, W. Weissflog, J. Risse, I. Wirth, D. Lose, S. Diele, G. Pelzl, S. Grande, H. Schmalfluss, H. Kresse, Poster Nr. 21 presented at the 7th International Conference on Ferroelectric Liq. Cryst., Darmstadt, Germany
- [82] D. L. Hughes, *Organic Reactions*, **42**, 335 (1992)
- [83] S. Coco, P. Espinet, J. M. Martín-Alvarez, A.-M. Levelut, *J. Mater. Chem.*, **7**, 19 (1997)
- [84] W.-C. Sun, K. R. Gee, D. H. Klaubert, R. P. Haugland, *J. Org. Chem.*, **62**, 6469 (1997)
- [85] P. R. Brooks, M. C. Wirtz, M. G. Vetelino, D. M. Rescek, G. F. Woodworth, B. P. Morgan, J. W. Coe, *J. Org. Chem.*, **64**, 9719 (1999)
- [86] J.-J. Yang, D. Su, A. Vij, T. L. Hubler, R. L. Kirchmeier, J. M. Shreeve, *Heteroatom Chemistry*, **9**, 229 (1998)
- [87] F. Lengfeld, J. Stieglitz, *Dtsch. Chem. Ges. Ber.*, **27**, 926 (1894)
- [88] M. Mikołajczyk, P. Kielbasiński, *Tetrahedron*, **37**, 233 (1981)
- [89] C.-K. Lee, L.-C. Chien, *Ferroelectrics*, **243**, 231 (2000)
- [90] G. Heppke, D. D. Parghi, H. Sawade, *Ferroelectrics*, **243**, 269 (2000)
- [91] H. Nádasi, Ch. Lischka, W. Weissflog, I. Wirth, S. Diele, G. Pelzl, and H. Kresse, *Mol. Cryst. Liq. Cryst.*, **399**, 69 (2003)
- [92] D. Walba, E. Körblova, R. Shao, J.E. Maclennan, D.R. Link, N.A. Clark, *Mat. Res. Soc. Symp. Proc.*, **559**, 3 (1999)
- [93] S. V. Shilov, S. Rauch, H. Skupin, G. Heppke, F. Kremer, *Liq. Cryst.*, **26**, 1409 (1999)
- [94] G. Heppke, A. Jákli, S. Rauch, H. Sawade, *Phys. Rev. E*, **60**, 5575 (1999)
- [95] M. I. Barnik, L. M. Blinov, N. M. Shtykov, S. P. Palto, G. Pelzl, W. Weissflog, *Liq. Cryst.*, **29**, 597 (2002)
- [96] J. Salfetnikova, H. Nádasi, W. Weissflog, A. Hauser, H. Kresse, *Liq. Cryst.*, **29**, 115 (2002)
- [97] H.R. Brand, P. Cladis, H. Pleiner, *Macromolecules*, **25**, 7223 (1988)
- [98] H. Schlacken, P. Schiller and H. Kresse, *Liq. Cryst.*, **28**, 1235 (2001)
- [99] H. Nádasi, W. Weissflog, A. Eremin, G. Pelzl, S. Diele, B. Das, S. Grande, *J. Mater. Chem.*, **12**, 1316 (2002)
- [100] M. Monclus, C. Masson, A. Luxen, *J. Fluorine Chem.*, **70**, 39 (1995)

Symbols and abbreviations

α - bending angle between the wings of a bent-shaped mesogen

β - angle between the symmetry axis and the molecular long axis of a bent-shaped mesogen

γ - viscosity

δ - chemical shift

ε - angle between the long molecular axis and one of the wings of a bent-shaped mesogen

ε - dielectric permittivity

θ - tilt angle

λ - wavelength

ν - splitting

σ - dielectric conductivity

τ_s - switching time

φ - torsion angle

ΔH - transition enthalpy

AFE - antiferroelectric

Alk - alkyl

Ar-H - aromatic hydrogen

B₁- B₇ - designation of banana mesophases suggested in the workshop

Banana-Shaped Liquid Crystals:

“Chirality by Achiral Molecules” held in Berlin in December 1997

B_x - banana mesophases different from already defined ones

calcd - calculated

C_B, C_{B2} - possible designation for B₂ mesophase

C_G - mesophase with C₁ symmetry and one polarization vector

Col_r - columnar rectangular mesophase

C_p - heat capacity

C_P - mesophase with C_{2v} symmetry and one polarization vector

Cr - crystalline

d - doublet

d - layer thickness

D - transversal order parameter

DCC - N, N'-dicyclohexylcarbodiimide

DCM - dichloromethane

DCU - N, N'-dicyclohexylurea

dd - double doublet

DEAD - diethyl azodicarboxylate

deg - degree

DMAP - 4-dimethylaminopyridine

DMF - dimethylformamide

DSC - differential scanning calorimetry

E - electric field

E_A - activation energy

EIMS - electron impact mass spectroscopy

EN - electronegativity

E_{th} - threshold field

f - frequency

FE - ferroelectric

I - isotropic

I - current	SmC_AP_A – antiferroelectric SmCP phase in which the interface arrangement of the molecules is anticlinic
IUPAC – international union of pure and applied chemistry	SmC_AP_F - ferroelectric SmCP phase in which the interface arrangement of the molecules is anticlinic
J – coupling constant	SmC_G - mesophase with C_1 symmetry and one polarization vector
iJ - coupling constant of ipso coupling	SmCP – designation for B_2 phase
3J – coupling constant of ortho coupling	SmC_SP_A - antiferroelectric SmCP phase in which the interface arrangement of the molecules is synclinic
4J - coupling constant of meta coupling	SmC_SP_F - ferroelectric SmCP phase in which the interface arrangement of the molecules is synclinic
5J - coupling constant of para coupling	SmX – smectic X phase: different from the already defined smectic phases
K – elastic constant	T - temperature
\mathbf{k} – layer normal vector	t – triplet
m – multiplet	t - time
m/z – mass/charge	THF – tetrahydrofuran
MF – molecular fixed frame	U_{th} – threshold voltage
N - nematic	W_{XY} – matrix elements of the interaction tensor
\mathbf{n} – vector along the long molecular axis of the molecule	XRD – X-ray diffraction
NMR – nuclear magnetic resonance	
\mathbf{p} – polarization vector	
PAS – principle axis system	
P_s – switching polarization	
q - quartet	
rel. int. – relative intensity	
R_f – migration ratio of the substance and the solvent on thin layer	
S – longitudinal order parameter	
s – singlet	
Sign. - signature	
SmA – smectic A phase	
SmAP - mesophase with C_{2v} symmetry and one polarization vector	
SmC – smectic C phase	

Hajnalka Nádas

Personal Information

Nationality: Hungarian
Date of Birth: 14. 08. 1975
Place of Birth: Budapest, Hungary

Education

1993-99 University Eötvös Loránd (ELTE) MSc degree in Chemistry specialized in drug research
1989-93 High School Eötvös József certificate of final examination in Hungarian High School

Professional Experience

1999- Martin-Luther-University Halle-Wittenberg
Scientific co-worker
1998-99 Institute of Peptide Research University Eötvös Loránd
Diploma worker
1998 Richter Gedeon Pharmaceutical Company Budapest
Practitioner
1996-98 Institute of Peptide Research University Eötvös Loránd
Student researcher

Languages

English – advanced
German – fluent in speech and reading
Russian – pre-intermediate
French – elementary
Hungarian – native

Community activities

1993-95 Member of the University self-government of ELTE
1994-95 Co-worker of the university journal of ELTE

Interests

Languages, Reading, Music, Movies, Journalism

Awards received

1999 Excellent student of the Faculty of Natural Sciences, University Eötvös Loránd
1999 First place on the competition of student researchers in the Department of Chemistry

Acknowledgments

The driving force behind the nurturing process which brought each chapter to maturity was my supervisor Professor Wolfgang Weissflog who also guided my work in his working group. I thank for it.

The electro-optical and X-Ray measurements were made in the working group of Professor Gerhard Pelzl. I would like to express my sincere appreciation to him for fruitful scientific discussions and the wholehearted support.

I sincerely thank to Dr. Katalin Fodor-Csorba, the kindest and most natural person I have ever met, for introducing me the world of liquid crystals and supporting me even from far distance. Furthermore I thank her for preparing the deuterated starting materials.

The dielectric measurements were made by Professor Horst Kresse. I thank for it.

I also thank Dr. Siegmur Diele and his student Ina Wirth for the X-Ray measurements.

I thank for the NMR measurements to Professor Siegbert Grande.

I really enjoyed working together with Ulrike Dunemann, Laura Kovalenko, Karsten Pelz, Jens Risse and Martin Schröder.

I am grateful for the technical support to Ms. Gottschlich, Ms. Hillmann, Ms. Kirkamm and Ms. Naumann.

I would like to express my most sincere and grateful appreciation to my family that never ceased believing in me and they have been behind me all the way.

Finally, I simply thank to Alexey Eremin because there is no way to express my gratitude in words.

The author wishes to express his sincere appreciation to Deutsche Forschungsgemeinschaft (DFG) for the financial support.

Erklärung

Hiermit versichere ich, daß ich die vorliegende Arbeit selbstständig verfaßt habe und keine anderen als die von mir angegebenen Quellen und Hilfsmittel verwendet habe. Diese Dissertation wurde bisher an keiner anderen Hochschule oder Universität vorgelegt.

Halle, den 06. 05. 2004